June 2018

Surface water and groundwater in a changing climate: applications of hydrogeophysics and trend analysis to understand hydrologic systems

Robin Glas
Syracuse University

Abstract

Water resources are being impacted by anthropogenic climate change worldwide, the nature and severity of that impact is determined by geographic position, local topography, underlying geology, and human influences such as land use, water availability, and water regulation. As global temperatures continue to rise due to greenhouse gas emissions, it is imperative that we better understand how water availability fluctuates with changes in air temperature, rainfall, snowpack, and glacial ice. This dissertation provides an analysis of the hydrologic response to both short-term and long-term climatic changes in both humid-temperate and semi-arid tropical regions. Within the tropical alpine zone, shifts in water availability have turned investigators' attention to groundwater systems that may function to buffer water losses due to climate change, and these systems are characterized and reviewed herein.

In the arid outer tropics of Peru, alpine proglacial valleys are storing groundwater that supplies a significant quantity of base flow to the regional surface water system. This is especially evident during the region's dry season from May to October, during the Austral winter. The Cordillera Blanca contains the world's highest coverage of tropical glacial ice, and this ice is melting at an unprecedented rate due to warming regional temperatures. As glacial meltwater and dry season streamflow decline, we focus on the groundwater storage potential of high-altitude wetlands and grasslands that are located in Cordillera Blanca's proglacial valleys. The valley aquifers, known as pampas, are composed of alpine gravitational slope deposits, such as talus cones and debris fans. These slope deposits are buried beneath thick (5 to 10 m) fine lacustrine sediment, indicating that they were first deposited in proglacial lakes, where their large pore space was infilled slowly with lake sediments over time.

Multiple geophysical surveys were carried out to study the internal structure of a buried talus aquifer in the Quilcayhuanca valley of the Cordillera Blanca, which lies in the center of the range, upstream from the city of Huaraz. Seismic and electrical methods were interpreted with borehole data from five piezometers that were installed in a transect that extends outward from the exposed portion of talus. The boreholes were drilled through fine-grained lacustrine sediments until the depth of auger refusal, which deepens with proximity to the stream and consists of large (.1 to 1 m in diameter) talus boulders. Geophysical evidence suggests that these boulders are part of a clast-supported deposit of talus at depth, where the shallower portions of the deposit are infilled with low-permeability sediment. The resulting confined aquifer discharges to surface springs via preferential flow pathways, providing year-round supply to tributaries and eventually the Quilcay stream. Total sediment thickness in this area is likely between 20 and 85 m, which likely includes glacial deposits beneath the talus aquifer.

This research highlights the importance of future aquifer studies in other valleys of the Cordillera Blanca in order to assess their spatial distribution, as well as differences in structure and thickness. For residents and industries in the Callejon de Huaylas watershed, which receives a high proportion of glacial runoff, future water availability is highly uncertain. Although hydropower operations along the Callejon de Huaylas utilize reservoirs to offset water losses, large-scale water diversions for agricultural operations are at risk for reduced dry season streamflow of the principal river, the Rio Santa. As the glaciers continue to recede, dependence on groundwater will increase both at the basin-wide scale and across individual proglacial catchments. Small-scale farmers, villages and cities that lie directly downstream of larger pampa aquifer systems will benefit from the buffering effects of groundwater to water losses caused by glacial melt.

To compliment the aforementioned investigations into tropical alpine hydrogeology, hydrology, and water resources, this dissertation also focuses on the effects of anthropogenic climate change in the Northern Hemisphere in the mid-latitude region of New York State. Because the state is so diverse in topography and land cover, we conduct a state-wide statistical analysis of streamflow from 1961 to 2016 that incorporates consideration of soil thickness, land cover, and water regulation across six spatial clusters that span New York State and adjacent areas. By incorporating the full spectrum of low, median, and high flows in the analysis, changes in specific flow regimes can be associated with seasonal precipitation and temperature changes. Change points, or temporal shifts in the long term mean of the series, are identified for both streamflow and precipitation, and the timing of those change points shows coincidence between summer precipitation and low flows, as well as post-drought increases in summer and winter precipitation in the early 1970s and 2000s. The early 1970s also saw an increase in peak flow frequency throughout the state of NY, which marked the beginning of an extended wet period that continues to the present day.

Long-term trends were detected in January streamflow and the winter-spring center of volume (WSCOV), which is a measure of volumetric streamflow timing in the winter and spring months. These trends will likely continue into the future as winters are projected to have more precipitation as rain and warmer temperatures, although winter temperatures may fluctuate more widely due to a shift in the Arctic polar vortex that cause colder temperatures in parts of North America. This study provides insight into the regional responses to changes in precipitation and temperature across New York State, providing a base study for future hydrologic predictions that include a warmer and wetter Northeastern US.

Surface water and groundwater in a changing climate: applications of hydrogeophysics and trend analysis to understand hydrologic systems

by

Robin Lee Glas

B.S., University of Maine, 2002
M.S., University of Southern Maine, 2008

Dissertation

Submitted in partial fulfillment of the requirements for the degree of

Doctor of Philosophy in Earth Sciences.

Syracuse University

June 2018

Acknowledgements

I'd like to thank my advisor, Dr. Laura Lautz, for supporting me and allowing me to creatively explore new questions and research methods. Without her unwavering trust and encouragement, this dissertation would not have been possible. Thank you to Drs. Don Siegel, Christa Kelleher, Jeffrey McKenzie, and Robert Moucha for serving on my dissertation committee. I'd like to acknowledge our research team in Peru, including Drs. Bryan Mark, Jeffrey McKenzie, Michel Baraer, Rob Hellstrom, and Ryan Gordon. This field work was completed with the help of Emily Baker, Lauren Somers, Pierric LaMontaigne, and Caroline Aubry-Wake. The field work was also made possible by Dr. John Lane and Dr. Martin Briggs, along with Eric White and Carole Johnson at the US Geological Survey branch of Hydrogeophysics. Further thanks goes to my mentor at the USGS New York State Water Science Center, Dr. Douglas Burns. The support of my family has been essential for my success, including my husband, Hamza Khalil and my parents, Bob and Dee Glas, as well as my brother, Dylan. I'd like to thank my friends Sally Curran and Tyler Slyker for further support through music, and Patty Ames in Huaraz, Peru for her hospitality between our excursions to the field. Thank you to Dr. Zeno Levy for guidance in figure design, and to Dr. W. Stephen Holbrook for geophysical mentoring and training.

Special thanks to the Syracuse University Education Model Program on Water-Energy Research (DGE-1449617), the National Science Foundation (EAR-1316429), Syracuse University Water Fellowship, the Geological Society of America Student Research Grant, and the K. Douglas Nelson Memorial Fund through the Syracuse University Department of Earth Sciences, for financial support of this work.

Table of Contents

List of Tables

Chapter 1

Chapter 2

Chapter 3

List of Figures

Chapter 1

Chapter 2

Chapter 3

Chapter 1

Aquifer Structure, Formation, and Groundwater Storage in Tropical Glaciated Catchments

Abstract

As glaciers continue to lose mass in the tropics, dry season water supplies for downstream communities will continue to decline. The world's largest concentration of tropical glaciers lies in the Cordillera Blanca range of the Peruvian Andes, where glacial runoff is declining and regional stresses are emerging over water resources. Throughout the Cordillera Blanca, groundwater inputs from alpine meadow- talus complexes, known as pampas, supply proglacial streams with up to 80% of their flow during the driest months of the year. Structural knowledge of the pampa aquifers is needed to estimate their total groundwater storage capacity and residence time, which are necessary estimates for future predictions of dry season streamflow. To address this, we used multiple near-surface geophysical methods in a prototypical proglacial valley near dense networks of spring- fed tributaries, in conjunction with existing borehole information. Our geophysical models suggest groundwater is stored in a confined aquifer composed of buried talus deposits overlain by lacustrine clay, while deeper portions of the unit, 10 to 15 m in depth, are relatively clay-free and more hydraulically conductive. Based on these findings, we estimate that the pampas of the Callejon de Huaylas have a maximum storage capacity of 0.2 to 0.6 km^3. Furthermore, our findings suggest that the talus aquifers of the Cordillera Blanca were formed in proglacial lakes, followed by infilling of the talus with fine lacustrine sediments that confine lower units and allow for groundwater discharge to springs via macropores and preferential flow.

1. Introduction

Mountain regions have been referred to as global 'water towers' because they supply a disproportionate share of freshwater to downstream populations, particularly in arid to semi-arid regions (Viviroli et al., 2007). In the tropics, mountain glaciers are especially sensitive to

warming because they exist near temperatures associated with melting conditions (Vuille et al., 2008), and compared with the mid- to higher latitudes, the tropics have been relatively understudied in terms of hydrologic processes that contribute to regional water resources. Warming in tropical zones around the globe is projected to surpass 4°C by the year 2100 at elevations higher than 4000 masl using the emissions scenario A2, which would result in a significant regional decline in ice mass (Bradley et al., 2006, Vuille et al., 2018). More than 99% of the world's tropical glaciers lie in the Andes Mountains, which divide the inner (continuous annual precipitation) from outer (seasonal precipitation) tropical zones (Kaser, 2001). Rivers and streams of the outer tropics that originate in the Peruvian Andes and drain to the arid Pacific coast are at risk for reduced flow, particularly during the dry season, due to accelerated glacial loss (Michel Baraer et al., 2012; Huss et al., 2017).

The Cordillera Blanca of northwestern Peru contains a quarter of the world's tropical glaciers, which supply meltwater to the downstream Santa River basin during the driest months of the year. The Santa River drains the western side of the Cordillera Blanca range, and is the primary water source for vast agricultural and industrial operations in the region, as well as hydroelectric power generation for approximately 10% of the country (Bury et al., 2013). Dry season flow rates in the Santa River watershed are projected to further decline with the retreat and ultimate loss of glacial melt as a source of flow to the river's headwater streams (Juen et al., 2007). Climate change in the Cordillera Blanca is driving the region's loss of glaciers (Schauwecker et al., 2014), with increasing temperature trends of 0.13°C/decade since the 1950s recorded for the tropical Andes (Vuille et al., 2015). As the glaciers retreat at accelerated rates (Burns & Nolin, 2014), groundwater will increasingly be a dominant source of flow during the dry season (Baraer et al., 2015).

During the dry months of May through October, over a quarter of a million people along the Santa River depend on a combination of glacial meltwater and alpine groundwater to supply streamflow (Mark et al., 2010). Although the glacial melt contribution to dry season streamflow for the Santa River is well documented (Baraer et al., 2009, 2012, 2015; Mark & Mckenzie, 2007; Mark et al., 2005; Pouyaud et al., 2005), the groundwater system that supplies the region's alpine tributaries has not been fully characterized (Baraer et al., 2009, 2015; Chavez, 2013; Gordon et al., 2015; Maharaj, 2011; Somers et al., 2016). Studies of groundwater hydrology in the Cordillera Blanca have reported a significant contribution of groundwater to proglacial streams during the dry season, and have inferred the aquifer structure of headwater valley aquifers based on groundwater chemistry and borehole logs from shallow wells (Chavez, 2013; Gordon et al., 2015). To predict the role of groundwater in sustaining streamflow during future dry seasons, estimates of total groundwater storage and residence time distributions are required. Such predictions require structural knowledge of the proglacial sediments and alpine slope deposits that are hypothesized to serve as the region's headwater aquifers.

Worldwide, glaciated alpine catchments contain slope deposits such as talus cones, debris fans, and moraines that are important landscape features that store groundwater and provide stream baseflow. Despite their importance, these features are relatively understudied in the tropics (Caballero, et al., 2002). Studies of the structure and aquifer function of slope deposits are generally restricted to the mid- latitudes of the Northern hemisphere (e.g. Clow et al., 2003; McClymont et al., 2010), where talus slopes, moraines, and debris fans are shown to recharge with precipitation and/ or snowmelt, and delay discharge to proglacial valley streams.

Slope deposits have been hypothesized as major components of the groundwater system of the Cordillera Blanca (Baraer et al., 2015; Chavez, 2013; Gordon et al., 2015; Maharaj, 2011).

Current conceptual models based on hydrochemistry, ground penetrating radar, borehole data, and dilution tracing experiments, all concur that permeable talus deposits exposed at the edges of proglacial headwater valleys are likely areas of aquifer recharge. These conceptual models hypothesize that buried talus supports the primary aquifer in proglacial valleys of the Cordillera Blanca, where these aquifers are confined by lacustrine sediments at the surface and transit time is long enough to sustain dry season flow.

To test the current conceptual models of groundwater recharge and discharge, this study provides the first structural classification of an aquifer in a representative valley of the Cordillera Blanca by using multiple near-surface geophysical methods integrated with previous borehole data. Near-surface geophysical methods are useful when studying the hydrogeology of remote alpine catchments where scant hydrologic data exist and deeper boreholes and road access are not feasible. Our study integrates results from both seismic (refraction and passive H/V) and electrical (1D and 2D resistivity) geophysical methods with current knowledge of geomorphology and hydrology to conceptualize changes in sediment and soil matrix with depth. We conclude with a refined conceptual model of the geomorphic evolution of glaciated valleys of the Cordillera Blanca, and of the sequential sediment deposition that created confined aquifers in headwater valleys that support groundwater storage and discharge to tributaries of the Santa River during the dry season.

2. Site Description

2.1 Callejon de Huaylas and Proglacial Valleys

The Cordillera Blanca lies between 8.5° and 10° S latitude and is Peru's highest mountain range (Kaser, & Georges, 1999). The majority of glacierized area of the Cordillera Blanca drains westward to the Santa River, which flows toward the northwest and eventually to the Pacific Ocean (Mark et al., 2005). Among Peru's rivers that drain to the Pacific, the Santa River is the second largest in discharge volume, and flows the most regularly throughout the year's wet and dry seasons (Mark & Seltzer, 2003). During the dry season, sources of discharge to the Santa River include runoff from the non-glaciated Cordillera Negra to the west, and glacial runoff with groundwater inputs from the Cordillera Blanca to the east (Mark et al., 2005). The upper portion of the Santa River watershed, known as the Callejon de Huaylas, contains the Cordillera Blanca and has a spatial extent of 4900 km^2. Within the Callejon de Huaylas, most of the glaciated peaks and corresponding watersheds lie within the boundary of Huascaran National Park (Figure 1).

The bedrock composition of the Cordillera Blanca consists of the Chicama Formation, a meta-sedimentary unit dominated by Jurassic Phyllites, which was intruded by a Neogene granodiorite batholith in the late Miocene (Giovanni et al., 2010). Valleys in the southern Cordillera Blanca reveal more exposed Chicama bedrock, and as a result tend to be wider and more expansive than the valleys to the north, which are predominately underlain by granodiorite. Northern and central valleys in the Cordillera Blanca have higher, steeper bedrock walls and relatively narrow valley widths, with greater proportions of glaciated catchment area (Baraer et al., 2015).

Typical proglacial valleys in the Cordillera Blanca consist of alpine meadows (called "pampas") that occur as wetlands and grasslands. The pampas are heavily grazed by livestock and are largely saturated throughout the wet and dry seasons (Polk, 2016). In the pampas, talus slopes and other lateral debris deposits line the valley walls, providing likely flow paths for wet

season-derived precipitation to recharge underlying aquifers, according to hydrochemical evidence in surface water samples (Baraer et al., 2015).

Throughout the Cordillera Blanca, pampas are punctuated by cross- valley moraines and landslide debris deposits that once dammed large proglacial lakes that have since filled in with fine-grained sediments (Rodbell & Seltzer, 2000). The last glacial maximum in this area was likely between 21 and 34 ka, with rapid glacial retreat underway by 16 ka (Farber et al., 2005) . These lakes infilled with lacustrine clays, silts, and sands beginning 12 ka (Glasser et al., 2009) leading to the terrestrialization of the lake environments. In the wetland- dominated pampas, the lake sediments are overlain by a thin (< 0.2 m) layer of peaty organic soil (Chavez, 2013; Maharaj, 2011). Networks of perennial and ephemeral springs emanate from the toes of lateral talus and debris deposits, as well as from mid-valley points. Spring water forms tributaries that flow into the valley stream and are the primary connection between the streams and the groundwater as evidenced by tracer experiments in the Quilcayhuanca Valley (Gordon et al., 2015; Somers et al., 2016)

2.2 Quilcayhuanca hydrogeomorphology

The Quilcayhuanca pampa is considered to feature prototypical geomorphology of the central and northern valleys of the Cordillera Blanca (Gordon et al., 2015). The Quilcayhuanca valley contains roughly 4 km^2 of pampa area, which can be considered the maximum potential spatial extent of a valley aquifer that contributes discharge to perennial springs, and ultimately to the Quilcay stream. Lower portions of the steep (>80°) bedrock slopes are covered by large talus deposits, which form a gentler slope of 20- 35° (Figure 2; slope A.), then transition to colluvial deposits on lower slopes of 10 to 20° (Figure 2; slope B) toward the valley center. The colluvial slope B intersects with the organic- and clay-rich pampa floor, which slopes gently up-valley

toward the glacier at angles less than 10°. Slopes A and B are infilled with loose, dry soils and are lightly vegetated with shrubs, grasses, and small alpine trees, whereas portions of the talus deposits higher in elevations are free of soil infilling.

Boreholes were drilled in the Quilcayhuanca pampa in 2012 and 2013 and completed as seven piezometers screened in the coarse sediments at the depth of refusal (Figure 3, Chavez, 2013). Borehole data from the Quilcayhuanca pampa valley floor show shallow sediments largely dominated by lacustrine silty clays and small amounts of fine sand with little to no coarse fragments. The maximum borehole depth is limited to approximately 7 m due to refusal at greater depths, where there are boulders ranging from 10 cm to 1 m in diameter, accompanied by small amounts of gravel and sand. The boulders are largely composed of granodiorite and andesite, with a small number originating from the metasedimentary Chicama formation (Chavez, 2013).

Positive pressure head exists in all seven piezometer boreholes, with one artesian well (GW2) that had to be permanently sealed to terminate water loss. During both the wet and dry season, the hydraulic gradient across the well transect (GW7- GW1-GW5-GW6) slopes toward the mid-valley stream, with the highest intra-annual head fluctuations in GW7, the piezometer located closest to the valley wall (Figure 3).

According to the most recent conceptual models, the interaction of slope deposits with lacustrine and glacial sediments in proglacial headwater catchments creates the conditions for aquifer storage of wet season precipitation, followed by sustained base flow throughout the Cordillera Blanca during the dry season (e.g. Baraer et al., 2015). Although the relative groundwater contribution to the Quilcay stream has been estimated at varying scales (Baraer et

al., 2015; Somers et al., 2016), the hydrogeology leading to these types of conditions has only been examined by point measurements in boreholes.

3. Methodology

In this study, we used four types of surface- based geophysical methods with existing well data (drill logs, piezometric head data, groundwater chemistry) to constrain the extent of buried colluvium, as well as its depth, sediment matrix composition, and valley bedrock depth in the Quilcayhuanca pampa. Geoelectrical and seismic methods are complementary and ideal for this study because these methods respond to differing physical properties of the subsurface and when used in conjunction, can diminish interpretive uncertainty associated with the methods when used in isolation (Cardarelli et al., 2010). Below, we review the field and analysis procedures for each geophysical survey conducted in the austral winters of 2015 and 2016.

3.1 Seismic refraction tomography

Two dimensional seismic refraction tomography consists of generating a 2D subsurface model of p-wave velocity distribution based on the timing of active energy sources (shots) received along a line of regularly spaced geophones. The geophones detect the arrival time of the refracted wavefront, and are used to generate a subsurface cross-sectional model of p-wave velocity distribution. Velocity models are produced iteratively by solving an inverse problem where infinite combinations of subsurface velocity distributions can lead to the same p-wave arrival times at the geophones. For this reason, a priori smoothing constraints are introduced, which provide limits to the solution space and allow the model to converge. Convergence is reached by minimizing differences between observed and synthetic arrival times, and resulting p-wave velocities in the final inverse model can be correlated to hydrogeologic structure based on ground-truthing and rock physics models. Seismic p-wave velocity is sensitive to hydrogeologic

properties such as lithology, porosity, density, and saturation of the subsurface media, where sediments with low porosity and high saturation propagate p-waves at higher speeds, as do more consolidated and crystalline materials (Haeni, 1986).

We conducted two seismic refraction surveys in the Quilcayhuanca pampa in July of 2015, targeting the interface between bedrock and unconsolidated valley sediments, as well as changes in sediment composition with depth. Seismic refraction surveys Q1 and Q7 (Figure 2) were performed to investigate changes in p-wave (acoustic) velocity with depth along the piezometer transect spanning the pampa floor (Figure 2b). We deployed 48 vertical component geophones spaced at 2.5 m along two parallel lines Q1 and Q7, for a total length in each survey of 117.5 m. The survey lines spanned the transition between the relatively flat pampa bottom and sloping hillside composed of colluvium and loose, dry soils (slope B). Signals were processed using two Geode exploration seismographs from Geometrics, Inc., with the accompanying Seisimager/2DTM software suite for in-field monitoring of data quality. To increase the signal- to- noise ratio, 8 to 10 shots were stacked (averaged) using a 6 kg sledgehammer striking a 2 cm thick, circular (30 cm diameter) stainless steel plate at 12 locations along each line.

The first arrival times were processed using Geogiga's DWTomo software, which employs ray tracing, also known as the "shortest path" method (Moser, 1991) in the forward modeling step. The forward model is a synthetic data set of p-wave arrival times generated from a predefined model of subsurface velocity. The calculated arrival times are compared with those observed in the field, and the subsurface velocity structure is updated using a regularized inversion with smoothing constraints. The model domain consists of gridded cells with dimensions of 0.625 m by 1.25 m (horizontal by vertical) for each model cell. The smoothing

(regularization) constraints allow the user to define the degree of heterogeneity desired in the final model. Smoothing lengths in the x and z directions were set to minimize artifacts and overfitting, while maintaining enough structure to resolve changes in lithology and/or saturation with depth. Under the assumption that the subsurface consists of horizontal or near- horizontal lacustrine sedimentary deposits, 5.0 m horizontal and 1.3 m vertical smoothing constraints were selected for the final model runs. Iterations of forward and inverse modeling were carried out until the difference between observed and synthetic travel times were minimized.

To characterize uncertainties in the inverted model, a sensitivity analysis was used to determine regions of the 2D tomogram that were dependent more on the data than the assigned starting model. To do this, we carried out 22 separate inversions using distinct starting models that encompass reasonable assumptions about the subsurface p-wave velocity distribution. The starting models consisted of a surface velocity that ranged from 500 to 1500 m/s, gradationally increasing downward toward a bedrock velocity of 5000 m/s. The depth to bedrock in the starting models was varied from 10 m to 60 m in depth. If model cells exhibit little variability despite diverse starting model structures, they can be considered sensitive to the data and reliable for interpretation. For each model cell, the coefficient of variation (CV) was calculated by dividing the standard deviation of the 22 resulting velocities in each cell by their mean.

3.2 Seismic horizontal to vertical spectral ratio

The horizontal to vertical spectral ratio (HVSR) technique is a passive seismic method (i.e. no active source such as a hammer is used) in which directional (north-south, east-west, up-down) components of ambient seismic noise are recorded in time series by a single station seismometer. The ratio of the horizontal to vertical frequency spectra are used to determine resonance frequencies of the underlying sediment, which varies with total sediment thickness

under certain physical conditions (Nakamura, 1989). HVSR methods are widely used in hydrogeology to characterize sediment thickness (e.g. Briggs et al., 2016; Sauret et al., 2015), given that the unconsolidated overburden and underlying bedrock interface contrast in acoustic velocity by a factor of 2 or more (Lermo & Chavez-Garcia, 1994). We conducted six HVSR surveys in the Quilcayhuanca valley in August of 2016 using a Tromino® (MoHo s.r.l.) multicomponent seismic recorder with acquisition lengths ranging from 15 to 45 min and sampling rate of 128 Hz. Irregularly spaced, the locations of the HVSR survey points were determined by quality of coupling to the ground surface, and reasonable shielding from nearby livestock and high sustained winds. The data were processed using the software capabilities of Grilla (Tromino®) and Geopsy, which was developed as a part of the larger SESAME European Project (http://sesame.geopsy.org/). After manually filtering out transient signals and applying 20-second windows to the time series, each windowed component was transformed to Fourier amplitudes, and the ratio of the horizontal to vertical amplitudes were calculated and averaged.

3. 3 Electrical resistivity tomography and vertical electrical soundings

We conducted seven 2D ERT surveys in August of 2016 in the Quilcayhuanca pampa to complement information from the seismic surveys, targeting the shallow confined aquifer structure of the pampa. Geoelectrical methods are among the most widely used geophysical methods for hydrogeological characterization because they are robust and sensitive to changes in subsurface saturation, lithology, and clay content (e.g. Parsekian et al., 2015 and references therein). Higher degrees of saturation, along with clay content and smaller grain sizes contribute to a more electrically conductive subsurface, whereas larger fragments, crystalline rocks, and voids lead to higher resistivity. Electrical resistivity tomography surveys (ERT) and vertical electrical soundings (VES) provide information about the subsurface electrical conductivity

structure and are considered complimentary to seismic methods, which provide information about elastic properties (Draebing, 2016).

Using Supersting R1/IP instrumentation (Advanced Geosciences, Inc.), we collected ERT data with 28 stainless steel electrodes placed at 6 m intervals for lines E1- E6 ("deep" surveys), as well as a single 3 m spacing roll- along survey (RA1, "shallow") that doubles over line E1, resulting in transect lengths of 162 m and 144 m, respectively (Table 1). A roll- along survey is a way to overlap data from consecutive lines to increase survey length, but not depth of investigation, and was selected to cover the length of line E1. The roll-along survey data were merged with the deeper E1 survey to improve data density across the piezometer transect, and the merged data were inverted and are presented here as model E1*. To ensure low contact resistance between electrodes placed in the ground, electrode locations were watered with a saline solution until contact resistance test readings were well under 4000 Ω, allowing the current to sufficiently flow into the subsurface. ERT surveys did not extend onto slope B due to very dry porous soil conditions, which resulted in poor contact resistance. Instead, all seven ERT surveys were conducted on the flat pampa sediment surface. DC current was injected with 1.2 s signal pulse duration using a dipole- dipole electrode configuration, where the current source/ receiver (A, B) and potential (M,N) electrode pairs are coupled adjacent to one another. The dipole- dipole array was chosen for this study to maximize the depth of investigation; it provided a maximum density of data points without compromising battery duration. The assignment and switching of dipole pair (source and receiver) combinations was automated by Supersting switch box. Two measurements were stacked for each source- receiver combination and averaged in with a third measurement if the first two differed by more than 2%. The apparent resistivity values obtained in the field were inverted using the smooth model inversion from Earthimager

2D software (Advanced Geosciences, Inc.). A smoothing multiplier of 10 was used as a constraint on the ERT inversions. This is a Lagrange multiplier in the objective function that determines the degree of roughness in the model, a value of 10 being the recommended setting for surface data (Advanced Geosciences, Inc., 2009). Model convergence criteria were set such that differences between measured and calculated resistivity values exhibit root mean square errors less than 10% and L2- norm least squares measure is less than 1.

The Depth of Investigation (DOI) indexing method (Oldenburg and Li, 1999) was used to determine the depth below which the 2D resistivity model is no longer highly influenced by the data. This was achieved by performing each inversion with two divergent, homogeneous half-space starting models and computing the normalized difference between the two resistivity values for each model cell. Model cells resulting in a DOI index greater than 0.1 were not plotted for interpretation.

3.4 Vertical electrical soundings

One dimensional VES methods are among the oldest and simplest geoelectrical methods in use, and can be advantageous in alpine environments where access is limited and deep probing of the subsurface structure is desired (Bechtel & Goldscheider, 2017). Although VES only provides models of resistivity in the vertical direction without consideration of 2 or 3 dimensional influences and anomalies, the method was chosen for this study because the maximum separation allowable by the VES cables increases the depth of investigation from the shorter 2D ERT surveys. Because VES requires the assumption that the subsurface consists of horizontal homogeneous layers, resulting models should reveal the simplest resistivity structure possible and can be presented as resistivity and depth ranges, as opposed to detailed models of subsurface electrical structure (Kneisel, 2004). For this study, six VES soundings were

performed on the center of each ERT line using a Schlumberger array, where the current injection and receiver electrodes (electrodes A, B) were placed on either side of the voltage (potential) electrodes M and N. The maximum AB electrode separation varied from 150 to 300 m, depending on the length of accessible terrain in the study area (Table 2). Theoretically, the depth of investigation for each sounding depends on the maximum electrode separation and the conductivity of the subsurface. In this case, our maximum DOI for an AB separation of 300 m is between 30 and 90 meters, although these depths can be reduced with lower ground resistivity and decreased signal strength (Edwards, 1977).

Each sounding was conducted by manually relocating the source and receiver electrodes after each measurement to a spacing that varied logarithmically from 2 m to the maximum available separation distance, consisting of up to 18 manual data collection points. When the inner potential electrodes (M and N) were repositioned to wider spacing, repeat measurements were taken at the previous and new MN locations to account for data offset. The VES apparent resistivity data were inverted using Earthimager 1D software (Advanced Geosciences, Inc.), which employs a damped least squares method to construct a layered resistivity model, where the number of layers were minimized according to data fit.

4. Results

4.1 Seismic Refraction Tomography

Picked first arrivals were generally limited to geophones overlying slope B, as the organic- rich, saturated sediments of the pampa floor resulted in lower signal-to-noise ratios by signal attenuation (Supplemental figure S1a, S1b). Because the majority of noise in each seismogram was caused by higher frequency wind, a combination of low pass and band pass filters were used to identify and manually pick the first arrivals for each channel. Using the

principle of reciprocity, which states that p-wave travel times are equivalent upon the interchange of point source and receiver positions (Zelt & Smith, 1992), the average reciprocal pick error was 1 ms for line Q1 and 3 ms for line Q7.

Results from the starting model sensitivity analysis show large variations in the portions of the model that are deeper and closer to the valley center, where signals were attenuated in the peaty organic soil (Supplemental figure S2a, S2b). In both lines Q1 and Q7, the upper 10 m varied by 10% or less, and can be considered sensitive to the data. Deeper regions of the models and those toward the center of the pampa valley were more sensitive to the starting model scenarios, and varied by 15- 35% between model sensitivity runs below depths of ~10 m. The lower regions of the model are considered unreliable, and are excluded from analysis in this study.

For the final inversions, a two layer gradational starting model was assigned for both Q1 and Q7, transitioning from 400 m/s at the surface to 2500 m/s at 10 m in depth, with a maximum depth assigned at 25 m for each model. The final Q1 model converged after 10 iterations with a fitting error of 1.97 ms, and Q7 model converged after 10 iterations with a fitting error of 3.15 ms. Two dominant seismic velocity ranges were observed under lines Q1 (Figure 4a) and Q7 (Figure 4b), with shallow areas being relatively slow (500-700 m/s) and faster velocities at depths >5 m (2000-3000 m/s). The reliability of the velocity models was considered using reconstructed seismic raypaths that connect each source to each receiver along the line (Figure 4a and 6b). Regions where many raypaths intersect are considered to be well constrained by the data (arrival times), whereas regions that lack raypaths are interpolations and were not considered for interpretation. In models Q1 and Q7, dense intersections of modeled ray paths in

the top 10 to 15 m overlap with the clay- boulder interface at depth, although piezometer GW1 extends into regions of moderate variation (5-10%, Figure 4).

The slower velocities (500- 700 m/s) that were closest to the surface toward the valley edge (Figure 4a, 6b, zone 1a) were consistent with other studies of talus slopes in North America (e.g. Brody et al., 2015), and can be associated with porous, unsaturated coarse sediments (Powers & Burton, 2012). The slope was audibly porous, producing strong reverberations after striking the sledge hammer. Because the hillslope comprised large boulder-sized clasts (0.5 - 2 m in diameter) that were partially exposed above dry soil, we interpret the slow velocities in zone 1a to correspond to unsaturated, highly porous colluvial deposits. At the base of the slope, similar velocities were observed in the partially saturated, organic and clay-rich sediments (Figure 4a, 6b; zone 1), which were devoid of any fragments or clasts (Chavez, 2013). Slow velocities in zone 1 appear to correspond to both slope B and to the fine-grained, variably saturated lacustrine sediments immediately underlying the pampa valley floor.

At depths of 5 to 10 m, the 1300 m/s iso-velocity contour (Figure 4c, 6d) corresponds to depths where boulders were encountered in the boreholes (Chavez, 2013). Below this line, the faster seismic velocities (2000 to 3000 m/s) are consistent with more compact, dense, and/or saturated media, likely reflecting the top of a buried, clast-supported body of talus with a higher overall seismic velocity. The vertical change in seismic velocity was plotted for each column of model cells, showing a step- increase in p-wave velocity with depth, rather than a gradational increase (Figure 4c, 6d). The transition to faster seismic velocities occurs 5 to 10 meters beneath the surface, and borehole observations above this transition at GW 7 are absent of any clasts or fragments. These lines of evidence indicate that zone 1 is a laterally continuous unit of fine-grained lacustrine sediments lying beneath the colluvial slope (zone 1a), and that the refracting

interface that corresponds to 1300 m/s does not appear to be a subsurface extension of slope B (Figure 4a; zone 1).

4.2 Electrical resistivity tomography

Using a starting model of the average apparent resistivity in each line, all 6 electrical resistivity tomography (ERT) models converged within 1 to 5 iterations with a root mean squared (RMS) error between predicted and measured data less than 5%, and normalized L2-norm values below 0.3 (Supplemental Table 1). The normalized L2- norm is a measure of data misfit, as the squared difference of weighted errors between the synthetic and modeled data, normalized by the total number of data points. Horizontal resolution was set to half the electrode spacing, 3 m for the deep survey and 1.5 m for the shallow roll-along. Vertically, the model cell size increased from 2 meters at the surface to 4 meters at depth. Because the deeper E1 survey and the more shallow roll- along were performed on two different days that had distinct soil moisture conditions and varying contact resistance, 91 erroneous data points were removed out of a total of 1013 measurements (9% removed) before the merged inversion of E1*. Repeated measurements show little to no noisy data points on surveys E2- E6 and no data points were removed for these lines.

The depth of investigation of the 2D resistivity surveys limits interpretation to the top ~20 m of sediment. Models of subsurface resistivity across the pampa floor indicate a region of varying resistivity (100 to 300 Ωm) in the shallow pampa subsurface (Figure 5a; zone 1), where lacustrine clays and silts were encountered during drilling and p-wave velocities are relatively slow. The upper, more electrically conductive (Figure 5a, zones 1 and 2, 50 to 300 Ωm) portion of the pampa subsurface transitions to a higher resistivity zone (Figure 5a, zone 3, 300 to 650

Ωm) at 10 to 15 m depth. Zones 1, 2 and 3 are present in all six ERT lines and show spatial continuity (Figure 5b), suggesting variable layer thicknesses and moisture content.

4.3 Vertical electrical soundings

All 1D resistivity profiles converged with less than 5% RMS data misfit between observed and modeled values, with the exception of V3, which converged with approximately 10% misfit (Supplemental Table 2, Supplemental Figure S3). The VES profiles are consistent with the ERT sections (Figure 6), showing: (1) high and variable resistivity (up to 1000 Ωm) at the shallowest depths of less than 5 m (zone 1); (2) lower resistivity (50 to 200 Ωm) at depths of 5 to 10 m (zone 2); and (3) higher resistivity (300- 600 Ωm) in regions deeper than 10 m (zone 3). All VES profiles show that the resistivity subsequently decreases at depths of 18 to 35 m below land surface (Figure 6; zone 4).

4.4 Horizontal-to-vertical spectral ratio

Clear resonance frequency peaks were found for all six HVSR survey points, ranging from 1.82 to 3.73 Hz (Figure 7b). The peak and trough shape of the resonance frequency curves indicate a high acoustic impedance contrast of the underlying material, likely due to a competent bedrock- sediment interface (Seht & Wohlenberg, 1999). When the depth to bedrock is unknown, overlying shear wave velocities of the unconsolidated sediment can be used to calculate overall sediment thickness (Johnson & Lane, 2016). Resonance frequencies calculated for each point of measurement in the pampa were converted to a range of likely bedrock depths, according to Equation (1).

$$Z = \frac{Vs}{4\,F_0} \qquad (1)$$

Where Z is the depth (m) from the land surface to the bedrock or other competent surface, V_s is the average shear wave velocity structure (ms^{-1}) of the overlying sediment column, and F_0 is the H/V resonance frequency (s^{-1}).

5. Discussion

Integrating the results from four geophysical methods along with borehole data, we present a refinement of Quilcayhuanca's conceptualized sediment structure and composition, and hypothesize possible stages in pampa evolution that have led to current conditions. This study presents the first use of multiple, integrated near-surface geophysical methods to characterize slope deposit and aquifer structure in tropical proglacial catchments. We add to the growing body of knowledge of the importance of high alpine slope deposits in the retention and delayed release of groundwater, the majority of studies having taken place in the mid- latitudes of the Northern Hemisphere.

5.1 Sediment composition and aquifer structure

Proglacial depositional environments generally exhibit a high degree of spatial complexity (Carrivick et al., 2013), however the pampas of the Cordillera Blanca contain organized structure due to their lacustrine origin. In the Quilcayhuanca pampa, as well as in other pampas of the range, a relatively thin (<.5 m) organic- rich layer of soil overlies a thicker (> 10 m) lacustrine clay aquitard (Chavez, 2013; Maharaj, 2011). Variable resistivity values (10-300 Ωm) in the uppermost 5 meters of sediment, which are dominated by lacustrine clays, are likely attributed to variable saturation and/or composition. The variability in this layer can be explained by unsaturated pore spaces and the presence of sand particles, which would contribute

to elevated resistivity readings from the background conductive clays (Samouëlian et al., 2005). Some of this more resistive material could be from portions of the clay permeated by macropore pathways that are either filled with sand particles or relatively lower amounts of saturated clay particles.

Prior work indicates the springs that emerge at the interface of the talus slope and the pampa floor are chemically distinct from glacial meltwater, sharing more hydrochemical properties with springs toward the center of the valley (Baraer et al., 2015) . These springs are likely connected to the talus aquifer via preferential flow pathways in the clay structure of the aquitard, which allow overpressured groundwater to discharge to the land surface (Dekker & Ritsema, 1996; Kurtzmane et al., 2016). Because these pathways hypothetically have lower levels of clay than their surroundings, they are reflected in the ERT surveys as resistivity values slightly higher (200 to 300 Ωm) than the surrounding lacustrine clays (50 to 200 Ωm in zone 2). The locations of springs and the tributaries they feed remained largely unchanged interannually, suggesting that the preferential flow pathways that lead to those tributary positions are also perennial.

Borehole observations show presence of crystalline boulders at depths with low resistivity (50 to 200 Ωm) in our sections, but the presence of large crystalline rock fragments are typically associated with higher resistivity values, depending on the extent of saturated fractures and weathering within the clasts (Loke, 2000; Samouëlian et al., 2005). The low resistivity in the presence of boulders in Zone 2 indicate that the sediments infilling the talus is saturated and clay-rich. The small grain size and conductive electrical properties of clay along with saturated pore spaces can mask a more resistive signal from large igneous rock fragments (Abu-Hassanein et al., 1996). This suggests that, in the dry season, moisture content and saturation are variable

near the pampa surface, but full saturation occurs at depths corresponding to the overpressured buried talus.

Lateral talus slopes line the Quilcayhuanca valley continuously and consist of boulders (.2 – 1 m in diameter) derived from the source rocks of the overlying cliffs, which are primarily granodiorite and metasedimentary (Chavez, 2013). In Quilcayhuanca and other northern and central valleys of the range, the talus slopes are incident on the pampa floor at an angle of 20-35° and buried beneath the less permeable lacustrine sediments. The top of the buried talus unit coincides with the 1300 m/s p-wave velocity contour, and this interface extends continuously eastward and upward toward the valley edge. The buried unit, therefore, is likely connected to an exposed portion of talus near the valley wall, recharging groundwater to deeper confined sediments during times of precipitation.

The uppermost portions of the buried talus at depths of 2 to 10 meters are infilled with saturated clay, contributing to a low (10- 100 Ωm) bulk resistivity (zone 2). The region of higher resistivity (zone 3) is interpreted to be a continuation of the buried talus deposit at depth, but infilled with a clay-poor matrix due to limited infiltration of lake bottom sediments into the talus material at the time of deposition. The lack of clay in deeper portions of the talus deposit suggests that pampa sediments are more permeable between depths of 10 to 25 m, contribute to a higher hydraulic conductivity, and form the productive aquifer storage volume. An alternative hypothesis for the increase in resistivity at depths of 10 to 15 m is that this boundary is the top of intact or weathered bedrock, rather than unconsolidated material. To further explore this possibility, bedrock depth ranges were estimated from the HVSR results using Equation (1), which requires the measure of shear wave velocity in the overlying sediment.

As more information is needed regarding the average shear wave velocity structure of the unconsolidated sediment, first estimates were made to begin to constrain the overall sediment thickness. Typical lacustrine clays and gravels have exhibited Vs ranges of 200- 500 m/s in published studies (Heureux & Long, 2016; Jongmans et al., 2009). The presence of a clast supported talus body should increase these averages because rock material has a high stiffness and contributes to higher shear wave velocities of over 800 m/s (Brocher, 2005). Given that the measured H/V resonance frequencies ranged from 2 to 4 Hz, and assuming a Vs structure that ranges from 300 to 600 m/s for clays intermixed with gravel or boulder sized fragments and glacial deposits, HVSR surveys indicate the competent bedrock surface is 20 to 85 m in depth beneath the pampa (Figure 7a).

Further constraints from the VES data also suggest that zone 3 is not indicative of bedrock. These lower resistivity values (50 to 200 Ωm) in zone 4 (Figure 6) can be explained by the presence of a deeper unit composed of older lacustrine deposits or clay-rich glacial till, rather than bedrock. Thick glacial deposits above bedrock are prevalent throughout the proglacial valleys of the Cordillera Blanca upon glacial retreat (Chavez, 2013; Klimeš, 2012; López-Moreno et al., 2016) and are consistent with the drop off in resistivity at depth in the vertical electrical soundings, provided the glacial deposits contain electrically conductive material. The lower extent of the Quilcayhuanca pampa talus aquifer therefore lies at the top of zone 4, leading to an overall aquifer thickness ranging from 10 to 25 m. Further investigation into deeper sediments is needed to corroborate the lower portions of the VES models because geophysical methods used in isolation could produce artifacts and uncertainties, as well as multiple solutions for the same data set, especially with increasing depth where signal strength decreases (Barker, 1989).

5.2 Pampa formation and sediment deposition

Our results indicate that Quilcayhuanca and other pampas of the Cordillera Blanca underwent lacustrine phases in which high amounts of colluvium (talus and debris fans) were deposited on lake floors from steeply incised proglacial valley walls. We hypothesize that glacial lake infilling and deposition of fine grained lake sediments occurred over the subaqueous talus, with the lake draining slowly enough to allow for thick lacustrine clay deposition that infiltrated the upper 5 to 10 m of the talus deposit. The fine grained and relatively impermeable sediment matrix in the upper talus then continued to infill, resulting in a 2 to 8 meters of clay that is devoid of clasts or fragments in the shallowest portions.

Deeper parts of the talus deposit that were not directly exposed to the water column became a central zone of the talus structure that has a clay-poor matrix and is more hydraulically conductive (Figure 8). After the terrestrialization of the Quilcayhuanca valley lake, the accumulation of peat- rich organic soils accumulated by the process of paludification, which generally occurs over moist mineral soils and leads to conditions of poor drainage (Lavoie et al., 2005). Both peaty and peat- poor organic soils are commonly found in the pampas of the Cordillera Blanca (Polk, 2016), as are terrestrial and subaqueous talus deposits in the proglacial lakes of the range (Emmer et al., 2016; Vilímek et al., 2015) . Cordillera Blanca slope deposits submerged in proglacial lake environments are therefore the primary stage for the formation of confined aquifers upon the lakes' paludification or terrestrialization, and are likely found in other valleys of the range. Furthermore, because alpine proglacial wetlands occur globally (Jacobsen et al., 2012), talus aquifers likely influence the global hydrologic cycle by buffering interannual streamflow fluctuations caused by seasonal precipitation regimes.

Seismic velocities directly beneath slope B were similar to those found in zone 1 (500 – 700 m/s), and the sediment column directly at the toe of slope B were completely devoid of clasts. It does not appear that slope B connects with the buried talus aquifer, as these two units are separated by ~ 5 m of clay sediments. This indicates that the exposed colluvial slope at the valley edge was not deposited at the time of the buried talus layer, but rather after deposition of the organic and clay-rich sediments observed on the pampa valley floor.

5.3 Groundwater storage potential of the Cordillera Blanca

As most of the lower-elevation glaciers (< 5400 m) of the Cordillera Blanca are rapidly melting and are predicted to disappear within 2 to 3 decades (Racoviteanu et al., 2008), future dry season water shortages necessitate the quantification of total groundwater storage capacity in proglacial pampa systems that drain to the Santa River. There are approximately 64 km^2 of pampas in the Cordillera Blanca (Figure 1b.), many of which have similar geomorphology to Quilcayhuanca (Maharaj, 2011). Although proglacial geomorphology is highly variable (Ballantyne, 2002), groundwater storage volume can be estimated from first principles for areas similar to Quilcayhuanca that are surrounded by talus deposits and dense with perennial springs.

Our results suggest that confined talus aquifers underlying pampas are 10 to 25 m in thickness. If confined talus aquifers of comparable thickness underlie all 64 km^2 of pampas in the Cordillera Blanca, the total aquifer volume in the region is approximately 0.6 to 1.6 km^3. If we assume a typical porosity of coarse-grained talus deposits (30 to 40%), we can estimate that talus aquifers in pampas of the Cordillera Blanca can store from 0.2 to 0.6 km^3 of groundwater. To put this storage capacity into context, we consider the basin- wide precipitation and discharge for comparison. The outflow of the Rio Santa at the La Balsa gage, which drains the Callejon de Huaylas basin, discharges 2.8 km^3 annually (1954-1997, Mark and Seltzer, 2003). Hence, the

pampas of the Cordillera Blanca have the capacity to store between 7 and 20% of annual basin discharge, according to our estimates. Assuming an annual precipitation rate of 650 mm/year for the Callejon de Huaylas (Huaraz station, 3052 m.a.s.l., Mark & Seltzer, 2003), the pampa aquifers have the capacity to store 6-20% of annual precipitation for the basin.

In 2005, Mark et al. used a volumetric mixing model to determine that 10-20% of annual streamflow in the Cordillera Blanca comes from the glaciated catchments. It has since been found that during the dry season, 20- 80% the streamflow in these glaciated catchments is sourced as groundwater, depending upon the degree of glaciation (Baraer et al., 2015). Calculations of pampa groundwater residence time from prior work in the Yanamarey pampa (9.6766°S, 77.2707°W, Baraer et al., 2009) indicate that groundwater is stored in the pampas on the order of three months to three years. With these residence times in mind, estimates that the pampas supply 5-10% of annual streamflow in the Callejon de Huaylas appear reasonable. The pampas of the Cordillera Blanca may therefore contain primary aquifers that contribute significantly to both the dry season and annual hydrologic budget.

More work is needed to characterize the nature of deeper sediments in talus aquifers, which will improve estimates of porosity at depth. Additionally, these talus aquifers are likely intermittent in some pampas, and surveys are needed to map the occurrence of pampa talus and springs to better refine their spatial extent. Refining these parameters will allow for improved estimation of total groundwater storage capacity of the pampas, and when compared to basin discharge, will improve estimates of groundwater residence time in these aquifers.

6. Conclusion

To estimate aquifer thickness and composition in the Quilcayhuanca valley, we employed four near- surface geophysical methods, interpreted with existing borehole records. Results from seismic surveys and boreholes suggest that the top of a buried talus unit lies 2- 8 meters below the surface, and electrical surveys indicate that the shallower portion of the talus is infilled with lacustrine clay. Groundwater is likely stored beneath this layer in clay- poor talus at depth, as the bulk resistivity of the subsurface increases with depth. Groundwater likely discharges to the surface through preferential flow paths that penetrate the surficial material, forming springs that flow to the valley stream throughout the region's wet and dry seasons.

Based on this study, we estimate the maximum pampa storage capacity of the Cordillera Blanca to be between 0.2 to 0.6 km^3. When compared with basin discharge at the La Balsa gaging station and basin- wide precipitation, this estimate is consistent with pampa groundwater residence times on the order of 1-3 years. Refinement of this estimate will allow for basin- wide calculations of hydrologic processes in a region that is becoming increasingly water- stressed. Future work should be aimed at refining the storage capacity of deeper sediments and evaluating the spatial extent of buried talus aquifers that likely occur where large talus deposits intersect proglacial wetlands and grasslands, as evidenced by the presence of spring- sourced tributaries. The talus aquifers of the Cordillera Blanca represent a hydrogeologic system that relies on interactions between glacial erosion, gravitational slope deposits, and the formation and sedimentation of proglacial lakes in a tropical climate. The water from these aquifers will become the primary source of dry season discharge for the Callejon de Huaylas basin over the next few decades, when many of the glaciers of the range are predicted to disappear.

References

Abu-Hassanein, Z. S., Benson, C. H., & Blotz, L. R. (1996). Electrical Resistivity of Compacted Clays. *Journal of Geotechnical Engineering*, 122(5), 397–406. http://doi.org/10.1061/(ASCE)0733-9410(1996)122:5(397)

Ballantyne, C. K. (2002). Paraglacial geomorphology. *Quaternary Science Reviews*, 21(18–19), 1935–2017. http://doi.org/10.1016/S0277-3791(02)00005-7

Baraer, M., Mark, B. G., McKenzie, J. M., Condom, T., Bury, J., Huh, K.-I., Portocarrero, C., Gomez, J., Rathay, S. (2012). Glacier recession and water resources in Peru's Cordillera Blanca. *Journal of Glaciology*, 58(207), 134–150. http://doi.org/10.3189/2012JoG11J186

Baraer, M., Mckenzie, J. M., Mark, B. G., Bury, J., Knox, S. (2009). Characterizing contributions of glacier melt and groundwater during the dry season in a poorly gauged catchment of the Cordillera Blanca (Peru). *Advances in Geosciences*, 41–49.

Baraer, M., McKenzie, J., Mark, B. G., Gordon, R., Bury, J., Condom, T., Gomez, J., Knox, S., Fortner, S. K. (2015). Contribution of groundwater to the outflow from ungauged glacierized catchments: a multi-site study in the tropical Cordillera Blanca, Peru. *Hydrological Processes*, 29(11), 2561–2581. http://doi.org/10.1002/hyp.10386

Barker, R. D. (1989). Depth of investigation of collinear symmetrical four-electrode arrays. *Geophysics*, 54(8), 1031–1037. http://doi.org/10.1190/1.1442728

Bechtel, T. D., & Goldscheider, N. (2017). Geoelectrical Fingerprinting of Two Contrasting Ecohydrological Peatland Types in the Alps. *Wetlands*. http://doi.org/10.1007/s13157-017-0921-5

Bradley, R. S., Vuille, M., Diaz, H. F., & Vergara, W. (2006). Threats to water supplies in the tropical Andes. *Science*, 312(5781), 1755-1756.

Briggs, M. A., Lane, J. W., Snyder, C. D., White, E. A., Johnson, Z. C., Nelms, D. L., & Hitt, N. P. (2016). Shallow bedrock controls on headwater climate refugia. *Geophysical Research Letters*, 1216–1225. http://doi.org/10.1002/2013GL058951.

Brocher, T. M. (2005). Compressional and shear wave velocity versus depth in the San Francisco Bay Area, California: rules for USGS Bay Area Velocity Model 05.0. 0 (pp. 05-1317). US Geological Survey.

Brody, A. G., Pluhar, C. J., Stock, G. M., & Greenwood, W. J. (2015). Near-surface geophysical imaging of a talus deposit in Yosemite Valley, California. *Environmental & Engineering Geoscience*, 21(2), 111-127.

Burns, P., & Nolin, A. (2014). Using atmospherically-corrected Landsat imagery to measure glacier area change in the Cordillera Blanca, Peru from 1987 to 2010. *Remote Sensing of Environment*, 140, 165–178. http://doi.org/10.1016/j.rse.2013.08.026

Bury, J., Mark, B. G., Carey, M., Young, K. R., Mckenzie, J. M., Baraer, M., French, A., Polk, M. H. (2013). New Geographies of Water and Climate Change in Peru : Coupled Natural and Social Transformations in the Santa River Watershed. *Annals of the Association of American Geographers*, 103(October 2012), 363–374. http://doi.org/10.1080/00045608.2013.754665

Caballero, Y., Jomelli, V., Chevallier, P., & Ribstein, P. (2002). Hydrological characteristics of slope deposits in high tropical mountains (Cordillera Real, Bolivia). *Catena*, 47(2), 101–116. http://doi.org/10.1016/S0341-8162(01)00179-5

Cardarelli, E., Cercato, M., Cerreto, A., & Di Filippo, G. (2010). Electrical resistivity and seismic refraction tomography to detect buried cavities. *Geophysical Prospecting*, 58(4), 685-695.

Carrivick, J. L., Geilhausen, M., Warburton, J., Dickson, N. E., Carver, S. J., Evans, A. J., & Brown, L. E. (2013). Contemporary geomorphological activity throughout the proglacial area of an alpine catchment. *Geomorphology*, 188, 83-95.

Chavez, D. (2013). Groundwater potential of pampa aquifers in two glacial watersheds, Cordillera Blanca, Peru. M.Sc. Thesis, McGill University, Montreal, PQ.

Clow, D. W., Schrott, L., Webb, R., Campbell, D. H., Torizzo, a, & Dornblaser, M. (2003). Ground water occurrence and contributions to stream ow in an alpine catchment, Colorado Front Range. *Groundwater*, 41937e950(7), 937–950. http://doi.org/10.1111/j.1745-6584.2003.tb02436.x

Dekker, L. W., & Ritsema, C. J. (1996). Preferential flow paths in a water repellent clay soil with grass cover taken in close order over a distance of 195 cm at depths. *Water Resources Research*, 32(5), 1239–1249.

Draebing, D. (2016). Application of refraction seismics in alpine permafrost studies: A review. *Earth-Science Reviews*, 155, 136–152. http://doi.org/10.1016/j.earscirev.2016.02.006

Edwards, L. S. (1977). A modified pseudosection for resistivity and IP. *Geophysics*, 42(5), 1020-1036.samoue

Emmer, A., Klimeš, J., Mergili, M., Vilímek, V., & Cochachin, A. (2016). 882 lakes of the Cordillera Blanca: An inventory, classification, evolution and assessment of susceptibility

to outburst floods. *Catena*, 147, 269–279. http://doi.org/10.1016/j.catena.2016.07.032

Farber, D. L., Hancock, G. S., Finkel, R. C., & Rodbell, D. T. (2005). The age and extent of tropical alpine glaciation in the Cordillera Blanca, Peru. *Journal of Quaternary Science*, 20(7–8), 759–776. http://doi.org/10.1002/jqs.994

Giovanni, M. K., Horton, B. K., Garzione, C. N., McNulty, B., & Grove, M. (2010). Extensional basin evolution in the Cordillera Blanca, Peru: Stratigraphic and isotopic records of detachment faulting and orogenic collapse in the Andean hinterland. *Tectonics*, 29(6), 1–21. http://doi.org/10.1029/2010TC002666

Glasser, N. F., Clemmens, S., Schnabel, C., Fenton, C. R., & McHargue, L. (2009). Tropical glacier fluctuations in the Cordillera Blanca, Peru between 12.5 and 7.6 ka from cosmogenic 10-Be dating. *Quaternary Science Reviews*, 28(27–28), 3448–3458. http://doi.org/10.1016/j.quascirev.2009.10.006

Gordon, R. P., Lautz, L. K., McKenzie, J. M., Mark, B. G., Chavez, D., & Baraer, M. (2015). Sources and pathways of stream generation in tropical proglacial valleys of the Cordillera Blanca, Peru. *Journal of Hydrology*, 522, 628–644. http://doi.org/10.1016/j.jhydrol.2015.01.013

Haeni, F. P. (1986). Application of seismic refraction methods in groundwater modeling studies in New England. *Geophysics*, 51(2), 236-249

Huss, M., Bookhagen, B., Huggel, C., Jacobsen, D., Bradley, R. S., Clague, J. J., Vuille, M., Buytaert, W., Cayan, D.R., Greenwood, J., Mark, B., Milner, A., Weingartner, R., Winder, M. (2017). Toward mountains without permanent snow and ice Earth's Future. *Earth's Future*, 5(May), 418–435. http://doi.org/10.1002/eft2.207

Jongmans, D., Bievre, G., Renalier, F., Schwartz, S., Beaurez, N., & Orengo, Y. (2009). Geophysical investigation of a large landslide in glaciolacustrine clays in the Trièves area (French Alps). *Engineering Geology*, 109(1), 45-56.

Jacobsen, D., Milner, A. M., Brown, L. E., & Dangles, O. (2012). Biodiversity under threat in glacier-fed river systems. *Nature Climate Change*, 2(5), 361–364. http://doi.org/10.1038/nclimate1435

Johnson, C., & Lane, J. (2016, March). Statistical comparison of methods for estimating sediment thickness from Horizontal-to-Vertical Spectral Ratio (HVSR) seismic methods: An example from Tylerville, Connecticut, USA. In Symposium on the Application of Geophysics to Engineering and Environmental Problems 2015 (pp. 317-323). Society of Exploration Geophysicists and Environment and Engineering Geophysical Society.

Juen, I., Kaser, G., & Georges, C. (2007). Modelling observed and future runoff from a glacierized tropical catchment (Cordillera Blanca, Peru). *Global and Planetary Change*, 59(1–4), 37–48. http://doi.org/10.1016/j.gloplacha.2006.11.038

L'Heureux, J. S., & Long, M. (2016). Correlations between shear wave velocity and geotechnical parameters in Norwegian clays. In Proceedings of the 17th Nordic Geotechnical Meeting.

Kaser, G., & Georges, C. (1999). On the mass balance of low latitude glaciers with particular consideration of the Peruvian Cordillera Blanca. *Geografiska Annaler: Series A, Physical Geography*, 81(4), 643-651.

Kaser, G. (2001). Glacier-climate interaction at low latitudes. *Journal of Glaciology*, 47(157), 195-204.

Kaser, G., Juen, I., Georges, C., Gómez, J., & Tamayo, W. (2003). The impact of glaciers on the runoff and the reconstruction of mass balance history from hydrological data in the tropical Cordillera Blanca, Perú. *Journal of Hydrology*, 282(1–4), 130–144. http://doi.org/10.1016/S0022-1694(03)00259-2

Klimeš, J. (2012). Geomorphology and natural hazards of the selected glacial valleys,Cordillera Blanca, Peru. *Acta Universitatis Carolinae, Geographica*, 47(2), 25–31.

Kneisel, C. (2004). New insights into mountain permafrost occurrence and characteristics in glacier forefields at high altitude through the application of 2D resistivity imaging. *Permafrost and Periglacial Processes*, 15(3), 221-227.

Kurtzman, D., Baram, S., & Dahan, O. (2016). Soil-aquifer phenomena affecting groundwater under vertisols: A review. *Hydrology and Earth System Sciences*, 20(1), 1–12. http://doi.org/10.5194/hess-20-1-2016

Lavoie, M., Paré, D., Fenton, N., Groot, A., & Taylor, K. (2005). Paludification and management of forested peatlands in Canada: a literature review. *Environmental Reviews*, 13(2), 21-50. http://doi.org/10.1139/A05-006

Lermo, J., & Chavez-Garcia, F. J. (1994). Are microtremors useful in site response evaluation? *Bulletin of the Seismological Society of America*, 84(5), 1350–1364. http://doi.org/10.1306/080700710318

Loke, M. H. (2000). Electrical imaging surveys for environmental and engineering studies. A practical guide to 2-D and 3-D surveys, 59. http://www.georentals.co.uk/Lokenote.pdf

López-Moreno, J. I., Valero-Garcés, B., Mark, B., Condom, T., Revuelto, J., Azorín-Molina, C.,

Valero- Garces, B., Moran- Tejeda, E., Vicente- Serrano, S., Zubieta, R., Alejo-Cochachin, J. (2016). Hydrological and depositional processes associated with recent glacier recession in Yanamarey catchment, Cordillera Blanca (Peru). *Science of The Total Environment*, 579, 272–282. http://doi.org/10.1016/j.scitotenv.2016.11.107

Maharaj, L. (2011). Investigating proglacial groundwater systems in the Quilcayhuanca and Yanamarey Pampas, Cordillera Blanca, Peru. M.Sc. Thesis, McGill University, Montreal, PQ.

Mark, B. G., Bury, J., McKenzie, J. M., French, A., & Baraer, M. (2010). Climate Change and Tropical Andean Glacier Recession: Evaluating Hydrologic Changes and Livelihood Vulnerability in the Cordillera Blanca, Peru. *Annals of the Association of American Geographers*, 100(4), 794–805. http://doi.org/10.1080/00045608.2010.497369

Mark, B. G., & Mckenzie, J. M. (2007). Tracing increasing tropical Andean glacier melt with stable isotopes in water. *Environmental Science and Technology*, 41(20), 6955–6960. http://doi.org/10.1021/es071099d

Mark, B. G., McKenzie, J. M., & Gómez, J. (2005). Hydrochemical evaluation of changing glacier meltwater contribution to stream discharge: Callejon de Huaylas, Peru *Hydrological Sciences Journal*, 50(6), 975–988. http://doi.org/10.1623/hysj.2005.50.6.975

Mark, B. G., & Seltzer, G. O. (2003). Tropical glacier meltwater contribution to stream discharge: a case study in the Cordillera Blanca, Peru. *Journal of Glaciology*, 49(165), 271–281.

McClymont, a. F., Hayashi, M., Bentley, L. R., & Liard, J. (2012). Locating and characterising groundwater storage areas within an alpine watershed using time-lapse gravity, GPR and

seismic refraction methods. *Hydrological Processes*, 26(May), 1792–1804. http://doi.org/10.1002/hyp.9316

McClymont, a. F., Hayashi, M., Bentley, L. R., Muir, D., & Ernst, E. (2010). Groundwater flow and storage within an alpine meadow-talus complex. *Hydrology and Earth System Sciences*, 14, 859–872. http://doi.org/10.5194/hess-14-859-2010

Moser, T. J. (1991). Shortest path calculation of seismic rays. *Geophysics*, 56(1), 59-67.

Nakamura, Y. (1989). A method for dynamic characteristics estimation of subsurface using microtremor on the ground surface. Railway Technical Research Institute, Quarterly Reports, 30(1).

Oldenburg, D. W., & Li, Y. (1999). Estimating depth of investigation in DC resistivity and IP surveys. *Geophysics*, 64(2), 403-416.

Parsekian, A. D., Singha, K., Minsley, B. J., Holbrook, W. S., & Slater, L. (2015). Multiscale geophysical imaging of the critical zone. *Reviews of Geophysics*, 53(1), 1-26. http://doi.org/10.1002/2013RG000441.Received

Polk, M. H. (2016). "They are drying out": social-ecological consequences of glacier recession on mountain peatlands in Huascarán National Park, Peru (Doctoral dissertation).

Pouyaud, B., Zapata, M., Yerren, J., Gomez, J., Rosas, G., Suarez, W., & Ribstein, P. (2005). On the future of the water resources from glacier melting in the Cordillera Blanca, Peru. *Hydrological Sciences Journal*, 50(6), 999–1022. http://doi.org/10.1623/hysj.2005.50.6.999

Powers, M. H., & Burton, B. L. (2012). Measurement of Near-Surface Seismic Compressional Wave Velocities Using Refraction Tomography at a Proposed Construction Site on the

Presidio of Monterey, California (No. 2012-1191). US Geological Survey.

Racoviteanu, A. E., Arnaud, Y., Williams, M. W., & Ordoñez, J. (2008). Decadal changes in glacier parameters in the Cordillera Blanca, Peru, derived from remote sensing. *Journal of Glaciology*, 54(186), 499–510. http://doi.org/10.3189/002214308785836922

Rodbell, D. T., & Seltzer, G. O. (2000). Rapid Ice Margin Fluctuations during the Younger Dryas in the Tropical Andes. *Quaternary Research*, 338, 328–338. http://doi.org/10.1006/qres.2000.2177

Samouëlian, A., Cousin, I., Tabbagh, A., Bruand, A., & Richard, G. (2005). Electrical resistivity survey in soil science: a review. *Soil and Tillage Research*, 83(2), 173–193. http://doi.org/10.1016/j.still.2004.10.004

Sauret, E. S. G., Beaujean, J., Nguyen, F., Wildemeersch, S., & Brouyere, S. (2015). Characterization of superficial deposits using electrical resistivity tomography (ERT) and horizontal-to-vertical spectral ratio (HVSR) geophysical methods: A case study. *Journal of Applied Geophysics*, 121(November), 140–148. http://doi.org/http://dx.doi.org/10.1016/j.jappgeo.2015.07.012

Schauwecker, S., Rohrer, M., Acuña, D., Cochachin, A., Dávila, L., Frey, H., Giraldez, C., Gomez, J., Huggel, C., Jacques- Coper, M., Loarte, E., Salzmann, N, & Vuille, M. (2014). Climate trends and glacier retreat in the Cordillera Blanca, Peru, revisited. *Global and Planetary Change*, 119, 85-97. http://doi.org/10.1016/j.gloplacha.2014.05.005

Seht, M. I. V, & Wohlenberg, J. (1999). Microtremor Measurements Used to Map Thickness of Soft Sediments. *Bulletin of the Seismological Society of America*, 89(1), 250–259.

Somers, L., Gordon, R., McKenzie, J., Lauta, L., Wigmore, O., Glose, A., Glas, R., Aubry-Wake, C., Mark, B., Baraer, M., Condom, T. (2016). Quantifying groundwater- surface water interactions in a proglacial valley, Cordillera Blanca, Peru. *Hydrological Processes*, 2929(June), 2915–2929. http://doi.org/10.1002/hyp.10912

Vilímek, V., Klimeš, J., & Červená, L. (2015). Glacier-related landforms and glacial lakes in Huascarán National Park, Peru. *Journal of Maps*, 5647(January), 1–10. http://doi.org/10.1080/17445647.2014.1000985

Viviroli, D., Dürr, H. H., Messerli, B., Meybeck, M., & Weingartner, R. (2007). Mountains of the world, water towers for humanity: Typology, mapping, and global significance. *Water Resources Research*, 43(7).

Vuille, M., Francou, B., Wagnon, P., Juen, I., Kaser, G., Mark, B. G., & Bradley, R. S. (2008). Climate change and tropical Andean glaciers: Past, present and future. *Earth Science Reviews*, 89(3), 79-96.

Vuille, M., Franquist, E., Garreaud, R., Sven, W., Casimiro, L., & Cáceres, B. (2015). *Journal of Geophysical Research : Atmospheres*. http://doi.org/10.1002/2015JD023126.

Vuille, M., Carey, M., Huggel, C., Buytaert, W., Rabatel, A., Jacobsen, D., Soruco, A., Villacis, M., Yarleque, C., Timm, O., Condom, T, Salzmann, N., Sicart, J. (2018). Rapid decline of snow and ice in the tropical Andes–Impacts, uncertainties and challenges ahead. *Earth-Science Reviews*, 176, 195-213.

Wigmore, O., & Bryan, M. (2017). Monitoring tropical debris-covered glacier dynamics from high-resolution unmanned aerial vehicle photogrammetry, Cordillera Blanca, Peru. *The Cryosphere*, 11(6), 2463.

Zelt, C. A., & Smith, R. B. (1992). Seismic traveltime inversion for 2-D crustal velocity structure. *Geophysical Journal International*, 108(1), 16-34.

Tables

Table 1. Survey and model conversion details for 2D resistivity and seismic lines.

2D line	Survey length (m)	Receiver spacing (m)	# of data points used	Data misfit	
				RMS (%)	L2
*E1**	162	NA	1013	3.87	0.29
RA1	144	3	NA	NA	NA
E1	162	6	NA	NA	NA
E2	162	6	346	3.86	0.15
E3	162	6	346	3.41	0.12
E4	162	6	346	3.39	0.12
E5	162	6	346	4.4	0.19
E6	162	6	346	5.02	0.25
Q1	117.5	2.5	354	3.58	NA
Q7	117.5	2.5	335	5.33	NA

Table 2. Maximum current source and receiver electrode spacing (AB), and model convergence for 1D vertical electrical soundings (VES).

1D sounding	Maximum AB separation (m)	Data misfit (RMS %)
V1	144.8	4.93
V2	300	0.91
V3	144.8	9.73
V4	261	2.89
V5	300	3.13
V6	144.8	2.01

Figures

Figure 1. a) Red star marks location of Cordillera Blanca range. (b) Delineation of Callejon de Huaylas basin, which drains to a gaging station at La Balsa via Santa River and tributaries. (c) Photograph of Quilcayhuanca Pampa with major geomorphologic features.

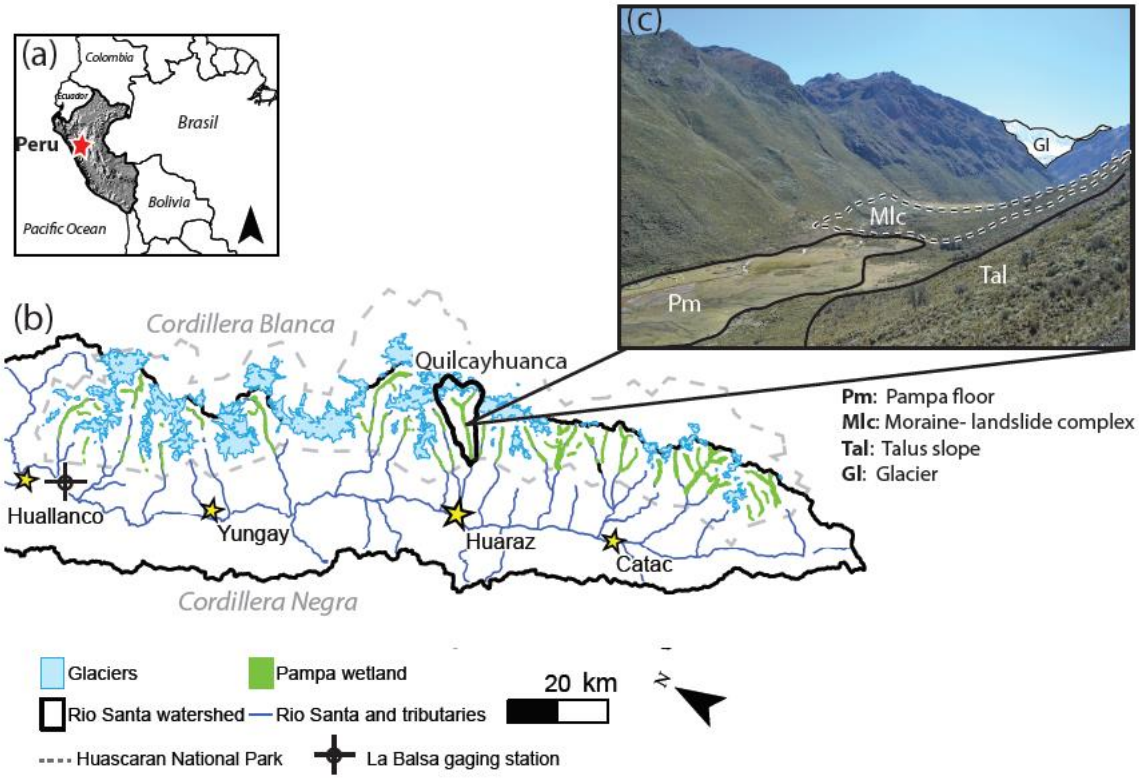

Figure 2. (a) Quilcayhuanca pampa, including geophysical study area in black box. Dominant topographical slopes indicated by shading. (b) Locations of geophysical transects and soundings, including vertical electrical soundings (VES), horizontal to vertical spectral ratio (HVSR), electrical resistivity tomography (ERT), and seismic refraction tomography (SRT). Locations of spring- fed tributaries delineated with light blue lines.

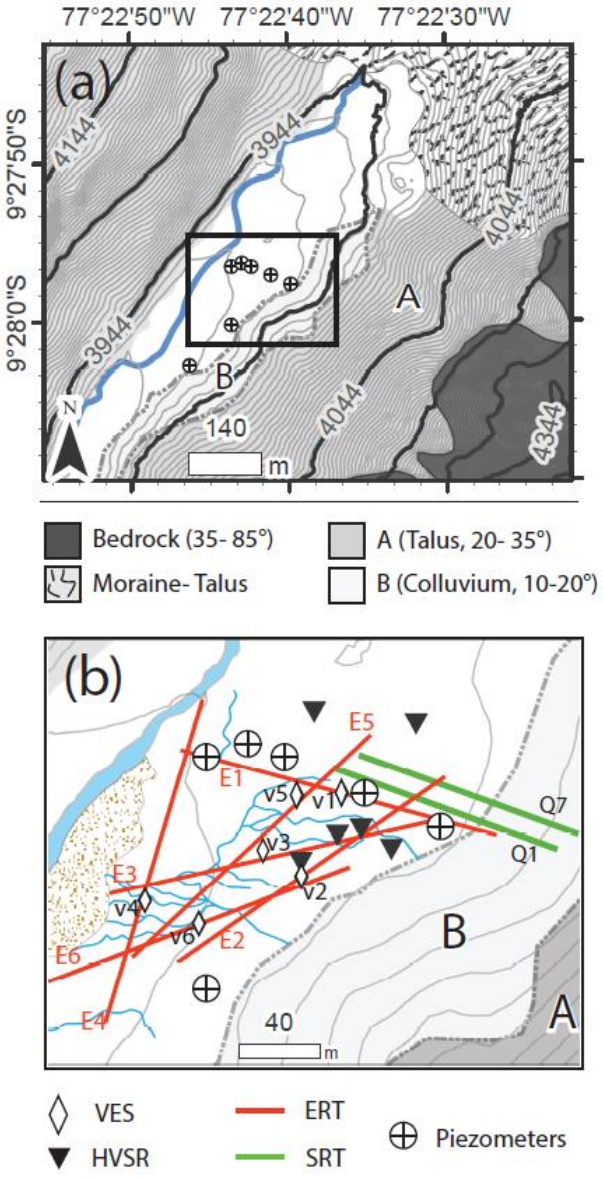

Figure 3. Time series of hydraulic head levels in piezometer transect GW7- GW1- GW5- GW6, plotted with rainfall hyetograph for reference. Regional dry season from May 1- Oct 1 shaded in grey. Figure insets show plan view (left) and profile view (right) of well transect.

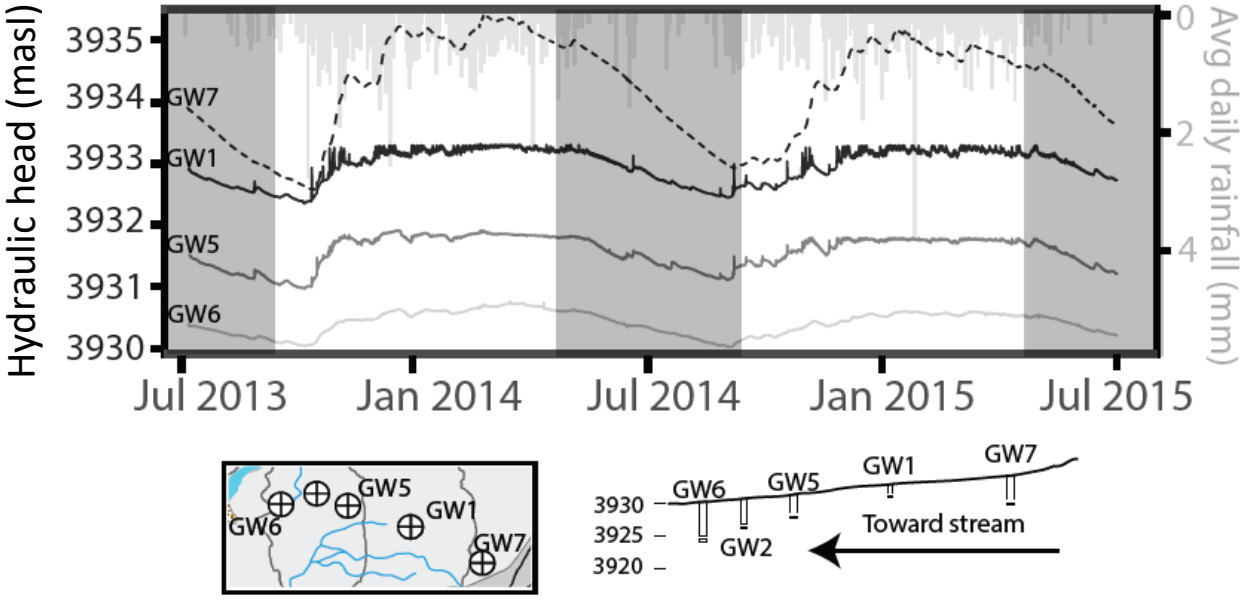

Figure 4. (a) P-wave velocity model, showing modeled ray paths as small black lines. Piezometer depths for GW7 and GW1 included for reference. (b) P-wave velocity model and ray paths for line Q7. (c) and (d) Change in velocity with every vertical meter for lines Q1 and Q7. (c) Shows hydrogeologic zones 1a, 1, and 2.

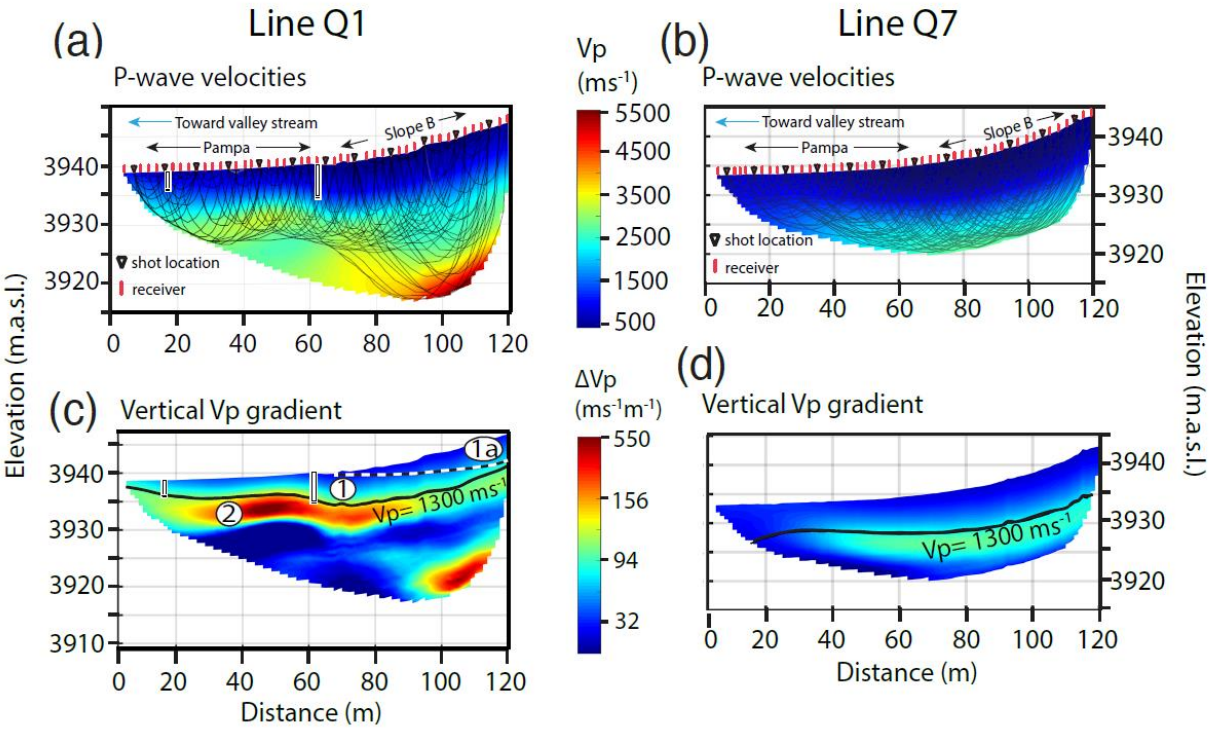

Figure 5. (a) 2D resistivity section for line E1*, which consists of merged data from E1 (6m spacing) and RA1 (3m spacing roll- along survey). Four hydrogeologic zones (1a, 1, 2, and 3) are marked, along with the 1300 m/s p-wave velocity contour (dotted line). (b) All six intersecting resistivity models plotted in 3D.

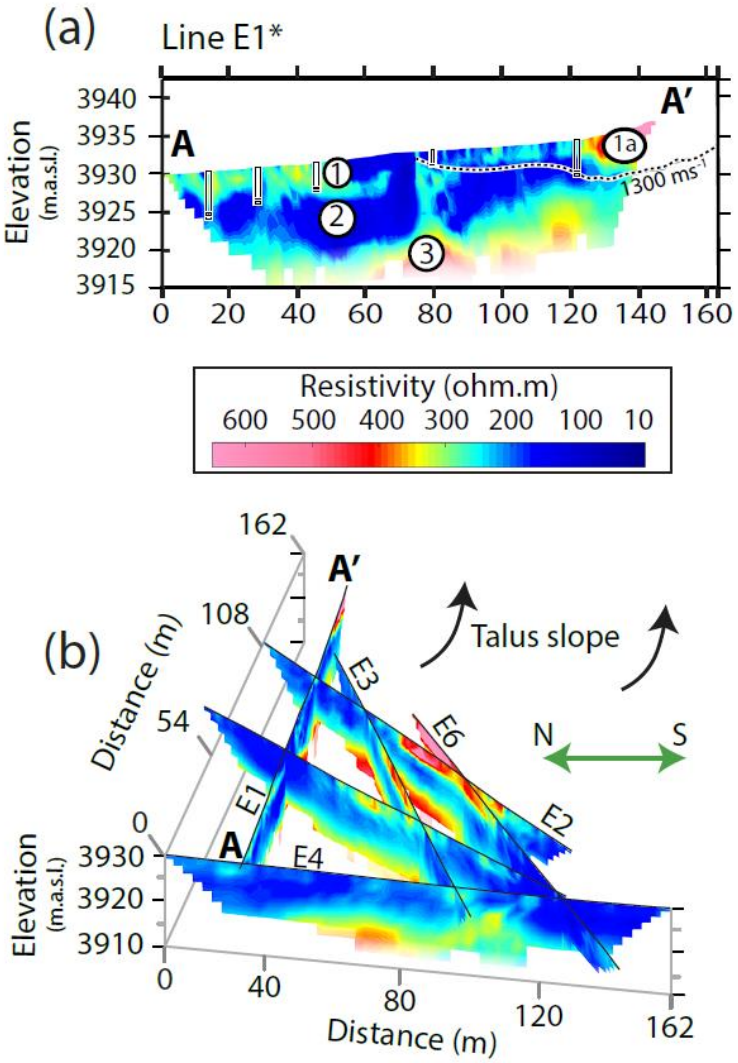

Figure 6. 1D resistivity plotted with depth (solid line), indicating zones of substantial aquifer storage (shaded area). 2D ERT resistivity represented as box plots for each model row, plotted at the mean row depth. Hydrogeologic zones 1, 2, 3, and 4 are marked on upper right.

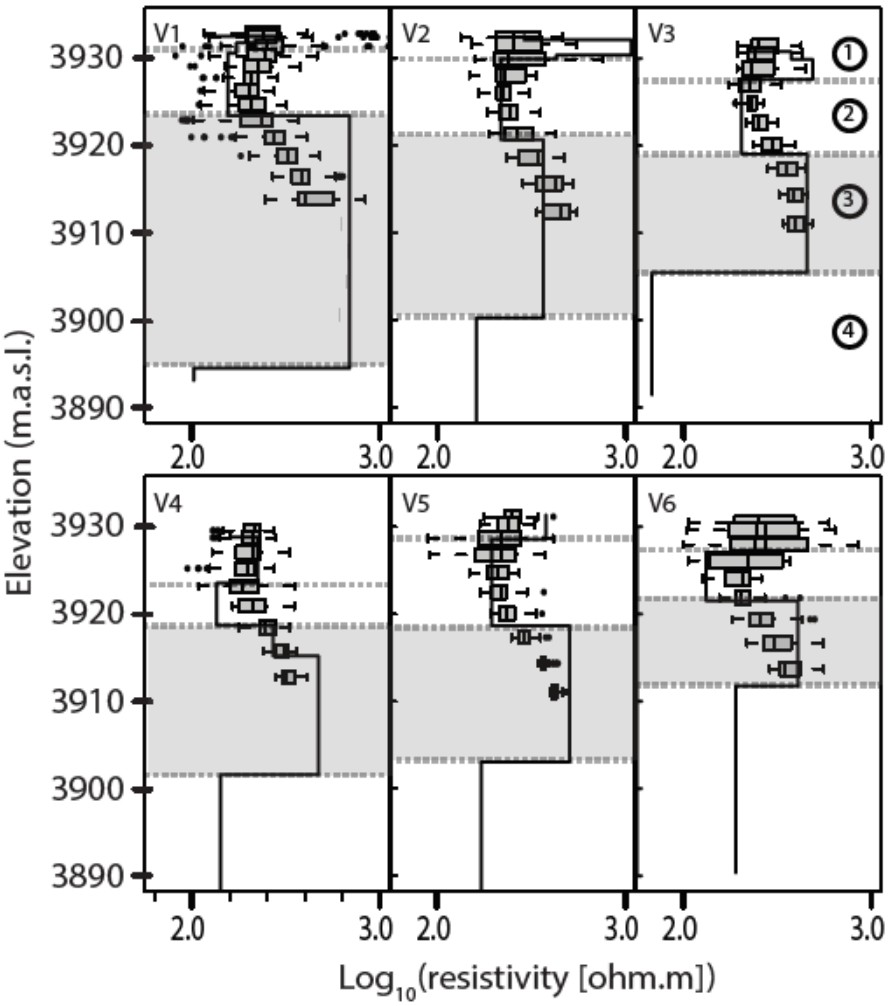

Figure 7. (a) Spatial locations of HVSR points in relation to other geophysical lines (background). Plot inset: Possible sediment thicknesses for each HVSR point based on estimated shear wave velocity ranges. (b) HVSR plots for all six locations. Standard deviation of H/V ratios in shaded grey region. Resonance frequency for each point is marked as f0. Aerial imagery from Wigmore & Mark (2017).

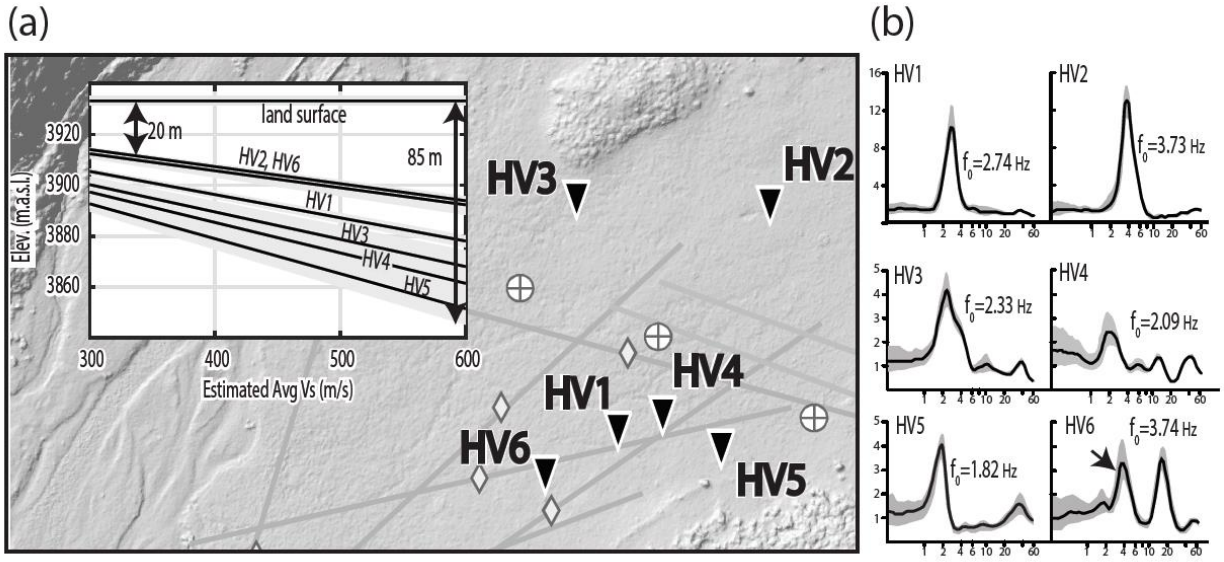

Figure 8. Conceptual model of Quilcayhuanca talus aquifer, including recharge zones at valley edge and zones of maximum storage.

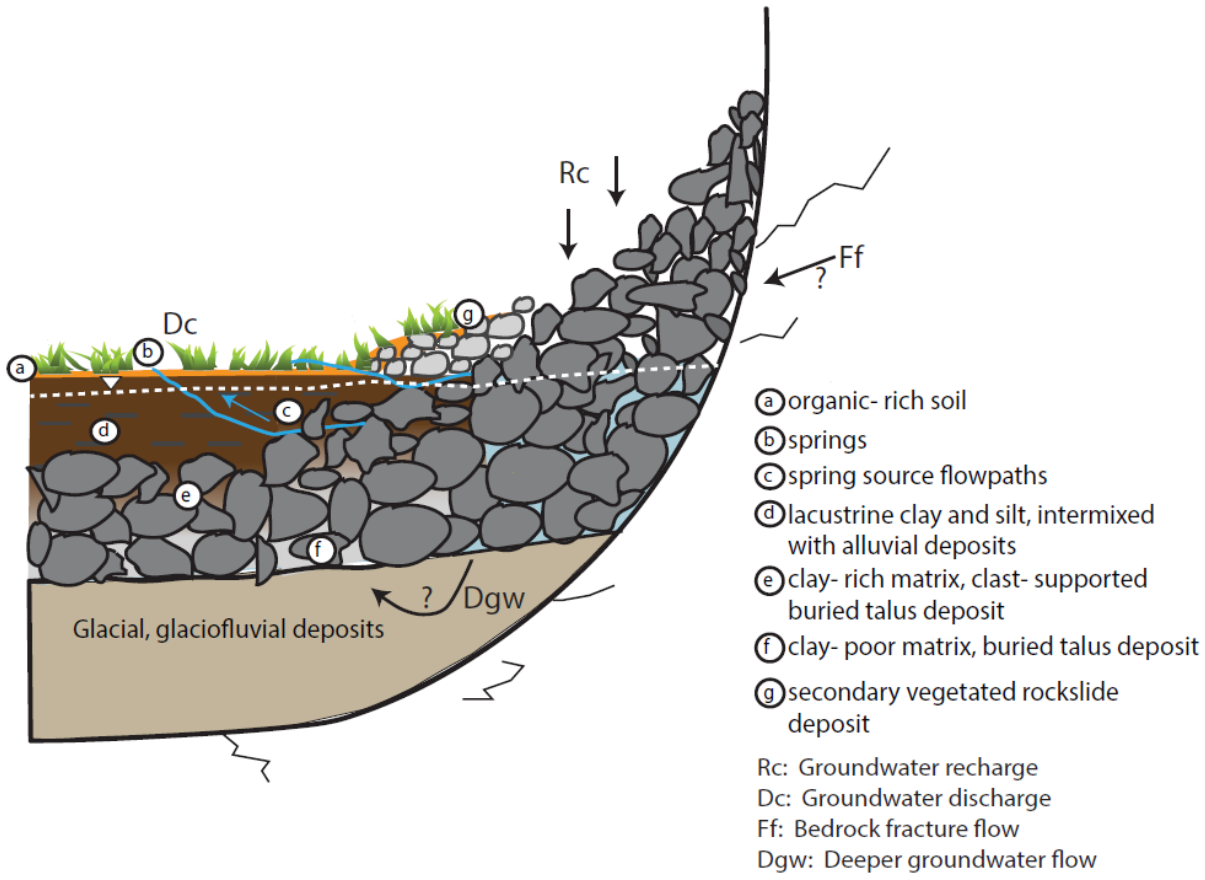

Supplementary Information

Figure S1. Seismic p-wave arrival time plots for (a) line Q1 and (b) line Q7. Figure insets show sample seismograms on each line with picked (grey) and modeled (black) arrival times.

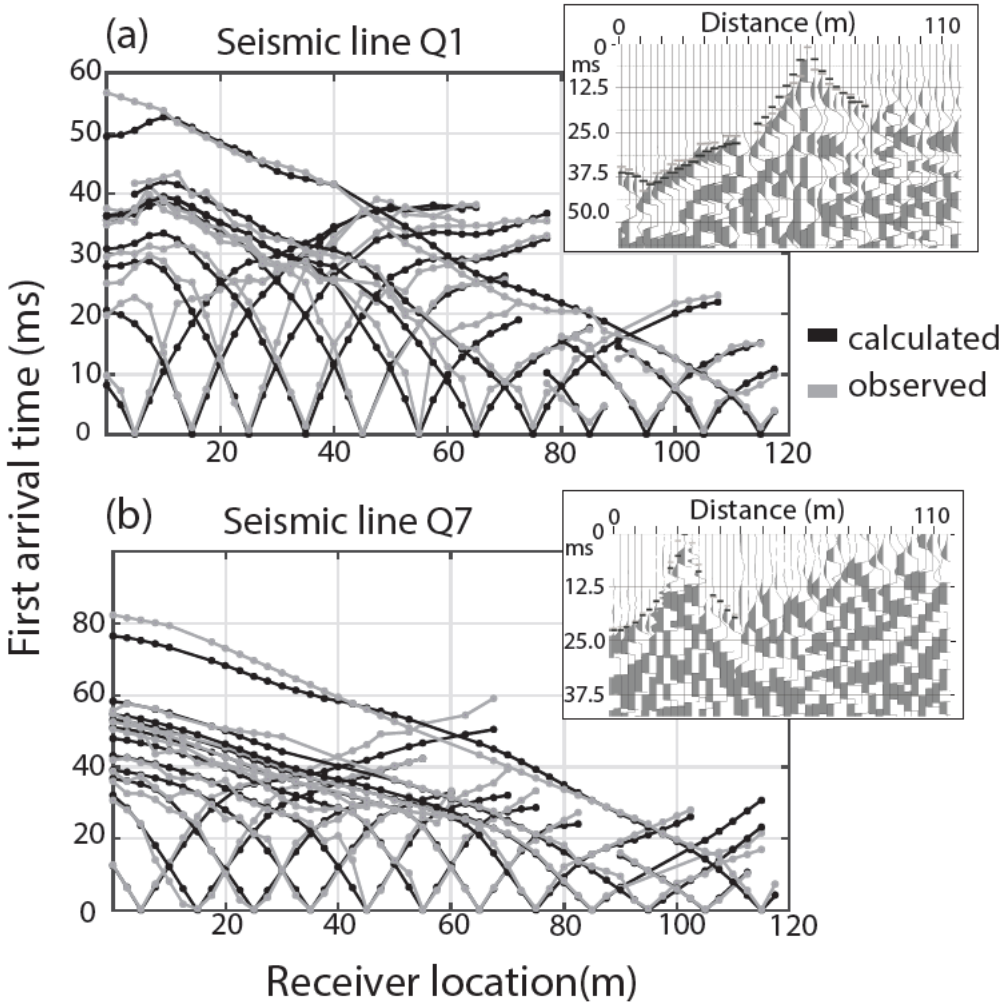

Figure S2. Analysis of variation across 22 distinct starting models. Dotted line follows the contour of highest velocity increase with depth. (a) Piezometer locations are shown on line Q1, indicating depth of borehole constraints on subsurface interpretation. (b) Coefficient of variation across model Q7.

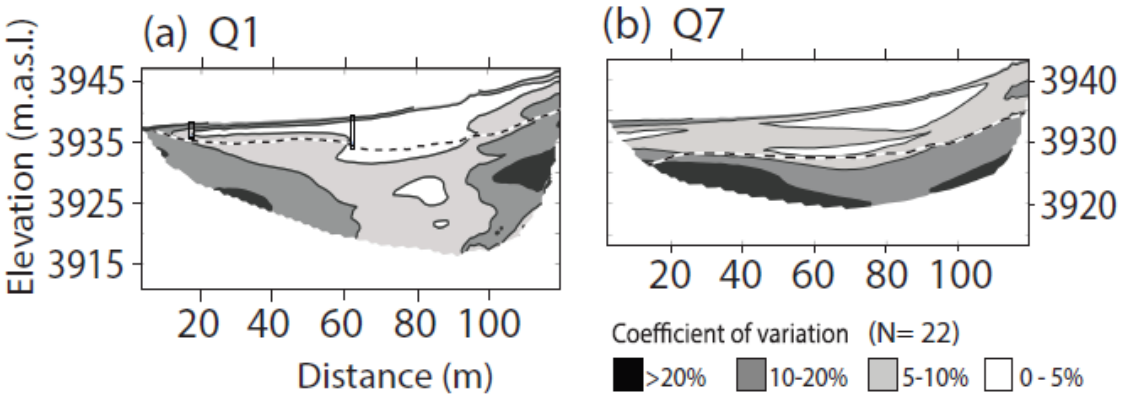

Chapter 2

A review of the current state of knowledge of proglacial hydrogeology in the Cordillera Blanca, Peru

Abstract

The rapidly melting glaciers of Peru are posing new risks to regional dry season water supplies, and this is evident in the Cordillera Blanca, the mountain range with the world's largest concentration of tropical glaciers. Permanent ice loss is causing reductions to dry season streamflow, which is coupled with shifting demands and control over water access and entitlements in the region. A full evaluation of hydrologic inputs is required to inform future water management in the relative absence of glaciers. Over the last decade, new studies have shown groundwater to be a significant component of the regional water budget during the dry season, and it cannot be ignored when accounting for water quality and quantity downstream of the Cordillera Blanca's alpine catchments. Distinctive common features of the Cordillera Blanca's proglacial catchments are sediment-filled valleys that were once under proglacial lake conditions. The combination of lake sediments with other alpine depositional features results in storage and inter-seasonal release of groundwater that comprises up to 80% of the valley's streamflow during the driest months of the year. We summarize the emerging understanding of hydrogeologic processes in proglacial headwater systems of the region's principal river, the Rio Santa, and make suggestions for future research that will more clearly characterize the spatial distribution of stored groundwater within the mountain range. As glaciers continue to recede, differences in aquifer thickness and groundwater residence time between alpine catchments in the region will increasingly control dry season water availability at the local and basin scale.

1. Introduction

Mountain glaciers are among the world's features most sensitive to global climate change due to increasing temperatures and changing precipitation patterns (Francou et al., 2005; Georg et al., 2010). Glacially-fed streams and rivers are the primary source of water for millions worldwide (Schaner, Voisin, Nijssen, & Lettenmaier, 2012; Vuille, Francou, et al., 2008), and in lower latitudes, the rapid retreat of tropical glaciers challenges water availability for arid and semi-arid regions downstream (Barnett et al., 2005; Chevallier et al., 2011; Kaser et al., 2006; Knight & Harrison, 2014; Thompson et al., 2011). Climate models predict that tropical glaciers will be exposed to more amplified tropospheric warming over the next century compared to mid-latitudes(Bradley, Vuille, Diaz, & Vergara, 2006a), which may explain the observed accelerated loss of ice in the tropics over the last few decades (Thompson et al., 2011).

Tropical glaciers are retreating worldwide, however those that drain to seasonally dry lowlands more significantly impact water resources. Along the Andean tropics, major cities such as La Paz, Quito, and Lima are dependent to some degree on water that originated in mountain glaciers (Chevallier et al., 2011). Tropical Andean catchments are experiencing shifts in hydrology associated with glacial loss, particularly those in the "outer tropics" with pronounced wet and dry seasons. Several reviews have documented the hydro-social, ecological, and societal impacts of glacier retreat in the tropical Andes, and have emphasized the need for adaptation strategies to consider social, economic, and cultural influences on water use (Drenkhan et al., 2015; Mark et al., 2017; Vuille et al., 2018).

The Cordillera Blanca (CB), which includes Huascaran National Park in Northwestern Peru, contains the world's largest concentration of tropical glaciers (Figure 1). The region experiences distinctly seasonal precipitation patterns, where approximately 80% of annual

precipitation falls during the wet season (November-April). During the dry months of May to October, glacial melt buffers streamflow to the region's principal river, the Rio Santa, and its tributaries that originate in glacierized catchments(Mark & Seltzer, 2003; Vuille, 2013).

Due to glacial mass loss, dry-season runoff of the Rio Santa is predicted to continue to decrease in the next few decades (Baraer et al., 2012), intensifying competition for water resources between large-scale agriculture, growing populations, mining, and hydropower operations (Bury et al., 2011; Drenkhan et al., 2015; Mark et al., 2017). Several hydroelectric power stations are located between the Cordillera Blanca and the Pacific coast along the Rio Santa (Mark, 2008), providing more than 10% of Peru's hydroelectric potential (Bury et al., 2013; Mark et al., 2010). Although the hydropower stations are regulated by reservoirs during the dry season, future water availability in the case of decreased glacial water storage is uncertain. The region has already experienced multiple water-related conflicts related to water regulation and management, complicated by both real and perceived threats of water shortages and glacial lake outburst floods (GLOF) (Carey et al., 2014; Carey et al., 2012; Li, 2016).

Over the past decade, research has shown groundwater is a significant component of the water budget in the Cordillera Blanca (Baraer et al., 2015). High altitude proglacial wetlands and meadows supply tributaries to the Rio Santa with flow during the dry season, but hydrogeologic processes in these systems are still largely uncharacterized. Similar proglacial peaty wetlands have been observed globally in both temperate and tropical proglacial catchments (Buytaert et al., 2011), and are attributed to the infilling of lakes with poorly drained and impermeable soils (Carrivick & Tweed, 2013). Both peat-rich and peat-poor wetlands are found in the proglacial catchments of the Cordillera Blanca, buffering both water quality and quantity, and are jeopardized by intensifying land use and the changing climate (Polk, 2016). While the

geomorphology of the Cordillera Blanca's alpine valleys allows for groundwater storage, the mechanisms governing groundwater storage and transmittance are not yet fully understood. More refined estimates of groundwater storage capacity, flow direction, and turnover is needed to improve dry season water quantity and quality predictions in the near future for the upper Rio Santa basin. As the glacial component of dry season streamflow diminishes, groundwater contributions will have relatively greater importance to the regional hydrology (Mark & Mckenzie, 2007; Mark et al., 2005).

The objective of this review is to synthesize contemporary groundwater studies of the Cordillera Blanca (CB), which are based on four individual proglacial catchments in the upper portion of the Rio Santa watershed known as the Callejon de Huaylas (Figure 1). In these alpine valleys, lake sediments interact with rock slides and glacial depositional features, leading to more significant groundwater storage than has been observed in both tropical and mid-latitude glacierized catchments (Baraer et al., 2015; Gordon et al., 2015). We describe the general landsystem stratigraphy and hydroclimatic context of these proglacial tropical highland systems that become the reservoirs for groundwater. We highlight the importance of these features as they relate to southern and northern CB geology and basin morphology, as well as the potential response of proglacial aquifers to warming temperatures and glacial mass loss. Finally, we place recent advances in understanding of CB alpine groundwater in the context of downstream water availability at the local and regional scale, illustrating the importance of further study of alpine hydrogeology in this remote region.

2. The Cordillera Blanca: Setting and Geology

A lack of thermal seasonality causes tropical glaciers to ablate throughout the year, in contrast with mid-latitude glaciers where winter freeze and spring melt amplify seasonal changes

in the annual hydrograph. As a result, tropical glacial melt has a smoothing effect on intra-annual runoff (Kaser et al., 2003). Within tropical latitudes, glacial ice is globally distributed in areas of high elevation, where freezing altitudes lie between 4500 to 5000 masl (Harris et al., 2000). Western New Guinea (Carstensz Glaciers, Papua Province, Indonesia), the East African Highlands (Rwenzori Mountains, Irian Yaya, Kilimanjaro, Mount Kenya), and the South American Andes between Bolivia and Venezuela comprise the global assemblage of glaciers in the tropics. More than 99% of these glaciers are located in the tropical Andes of South America, and more than 70% of the world's tropical glacier area coverage is located in Peru (Rabatel et al., 2013).

The Cordillera Blanca lies between 8.5° and 10° S latitude in Northwestern Peru and holds more than 25% of all the world's tropical glaciers by area (Kaser et al., 2003), covering approximately 480 km^2 (Burns & Nolin, 2014). The western slopes of the glacierized Cordillera Blanca and the eastern slopes of the non-glacierized Cordillera Negra to the west drain to the Rio Santa valley and eventually to the Pacific Ocean through arid terrain (Bury et al., 2011). The remaining portion of glacial melt in the Cordillera Blanca drains eastward toward the Amazon Basin, where proglacial hydrologic processes under these more humid tropical conditions have not yet been explored. Among Peru's rivers that drain to the Pacific, the Rio Santa is the second largest in discharge volume, and maintains flow throughout the year's wet and dry seasons (Mark & Seltzer, 2003). Located in Peru's Ancash region, the Rio Santa watershed occupies over 12,000 km^2 of land area. The upper portion of the Rio Santa watershed, the Callejon de Huaylas, receives glacial runoff and has a spatial extent of 4900 km^2.

The bedrock composition of the Callejon de Huaylas consists of the Chicama Formation, a meta-sedimentary unit composed largely of Jurassic Phyllites, which was intruded by a

granodiorite batholith in the late Miocene (Giovanni et al., 2010; Gonzalez & Pfiffner, 2012). The western edge of the Cordillera Blanca is demarcated by the Cordillera Blanca Normal Fault (McNulty & Farber, 2002). Valleys in the southern Cordillera Blanca show more exposed Chicama bedding with some exposure of volcanic ignimbrites (Margirier et al., 2016) and tend to be wider and more expansive than the valleys to the north that are more steeply incised with greater exposure of igneous bedrock (Giovanni et al., 2010). The valley bottoms of the Cordillera Blanca consist of alpine meadow-talus complexes featuring alpine grasses, shrubs, and wetland plant species. Lining the valley grasslands, colluvial slope deposits are prevalent due to tectonic conditions and glacial retreat, and they often interfinger with lacustrine deposits in the wetlands to form confined aquifers (Baraer et al., 2015; Gordon et al., 2015).

Investigators have made several distinctions between northern/central (north of the city of Huaraz) and southern (south of Huaraz) proglacial valleys within the Cordillera Blanca based on proportions of meadow and glacial area, precipitation patterns, and lithology. The northern portion of the range experiences higher precipitation rates than southern valleys, where the precipitation gradationally decreases southward from 770 mm y^{-1} to 470 mm y^{-1} (Vuille et al., 2008). Southern catchments have a lower proportion of glacial area, ranging from 6 to 12% of total catchment area, where glacial coverage increases northward to roughly half the catchment area toward Llanganuco and Parón (Burns & Nolin, 2014). These differences resulted in distinct geomorphology of southern and northern/central catchments of the Cordillera Blanca, likely resulting in differing hydrogeologic function, although high uncertainties persist in the context of complex topography and lacking subsurface data. In the southern catchments of Yanamarey and Pachacoto, the proportion of alpine meadow to total catchment area is roughly three times that of Quilcayhuanca and Llanganuco toward the north (Baraer et al., 2015). Relative dry season

groundwater contributions to catchment outflow are lower in catchments with more glacial coverage, supporting the prediction that groundwater will increasingly dominate the dry season hydrologic regime with continued loss of glaciers.

3. Hydroclimatic Change

Extensive research has been carried out to quantify climate trends, teleconnections, and glacial retreat in the Peruvian Andes (e.g. Hastenrath & Ames, 1995; Kasert et al., 1990; Mark et al., 2005; Rabatel et al., 2013; Salzmann et al., 2013; Schauwecker et al., 2014; Vuille et al., 2008). Observations starting in the mid-20th century reveal that temperature is increasing throughout the tropical Andes at a rate of 0.1° to 0.3° C per decade (Schauwecker et al., 2014; Vuille et al., 2008), although the rate of warming varies with overlying climatic oscillation patterns (Vuille et al., 2015). From 1969 to 1998, mean annual air temperature increased in the Cordillera Blanca at a rate of 0.31 ° C per decade, and slowed down during the overlapping period of 1983 to 2012 to a rate of 0.13° C per decade (Schauwecker et al., 2014). The stronger temperature increases in the 1970s could be explained by a positive phase in the Pacific Decadal Oscillation (PDO), a recurring pattern of atmospheric-oceanic variability with a cycling period of 20 to 30 years (Vuille et al., 2015).

Precipitation trends are less evident. While no clear trends in precipitation have been found for the tropical Andes on the whole during the 20th century (Rabatel et al., 2013), observations have shown both decreasing (Racoviteanu et al., 2008) and increasing (Schauwecker et al., 2014) trends for the Cordillera Blanca region. Because precipitation in the Cordillera Blanca is spatially heterogeneous due to orographic effects, low station density and data quality lead to a high degree of uncertainty with respect to spatial and elevational distributions of rain and snowfall (Mourre et al., 2016). Anomalously warm/dry El Niño years

and cold/wet La Niña years have been linked to fluctuations in glacial mass balances for the region, although this pattern has been less consistent since the mid-1970s (Vuille et., 2008). Over the past century, interactions of temperature, precipitation and cyclical climate oscillations have caused the negative mass balance in the glaciers of the Cordillera Blanca (Vuille et al., 2008).

Due to rising temperatures and reduced albedo, the rate of glacial area loss in the Cordillera Blanca is accelerating (Baraer et al., 2012). Between 2004 and 2010, the rate of glacial area loss (~87 km^2 $year^{-1}$) was more than five times the rate between 1996 and 2004, when glaciers lost approximately 15 km^2 each year, corresponding to a shrinkage rate of 2.5% and 0.3%y^{-1}, respectively [35]. Climate models with the most optimistic emissions scenarios predict that half the current glacial coverage of the Cordillera Blanca will vanish by the end of the century, leaving only the larger, higher (> 5400 masl) glaciers behind (Rabatel et al., 2013; Racoviteanu et al., 2008; Schauwecker et al., 2014; Schauwecker et al., 2017).

Continued glacial retreat causes a transitory increase in runoff, generated by increases in glacial melt ("peak water"), followed by a decline in discharge as the glacier continues to lose mass (Bury et al., 2013). Peak water has already been surpassed in the uppermost portions of the Rio Santa as well as in seven glacierized tributaries, indicating that the dry-season water levels will continue to fall (Baraer et al., 2012). Dry season discharge of the Rio Santa upon its exit from the basin could be reduced by up to 30% in reduction of glacial inputs (Baraer et al., 2012), although further study is needed to quantify relative contributions of dry season streamflow as glaciers continue to retreat. The effect of glacial retreat on streamflow has been extensively explored in the literature (e.g. Bradley et al., 2006b; Francou & Coudrain, 2005; Mark, 2008; Schaner et al., 2012; Vuille et al., 2008). These reviews aggregate the results of climatic and

hydrologic research in the Cordillera Blanca and conclude that glacial response to climatic forcing is predicted to have an adverse and severe effect on downstream dry-season water resources for both human and environmental systems.

4. Slope Deposits and Alpine Wetlands

In the Cordillera Blanca, slope deposits allow for groundwater recharge and transmittance, while the less permeable sediments of the overlying wetlands allow for groundwater retention and delayed discharge (Baraer et al., 2015; Chavez, 2013; Glas, 2018; Gordon et al., 2015; Maharaj, 2011). Alpine valleys are conducive to mass movements and paraglacial landform deposits because steep slopes and seismicity cause gravitational instabilities (Ballantyne, 2002; Hermanns & Longva, 2012). Slope deposits, such as talus cones, moraines, and debris fans, provide conduits for precipitation and meltwater to reach subsurface flowpaths in mountain environments (Caballero et al., 2002; Roy & Hayashi, 2009). These proglacial geomorphic features retain water and release it slowly to proglacial streams at variable rates, as has been observed in North American alpine catchments under seasonal temperature regimes (Hood et al., 2006; Liu et al., 2004; McClymont et al., 2012), as well as in a tropical proglacial catchment in the Cordillera Real, Bolivia (Caballero et al., 2002).

While temperate proglacial slope deposits are recharged by snowpack and contain permafrost, in tropical systems they provide temporary storage of precipitation and glacial inputs. The thermal seasonality of the mid-latitudes causes freeze-thaw processes, as well as low-lying seasonal snowpacks and permafrosts, making alpine slope deposits in temperate regions quite distinct from those of tropical latitudes in terms of hydrogeologic behavior (Caballero et al., 2002; Muir et al., 2011). Proglacial lakes are also common throughout the CB and are increasing in number with accelerated glacial loss (Emmer et al., 2016; Vilímek et al., 2015).

The role and interaction of slope deposits with proglacial lakes in these hydrogeologic systems varies by catchment, and their importance is highlighted in later sections of this paper.

The valley bottoms of the glacierized Cordillera Blanca are occupied by clay-rich wet meadows and organic-rich wetland systems known as 'bofedales'. Bofedales, sometimes referred to as 'highland bogs', occur throughout Andean highlands and consist of wetland vegetation and peat layers (Fonkén, 2014; Squeo et al., 2006). Collectively within the CB, the bofedal wetlands and grassy meadows are known locally and are referred to here as pampas. The pampas store groundwater that is recharged by both glacial melt and precipitation, and are transitioning to precipitation-derived groundwater as overlying glaciers recede (Polk et al., 2017). Figure 1 shows the extent of pampas in the CB, which were delineated according to a semi-automated method described by Maharaj (2011), distinguishing flat tributary valleys (<10°slope) above 3500 masl that occupy an area of approximately 64 km^2 (Maharaj, 2011).

Subsurface water storage in the pampas is likely contributing significantly to the regional hydrologic system, however there remain uncertainties about the relative contribution of pampa groundwater at the basin scale (Baraer et al., 2015). Pampas are considered to be a part of the Dry Puna ecoregion that occupies the central portion of the Andes, comprising high-altitude grasslands and meadows in the tropics located between ~3500 and ~5000 masl (Buytaert et al., 2006). The pampas' hydrologic function places them as a subset of the Páramo neotropical grasslands that span from Venezuela to Northern Peru, which provide sustained baseflow to downstream areas and contribute significantly to the hydrologic cycle in arid to semiarid tropical regions on the continental scale (Buytaert et al., 2011). Like the Páramo, the pampas of the Cordillera Blanca provide groundwater storage, along with carbon storage and nutrient filtration (Polk, 2016). The low-permeability and organic-rich soils retain porewaters, while thick clay

deposits interfinger with coarser slope deposits and facilitate groundwater recharge and subsurface flow, particularly in northern catchments (Glas, 2018; Mark et al., 2017).

The pampas were formed by proglacial lakes that were originally dammed by moraines and landslides and have since filled with sediment (Maharaj, 2011). As these lakes infilled, existing lateral slope deposits became partially buried beneath fine-grained lacustrine sediments with low permeability (Chavez, 2013; Glas, 2018). Overlying thick layers of lacustrine clays, organic soils were formed by the process of paludification (Figure 2b-d) (Mark & Mckenzie, 2007), eventually forming biodiverse wetlands and grasslands that provide ecosystem services and are used for livestock grazing and tourism (Polk, 2016). In many cases the wetland sediments are drained with ditches to increase pasture and grazing area for cattle and sheep (Bury et al., 2011). Like the glaciers themselves, the pampas have a buffering effect on the seasonality of streamflow and have recently been found to be an important component of the regional hydrologic budget, sustaining streamflow during the dry season to downstream users (Baraer et al., 2009). Within the four glacierized catchments represented in this review, pampa area ranges from ~1 to ~12% of land cover (Baraer et al., 2015). Pampa surface coverage in the Cordillera Blanca has been observed from satellite imagery to fluctuate in sync with valley stream "peak water" hydrographs, initially increasing as water is released from storage in the glaciers, and subsequently decreasing as glacial area continues to diminish (Polk et al., 2017). These results suggest hydrologic connectivity between pampas and glacier meltwater in stream flow, but many other factors including human land use were recognized as important controls on pampa extent. Future changes to pampa soils and vegetative cover will be partially controlled by glacial coverage on decadal time scales, likely affecting their hydrologic function (Young, 2014b).

5. Relative Contributions of Groundwater to Surface Water

5.1 Rio Santa Basin

Historical monthly discharge data from the La Balsa gauge at the outflow of the Callejon de Huaylas has provided a basis for analyzing long-term trends in the Rio Santa flow for relative contributions of glacial melt (1953-present) (Condom et al., 2012; Mark et al., 2010). Dry season discharge at La Balsa has been decreasing, and intra-annual runoff variability is expected to continue to increase with continued glacial loss (Juen et al., 2007). The Callejon de Huaylas watershed is roughly 8% glacierized, with ~66% of the dry season flow of the Rio Santa at La Balsa derived from the proglacial tributary catchments(Mark & Mckenzie, 2007; Mark et al., 2005).

Headwater catchments of the Callejon de Huaylas watershed vary in land area and geomorphology (Figure 3, Table 1). However, most of these catchments contain pampas with significant groundwater storage. In four of approximately 25 of these tributaries, relative dry season groundwater contributions have been estimated, revealing that 24% to 80% of streamflow in these catchments, depending on the degree of glacier coverage, is sourced from groundwater (Baraer et al., 2015; Somers et al., 2016). This leads to preliminary estimates that groundwater originating from tributary catchments contributes 16%-50% of dry season flow to the Rio Santa, representing 5-10% of annual discharge. The dry season inputs from the Cordillera Negra (~34%) are predicted to remain unchanged if precipitation patterns remain the same (Mark & Mckenzie, 2007). Under conditions of glacial loss, over the next century, the dry season baseflow for the upper Rio Santa could be reduced by 50%-84% of current levels, depending on refined estimates of groundwater contribution from the glacierized catchments.

Groundwater studies at the catchment scale are crucial to understanding the overall groundwater contribution to the Rio Santa because variation in valley geomorphology and glacier coverage could potentially lead to distinct inter-valley hydrogeologic processes. Below we review the findings from all available CB groundwater studies, which have focused on four proglacial catchments that span the range from south to north (Pachacoto, Querococha, Quilcayhuanca, and Llanganuco) (Table 2, Figure 3). In general, the alpine valley catchments in the CB contain pampas with low-density, organic-rich soils. High evapotranspiration rates lead to spatially variable soil moisture, which is highest near groundwater springs that originate in deeper aquifers and from valley sides (Mark et al., 2017).

5.2 Pachacoto

One of the most southern valleys of the Cordillera Blanca, the proglacial catchment of Pachacoto (9.90° S, 77.25° W), is relatively wide with about a tenth of its area covered by alpine meadows (Baraer et al., 2015). The catchment area is ~ 1.2% glacierized, containing the Pastoruri Glacier, which is one of the most visited glaciers in Peru. Pachacoto is underlain by volcanic ignimbrites and the Chicama formation, which form the wide, lower gradient valleys that are characteristic of the southern portion of the range (Giovanni et al., 2010). The proglacial valleys of Pachacoto are filled with alpine grasses and grazed by cattle, and are home to the Puya raimondii, a tall (>3 m), endangered endemic flowering plant in the same family as the pineapple (Cruz, 2004) (Figure 3a). Pachacoto contains a relatively large (>11 %) percentage of pampa area, corresponding to a high relative groundwater contribution at the catchment's outflow. Consistent with valleys having less glacial coverage and therefore smaller glacial inputs to streamflow, the relative groundwater contribution in Pachacoto is high, making up ~60% of the dry season streamflow at the catchment outlet (Michel Baraer et al., 2015).

5.3 Querococha

The Querococha basin (9.70° S, 77.30° W) also lies on the southern end of the range, between 4200 and 5400 masl in elevation. Lake Querococha is fed by two converging streams, carrying meltwater from two proglacial catchments headed by the Yanamarey and G2 glaciers (Baraer et al., 2009). The Yanamarey glacier is the most extensively studied in the Cordillera Blanca to quantify glacial retreat (e.g. Bury et al., 2011; Hastenrath & Ames, 1995; Mark et al., 2010; Mark & Seltzer, 2003; Schauwecker et al., 2014) and is predicted to completely disappear within the next few decades. Between 1970 and 1990, the Yanamarey glacier lost two-thirds its areal coverage (Georges, 2004), increasing exposure of Chicama bedrock and contributing to the transport of heavy metals to Yanamarey's proglacial lake, and to Lake Querococha at the pour point of the catchment. Glacial ice fluctuations at Yanamarey have been tightly coupled to temperature at nearby meteorological stations, and the highest rates of ice loss were during a string of moderate to strong El Niño years through the 1990s. Lower rates of ice loss since this time are associated with more frequent La Niña wet periods (López-Moreno et al., 2016).

The Yanamarey pampa forms an area of approximately 1.0 km^2 where the proglacial streams from Yanamarey and G2 meet. It is underlain by the Chicama formation, and infilled with quaternary sediments. The top eight meters of pampa sediment were imaged in 2011 with ground penetrating radar, revealing dry, organic rich soil in the first 0.5 m, followed by sandy soils with coarse fragments down to a depth of 2.0 m, underlain by a thick unit of clay (Maharaj, 2011). Among these quaternary sediments, springs and small streams have been reported as increasingly intermittent, according to local residents (Bury et al., 2011). At the outlet of the Querococha catchment, groundwater contributes ~80% of the total streamflow during the dry season (Baraer et al., 2015) due to the relative lack of glacial ice (< 4% glacierized).

5.4 Quilcayhuanca

The Quilcayhuanca proglacial catchment (9.50° S, 77.38° W) lies upstream of the city of Huaraz near the center of the Cordillera Blanca, and the catchment is drained by two proglacial streams, the Quilcay and Cayesh (Somers et al., 2016). The Quilcayhuanca basin is 17% glacierized, with exposed bedrock leading to sulfide weathering and a valley stream pH < 4. The continued glacial retreat at the catchment headwaters has exposed fresh sulfide minerals that leach toxic elements to the valley streams; heavy metal concentrations measured in these streams have exceeded both Peruvian and international drinking water standards for lead and nickel (Fortner et al., 2011). Valley geology in Quilcayhuanca differs from southern valleys of the Cordillera Blanca because the exposed bedrock valley walls are nearly vertical and are composed largely of miocene ganodiorite and Chicama (Vilímek et al., 2015).

The Quilcayhuanca pampa occupies roughly 4% of the catchment area and is composed of four shallow stratigraphic units: (1) dry, organic-rich soils (0-0.3 m); (2) saturated, sandy organic-rich soils (0.3-3.0 m); (3) a clay confining layer (3-6 m); and (4) coarse-grained gravels and colluvium (6-8+ m), with deeper units not yet identified (Chavez, 2013; Glas, 2018; Maharaj, 2011). These sediments store groundwater. However, the wetland extent of the Quilcayhuanca pampa has decreased since the year 2000 by 17.2% due to decreases in pore water content (Bury et al., 2013). At the catchment outflow (3835 masl), groundwater makes up ~40% of streamflow in Quilcayhuanca pampa during the dry season (Baraer et al., 2015).

5.5 Llanganuco

The Llanganuco catchment (9.02° S, 77.60° W) contains a high percentage of glacial coverage (39%) (Pouyaud et al., 2005) and is underlain by both Miocene granodiorite and Chicama formation (Petford & Atherton, 1996). Like Quilcayhuanca, Llanganuco has steeply

incised, almost vertical walls, and large amounts of talus and landslide deposits that continue from the upper to lower portions of the valley (Chavez, 2013). The Llanganuco catchment contains ~0.15 km^2 of wetland pampa area located above 4400 masl. Just below the pampa, the proglacial stream then falls over a bedrock waterfall to the valley below that is largely filled with floodplain and talus sediments (Portes et al., 2016). Based on hydrochemical mass balance analyses at the catchment outflow (3838 masl), 24% of streamflow is derived from groundwater during the dry season (Baraer et al., 2015).

6. Groundwater-Surface Water Interactions

Most of the water exiting the CB's tributary catchments has spent some time in the subsurface, to varying degrees depending on sediment type and landscape position (Chavez, 2013; Gordon et al., 2015; Maharaj, 2011; Somers et al., 2016). At the reach scale, groundwater-surface water interactions (GWSWI) are facilitated by proglacial landscape features, such as moraines, that exchange water with the valley stream through subsurface connections. Springs in the valley floor provide an important additional connection to valley streams via tributary flow (Bury et al., 2011; Mark et al., 2017; Somers et al., 2016). Below we highlight some key process-based understandings of alpine GWSWI in the Cordillera Blanca, and the linkages between valley geomorphology and groundwater exchange.

Groundwater residence time has been identified as a target for future research in the region (Baraer et al., 2015; Gordon et al., 2015) because it is a key parameter for modeling water resource availability (McGuire et al., 2005). Baraer et al., (2009) described a bimodal groundwater residence time distribution in the Querococha pampa. The meteorological station near the Yanamarey glacier (9.66° S, 77.27° W) contains precipitation measurements dating back to 1981, which were correlated with modeled relative groundwater contributions from years

1998, 1999, 2006, and 2007. Correlations between groundwater contributions and antecedent precipitation show that groundwater flow through the Yanamarey proglacial valley follows both rapid (~3 months) and slower (~ 3 years) flowpaths from recharge to discharge points at the bottom of the valley near Lake Querococha (Baraer et al., 2009). In the Yanamarey pampa, the valley stream loses volume to the subsurface and subsequently gains groundwater near the base of the valley as is typical of meandering alpine streams (Maharaj, 2011). This type of groundwater flowpath likely exists in the adjacent G2 valley as well as other southern pampas that have similar geomorphic characteristics and dry season groundwater contributions (Figure 4b) (Baraer et al., 2009).In the CB tributary catchments to the north, slope deposits are prominent hydrogeologic features, facilitating volumetric exchanges between surface water and groundwater (fractional hydrologic turnover) along the valley streams (Figure 4a) (Gordon et al., 2015; Somers et al., 2016). Utilizing field measurements of stream temperature and meteorological variables, energy balance modeling has been used to estimate relative groundwater contributions to the Quilcayhuanca valley stream over a 4-km reach, revealing that ~29% of the stream discharge is derived from groundwater during the dry season (Somers et al., 2016). Over this study reach, an upper pampa is separated from a lower pampa by a cross-valley landslide-moraine complex (Chavez, 2013). As the stream passes through this feature, it exchanges most of its flow volume with groundwater and regains losses via springs at the base (Gordon et al., 2015). These observations are consistent with the hydrologic role of moraines in mid-latitude alpine catchments, where they serve as primary features for groundwater-surface water exchange (Langston et al., 2011; McClymont et al., 2011).

In the CB, meadow and wetland springs connect groundwater with valley streams via tributary flow, and often occur in dense clusters at mid-valley points (Baraer et al., 2015; Mark et

al., 2017) and at the base of slope deposits incident upon the valley floor (Chavez, 2013). In the mid-valley setting of Quilcayhuanca, most of the artesian springs located in the mid-pampa and at the base of the talus deposits have similar geochemical signatures, indicating that the water from these springs is likely derived from the same source- meteoric water that has recharged the subsurface, where water-rock interaction drives water geochemistry. Furthermore, these springs are significantly different geochemically and isotopically from glacial meltwater that enters the valley, indicating that they are not directly sourced from glacial melt (Baraer et al., 2015; Gordon et al., 2015). In contrast, springs in the upper llanganuco valley that are fed by glaciers lie directly below proglacial lakes, which are the primary source of water these headwater springs (Gordon et al., 2015).

Proximal to the studied reach in Quilcayhuanca, piezometers have been installed spanning a transect from the lateral talus deposit to the valley stream and also along the talus base (Chavez, 2013). Sediment records from piezometer installation reveal largely silty and clayey lacustrine deposits with small amounts of sand. Similar to the springs, groundwater samples from piezometers in Quilcayhuanca are isotopically different from glacier meltwater, supporting the hypothesis that most of this groundwater is not recharged from glacial melt at the headwaters. The piezometers were screened at depths where large blocky debris was encountered, at ~4 to 7 meters depth. The boulders have diameters ranging from 0.1 to 0.9 m, primarily composed of diorites, granites, and andesites, with some metasedimentary rocks (Chavez, 2013). The assemblage of boulders belongs to a buried talus deposit that is clast-supported and likely infilled with clay in the most shallow portion, grading to a clay-poor, more hydraulically conductive zone at depth (Glas, 2018).

During the rainy season, the Quilcayhuanca talus aquifer is recharged at the permeable moraines and lateral talus deposits that line the valley, storing enough groundwater to supply small, perennial tributaries throughout the dry season (Baraer et al., 2015). After infiltrating, the groundwater flows toward the valley center and becomes overpressured, discharging via preferential flow paths and springs in a clay aquitard (Chavez, 2013; Glas, 2018). Comparable geomorphic features in other catchments of the range may have similar hydrologic storage and function, although the basin-wide distribution of talus aquifers remains unknown.

The geomorphology of the Llanganuco pampa demonstrates the hydrologic importance of debris fan, talus, and moraine deposits for both storage and transport of groundwater in a headwater environment (Gordon et al., 2015). This pampa aquifer receives a larger proportion of recharge from glacial ice, as opposed to the Quilcayhuanca pampa that is mostly recharged by precipitation. Glacial melt from two proglacial lakes (Broggi and Laguna 69) is channeled through slope deposits to the subsurface, emerging at pampa springs. The pampa sediments consist of a thick clay unit (> 5.85 m) intermixed with sand lenses underlain by hydraulically conductive (10-5 m/s) glacial till (Chavez, 2013). Just upstream of the clay-rich sediments, a large debris fan receives outflow from glacial lake Laguna 69, storing and releasing it slowly to the pampa during the dry season via perennial springs. Other debris fans, talus slopes, and moraines near the glacier provide storage and recharge mechanisms for melt-, lake-, and precipitation-derived water (Chavez, 2013).

7. Conclusion

In the proglacial valleys of the Cordillera Blanca, the current conceptual understanding of groundwater storage and flow largely involves the interaction of glacial and gravitational deposits with lacustrine and fluvial sediments. Talus and debris flows facilitate groundwater

recharge, while finer sediments aid in groundwater storage, delaying discharge to streams and tributaries. The underlying geology of northern, central, and southern CB valleys likely results in distinct groundwater flow patterns. The storage of wet season precipitation in colluvial aquifers occurs primarily in the northern and central valleys of the range where bedrock is primarily igneous, whereas southern valleys are wider and slope deposits are smaller and not as common (Baraer et al., 2015; Maharaj, 2011). In the southern pampas of the Cordillera Blanca, groundwater likely is recharged through scree and smaller talus deposits at the valley sides and transmitted down-valley via connections to glacial outwash deposits at depth, although more groundwater studies are needed to confirm these relationships (Maharaj, 2011). In both cases, clay-rich lacustrine deposits overlie coarser materials, forming a confining layer perforated by springs. Groundwater is likely recharged via coarse slope deposits and moraines, and subsequent discharge to valley springs is delayed by finer grained sediments.

Throughout the CB, alpine groundwater retention is controlled by geomorphic setting, and has the potential to be altered by glacial mass loss and human influence. Overgrazing in the valleys can affect vegetation type, soil compaction, and soil moisture content, which has links to groundwater table fluctuations via infiltration (Mark et al., 2017). Portions of alpine wetlands that are directly below ice formations will likely shrink in size as those ice patches melt, while portions of wetland that are recharged with precipitation will remain unchanged in terms of hydrologic storage and function. Proglacial aquifers in catchments that are occupied by low-lying glaciers below 5400 masl are at particular risk for wetland area depletion over the next century (Polk, 2016; Rabatel et al., 2013; Racoviteanu et al., 2008), and correspondingly to diminished alpine groundwater springs, available grazing land, and tributary streamflow during the dry season. This is especially true for southern and central catchments where the entirety of

glacial ice is predicted to disappear within the next century (Schauwecker et al., 2017), although these catchments already have the lowest glacial inputs and highest groundwater inputs to streamflow (Baraer et al., 2015).

As glacier ice is permanently lost, the groundwater that originates from both the CB and the Cordillera Negra will become the primary source for dry season water in the Callejon de Huaylas. Glacio-hydrologic change in the CB is coupled with shifting social dynamics and highly heterogeneous distributions of water accessibility throughout the basin (Mark et al., 2017). The spatial occurrence of wetland aquifers throughout the range will have an increasing effect on water quantity and quality directly downstream, particularly in the tributary valleys that lose the most glacial ice. There is a need to further elucidate the temporal relationship of groundwater and precipitation via water age and residence times across CB valley types and geomorphologic settings. Populations downstream of aquifers with longer residence times and slower hydrologic turnover may be more decoupled from water stresses caused by glacial loss.

Further study of hydrogeologic structure and processes in tropical proglacial systems will address gaps in current knowledge of how these systems store and transmit groundwater (Heckmann et al., 2016). Inferences can be made on the basis of commonalities between landscape features in hydrogeologic structure and function, such as the role of talus in groundwater storage. The common occurrence of talus throughout the CB tributary catchments provides a basis for scaling up findings from individual catchments to basin-wide generalizations about groundwater storage. To achieve this scaling up, similar talus-spring complexes should be identified in other valleys, using geophysical surveys or topographic analysis to estimate aquifer thickness. These observations will improve our understanding of the spatial distribution of

groundwater storage in the CB, which will refine predictions of future dry season water availability basin-wide.

Apart from the studies reviewed in this paper, there has been very little research in the field of tropical proglacial hydrogeology (Caballero et al., 2002). The geologic setting of the Cordillera Blanca leads to a hydrologic function of slope deposits that contrasts with those found in the North American Rockies and German Alps (Lauber et al., 2014; Roy & Hayashi, 2009). Whereas alpine slope deposits in mid-to high latitudes act to transmit snowmelt and contain permafrost layers that lead to preferential groundwater flow, the slope deposits in the CB are buried beneath thick clay beds and have the potential for increased storage and slower turnover. Because these alpine areas are remote and sparsely instrumented, field work is challenging and logistics are complex. The challenges of alpine research present opportunities for the use of innovative data collection methods that minimize the need for cumbersome equipment, such as synoptic sampling routines and geophysical surveys. Within the CB, these techniques should be applied to the tributary valleys of the range that are predicated to undergo the most change over the next century, namely the valleys with high glacier coverage at or below 5400 masl (Rabatel et al., 2013).

The hydrogeologic characterization of this region contributes new understanding to the field of alpine groundwater and is merited by the urgent need to quantify the spatial distribution of dry season water resources. The origin and subsurface flow characteristics of CB groundwater need to be better understood to quantify future water availability and refine adaptation strategies. As the role of groundwater in the water cycle becomes better understood, it should be integrated with an interdisciplinary hydro-social framework to manage complex and

shifting water stresses in the Cordillera Blanca and in other glacierized Andean catchments that depend on groundwater (Mark et al., 2017; Somers et al., 2018).

References

Ballantyne, C. K. (2002). Paraglacial geomorphology. *Quaternary Science Reviews*, *21*(18–19), 1935–2017. http://doi.org/10.1016/S0277-3791(02)00005-7

Baraer, M., Mark, B. G., Mckenzie, J. M., Condom, T., Bury, J., Huh, K., … Rathay, S. (2012). Glacier recession and water resources in Peru's cordillera Blanca. *Journal of Glaciology*, *58*(207), 134–150. http://doi.org/10.3189/2012JoG11J186

Baraer, M., Mckenzie, J. M., Mark, B. G., Bury, J., Knox, S., Sciences, P., … Cruz, S. (2009). Characterizing contributions of glacier melt and groundwater during the dry season in a poorly gauged catchment of the Cordillera Blanca (Peru). *Advances in Geosciences*, 41–49.

Baraer, M., McKenzie, J., Mark, B. G., Gordon, R., Bury, J., Condom, T., … Fortner, S. K. (2015). Contribution of groundwater to the outflow from ungauged glacierized catchments: a multi-site study in the tropical Cordillera Blanca, Peru. *Hydrological Processes*, *29*(11), 2561–2581. http://doi.org/10.1002/hyp.10386

Barnett, T. P., Adam, J. C., & Lettenmaier, D. P. (2005). Potential impacts of a warming climate on water availability in snow-dominated regions. *Nature*, *438*(November), 303–309. http://doi.org/10.1038/nature04141

Bradley, R. S., Vuille, M., Diaz, H. F., & Vergara, W. (2006). Threats to water supplies in the tropical Andes. *Science*, 312(5781), 1755-1756.

Burns, P., & Nolin, A. (2014). Using atmospherically-corrected Landsat imagery to measure glacier area change in the Cordillera Blanca, Peru from 1987 to 2010. *Remote Sensing of Environment*, *140*, 165–178. http://doi.org/10.1016/j.rse.2013.08.026

Bury, J., Mark, B. G., Carey, M., Young, K. R., Mckenzie, J. M., Baraer, M., … Polk, M. H. (2013). New Geographies of Water and Climate Change in Peru : Coupled Natural and Social Transformations in the Santa River Watershed. *Annals of the Association of American Geographers*, *103*(October 2012), 363–374. http://doi.org/10.1080/00045608.2013.754665

Bury, J. T., Mark, B. G., McKenzie, J. M., French, A., Baraer, M., Huh, K. I., … Gómez López, R. J. (2011). Glacier recession and human vulnerability in the Yanamarey watershed of the Cordillera Blanca, Peru. *Climatic Change*, *105*(1–2), 179–206. http://doi.org/10.1007/s10584-010-9870-1

Buytaert, W., Célleri, R., De Bièvre, B., Cisneros, F., Wyseure, G., Deckers, J., & Hofstede, R. (2006). Human impact on the hydrology of the Andean páramos. *Earth-Science Reviews*, *79*(1–2), 53–72. http://doi.org/10.1016/j.earscirev.2006.06.002

Buytaert, W., Cuesta-Camacho, F., & Tobón, C. (2011). Potential impacts of climate change on the environmental services of humid tropical alpine regions. *Global Ecology and Biogeography*, *20*(1), 19–33. http://doi.org/10.1111/j.1466-8238.2010.00585.x

Buytaert, W., & Domzalski, S. (2015). Climate chage impacts on water resources in the tropical Andes: Prioritizing scientific research for developing adaptation policies. UNESCO International Hydrology Program, https://en.unesco.org/themes/water-security/hydrology

Caballero, Y., Jomelli, V., Chevallier, P., & Ribstein, P. (2002). Hydrological characteristics of slope deposits in high tropical mountains (Cordillera Real, Bolivia). *Catena*, *47*(2), 101–116. http://doi.org/10.1016/S0341-8162(01)00179-5

Carey, M., Baraer, M., Mark, B. G., French, A., Bury, J., Young, K. R., & McKenzie, J. M.

(2014). Toward hydro-social modeling: Merging human variables and the social sciences with climate-glacier runoff models (Santa River, Peru). *Journal of Hydrology*, *518*(PA), 60–70. http://doi.org/10.1016/j.jhydrol.2013.11.006

Carey, M., Huggel, C., Bury, J., Portocarrero, C., & Haeberli, W. (2012). An integrated socio-environmental framework for glacier hazard management and climate change adaptation: Lessons from Lake 513, Cordillera Blanca, Peru. *Climatic Change*, *112*(3–4), 733–767. http://doi.org/10.1007/s10584-011-0249-8

Carrivick, J. L., & Tweed, F. S. (2013). Proglacial Lakes: Character, behaviour and geological importance. *Quaternary Science Reviews*, *78*, 34–52. http://doi.org/10.1016/j.quascirev.2013.07.028

Chavez, D. (2013). *Groundwater potential of pampa aquifers in two glacial watersheds, Cordillera Blanca, Peru*. Master's thesis, McGill University, Montreal, PQ

Chevallier, P., Pouyaud, B., Suarez, W., & Condom, T. (2011). Climate change threats to environment in the tropical Andes: Glaciers and water resources. *Regional Environmental Change*, *11*(SUPPL. 1), 179–187. http://doi.org/10.1007/s10113-010-0177-6

Condom, T., Escobar, M., Purkey, D., Pouget, C., Suarez, W., Ramos, C., … Gomez, J. (2012). Simulating the implications of glaciers' retreat for water management: a case study in the Rio Santa basin, Peru. *Water International*, (August), 37–41.

Cruz, D. La. (2004). La Geologia en Relacion al Sistema Ecologico en el Peru. *Revista Del Instituto de Investigacion FIGMMG*, *7*(13), 9–15.

Drenkhan, F., Carey, M., Huggel, C., Seidel, J., & Oré, M. T. (2015). The changing water cycle:

climatic and socioeconomic drivers of water-related changes in the Andes of Peru. *Wiley Interdisciplinary Reviews: Water*, *2*(December), n/a-n/a. http://doi.org/10.1002/wat2.1105

Emmer, A., Klimeš, J., Mergili, M., Vilímek, V., & Cochachin, A. (2016). 882 lakes of the Cordillera Blanca: An inventory, classification, evolution and assessment of susceptibility to outburst floods. *Catena*, *147*, 269–279. http://doi.org/10.1016/j.catena.2016.07.032

Fonkén, M. S. M. (2014). An introduction to the bofedales of the Peruvian High Andes. *Mires and Peat*, *15*, 1–13.

Fortner, S. K., Mark, B. G., McKenzie, J. M., Bury, J., Trierweiler, A., Baraer, M., … Munk, L. (2011). Elevated stream trace and minor element concentrations in the foreland of receding tropical glaciers. *Applied Geochemistry*, *26*(11), 1792–1801. http://doi.org/10.1016/j.apgeochem.2011.06.003

Francou, B., & Coudrain, A. (2005). Glacier shrinkage and water resources in the Andes. *Eos, Transactions American Geophysical Union*, *86*(43), 415. http://doi.org/10.1029/2005EO430005

Francou, B., Ribstein, P., Wagnon, P., Ramirez, E., & Pouyaud, B. (2005). Glaciers of the tropical Andes: indicators of global climate variability. In *Global change and mountain regions* (pp. 197-204). Springer, Dordrecht. http://doi.org/10.1007/1-4020-3508-X

Georges, C. (2004). 20th-Century Glacier Fluctuations in the Tropical Cordillera Blanca , Perú Author (s): Christian Georges Published by : INSTAAR , University of Colorado Stable URL : http://www.jstor.org/stable/1552433 Linked references are available on JSTOR, *36*(1), 100–107.

Giovanni, M. K., Horton, B. K., Garzione, C. N., McNulty, B., & Grove, M. (2010). Extensional basin evolution in the Cordillera Blanca, Peru: Stratigraphic and isotopic records of detachment faulting and orogenic collapse in the Andean hinterland. *Tectonics*, *29*(6), 1–21. http://doi.org/10.1029/2010TC002666

Glas, R. (2018). Surface water and groundwater in a changing climate: applications of hydrogeophysics and trend analysis to understand hydrologic systems. Doctoral Dissertation, Syracuse University, Syracuse, NY.

Gonzalez, L., & Pfiffner, O. A. (2012). Morphologic evolution of the Central Andes of Peru. *International Journal of Earth Sciences*, *101*(1), 307–321. http://doi.org/10.1007/s00531-011-0676-9

Gordon, R. P., Lautz, L. K., McKenzie, J. M., Mark, B. G., Chavez, D., & Baraer, M. (2015). Sources and pathways of stream generation in tropical proglacial valleys of the Cordillera Blanca, Peru. *Journal of Hydrology*, *522*, 628–644. http://doi.org/10.1016/j.jhydrol.2015.01.013

Harris, J., Bowman, K. P., & Shin, D. B. (2000). Comparison of freezing-level altitudes from the NCEP reanalysis with TRMM precipitation radar brightband data. *Journal of Climate*, *13*(23), 4137–4148. http://doi.org/10.1175/1520-0442(2000)013<4137:COFLAF>2.0.CO;2

Hastenrath, S., & Ames, A. (1995). Recession of Yanamarey Glacier in Cordillera-Blanca, Peru, During the 20th-Century. *Journal of Glaciology*, *41*, 191–196.

Heckmann, T., Mccoll, S., & Morche, D. (2016). Retreating ice: Research in pro-glacial areas matters. *Earth Surface Processes and Landforms*, *41*(2), 271–276. http://doi.org/10.1002/esp.3858

Hermanns, R. L., & Longva, O. (2012). Rapid rock-slope failures. *Landslides*, (January), 59–70. http://doi.org/10.1017/CBO9780511740367.007

Hood, J. L., Roy, J. W., & Hayashi, M. (2006). Importance of groundwater in the water balance of an alpine headwater lake. *Geophysical Research Letters*, *33*(April), 1–5. http://doi.org/10.1029/2006GL026611

Juen, I., Kaser, G., & Georges, C. (2007). Modelling observed and future runoff from a glacierized tropical catchment (Cordillera Blanca, Peru). *Global and Planetary Change*, *59*(1–4), 37–48. http://doi.org/10.1016/j.gloplacha.2006.11.038

Kaser, G., Ames, A., & Zamora, M. (1990). Glacier fluctuations and climate in the Cordillera Blanca, Peru. *Annals of Glaciology*, *14*(July), 136–140.

Kaser, G., Cogley, J. G., Dyurgerov, M. B., Meier, M. F., & Ohmura, A. (2006). Mass balance of glaciers and ice caps: Consensus estimates for 1961–2004. *Geophysical Research Letters*, *33*(19), L19501. http://doi.org/10.1029/2006GL027511

Kaser, G., Großhauser, M., Marzeion, B., & Barry, R. G. (2010). Contribution potential of glaciers to water availability in different climate regimes. *Proceedings of the National Academy of Sciences of the United States of America*, *107*(47), 21300–21305. http://doi.org/10.1073/pnas.

Kaser, G., Juen, I., Georges, C., Gómez, J., & Tamayo, W. (2003). The impact of glaciers on the runoff and the reconstruction of mass balance history from hydrological data in the tropical Cordillera Bianca, Perú. *Journal of Hydrology*, *282*(1–4), 130–144. http://doi.org/10.1016/S0022-1694(03)00259-2

Knight, J., & Harrison, S. (2014). Mountain glacial and paraglacial environments under global climate change: Lessons from the past, future directions and policy implications. *Geografiska Annaler, Series A: Physical Geography*, *96*(3), 245–264. http://doi.org/10.1111/geoa.12051

Langston, G., Bentley, L. R., Hayashi, M., Mcclymont, A., & Pidlisecky, A. (2011). Internal structure and hydrological functions of an alpine proglacial moraine. *Hydrological Processes*, *25*(19), 2967–2982. http://doi.org/10.1002/hyp.8144

Lauber, U., Kotyla, P., Morche, D., & Goldscheider, N. (2014). Hydrogeology of an Alpine rockfall aquifer system and its role in flood attenuation and maintaining baseflow. *Hydrology and Earth System Sciences*, 18(11), 4437. http://doi.org/10.5194/hess-18-4437-2014

Li, F. (2016). In Defense of Water: Modern Mining, Grassroots Movements, and Corporate Strategies in Peru. *Journal of Latin American and Caribbean Anthropology*, *21*(1), 109–129. http://doi.org/10.1111/jlca.12198

Liu, F., Williams, M. W., & Caine, N. (2004). Source waters and flow paths in an alpine catchment, Colorado Front Range, United States. *Water Resources Research*, 40(9). http://doi.org/10.1029/2004WR003076

López-Moreno, J. I., Valero-Garcés, B., Mark, B., Condom, T., Revuelto, J., Azorín-Molina, C., … Alejo-Cochachin, J. (2016). Hydrological and depositional processes associated with recent glacier recession in Yanamarey catchment, Cordillera Blanca (Peru). *Science of The Total Environment*, *579*, 272–282. http://doi.org/10.1016/j.scitotenv.2016.11.107

Maharaj, L. (2011). *Investigating proglacial groundwater systems in the Quilcayhuanca and*

Yanamarey Pampas, Cordillera Blanca, Peru. Master's thesis, McGill University, Montreal, PQ

Margirier, A., Audin, L., Robert, X., Herman, F., Ganne, J., & Schwartz, S. (2016). Journal of Geophysical Research : Solid Earth. *Journal of Geophysical Research: Solid Earth*, *121*, 6235–6249. http://doi.org/10.1002/2014JB011765.Received

Mark, B. G. (2008). Tracing tropical Andean glaciers over space and time: Some lessons and transdisciplinary implications. *Global and Planetary Change*, *60*(1–2), 101–114. http://doi.org/10.1016/j.gloplacha.2006.07.032

Mark, B. G., Bury, J., McKenzie, J. M., French, A., & Baraer, M. (2010). Climate Change and Tropical Andean Glacier Recession: Evaluating Hydrologic Changes and Livelihood Vulnerability in the Cordillera Blanca, Peru. *Annals of the Association of American Geographers*, *100*(4), 794–805. http://doi.org/10.1080/00045608.2010.497369

Mark, B. G., French, A., Baraer, M., Carey, M., Bury, J., Young, K. R., … Lautz, L. (2017). Glacier loss and hydro-social risks in the Peruvian Andes. *Global and Planetary Change*, *159*(April), 61–76. http://doi.org/10.1016/j.gloplacha.2017.10.003

Mark, B. G., & Mckenzie, J. M. (2007). Tracing increasing tropical Andean glacier melt with stable isotopes in water. *Environmental Science and Technology*, *41*(20), 6955–6960. http://doi.org/10.1021/es071099d

Mark, B. G., McKenzie, J. M., & Gómez, J. (2005). Hydrochemical evaluation of changing glacier meltwater contribution to stream discharge: Callejon de Huaylas, Peru / Evaluation hydrochimique de la contribution évolutive de la fonte glaciaire à l'écoulement fluvial: Callejon de Huaylas, Pérou. *Hydrological Sciences Journal*, *50*(6), 975–988.

http://doi.org/10.1623/hysj.2005.50.6.975

Mark, B. G., & Seltzer, G. O. (2003). Tropical glacier meltwater contribution to stream discharge: a case study in the Cordillera Blanca, Peru. *Journal of Glaciology*, *49*(165), 271–281.

McClymont, a. F., Hayashi, M., Bentley, L. R., & Liard, J. (2012). Locating and characterising groundwater storage areas within an alpine watershed using time-lapse gravity, GPR and seismic refraction methods. *Hydrological Processes*, *26*(May), 1792–1804. http://doi.org/10.1002/hyp.9316

McClymont, A. F., Roy, J. W., Hayashi, M., Bentley, L. R., Maurer, H., & Langston, G. (2011). Investigating groundwater flow paths within proglacial moraine using multiple geophysical methods. *Journal of Hydrology*, *399*(1–2), 57–69. http://doi.org/10.1016/j.jhydrol.2010.12.036

McGuire, K. J., McDonnell, J. J., Weiler, M., Kendall, C., McGlynn, B. L., Welker, J. M., & Seibert, J. (2005). The role of topography on catchment-scale water residence time. *Water Resources Research*, *41*(5), 1–14. http://doi.org/10.1029/2004WR003657

McNulty, B., & Farber, D. (2002). Active detachment faulting above the Peruvian flat slab. *Geology*, *30*(6), 567–570. http://doi.org/10.1130/00917613(2002)030<0567:ADFATP>2.0.CO;2

Mourre, L., Condom, T., Junquas, C., Lebel, T., E. Sicart, J., Figueroa, R., & Cochachin, A. (2016). Spatio-temporal assessment of WRF, TRMM and in situ precipitation data in a tropical mountain environment (Cordillera Blanca, Peru). *Hydrology and Earth System Sciences*, *20*(1), 125–141. http://doi.org/10.5194/hess-20-125-2016

Muir, D. L., Hayashi, M., & Mcclymont, A. F. (2011). Hydrological storage and transmission characteristics of an alpine talus. *Hydrological Processes, 25*(19), 2954–2966. http://doi.org/10.1002/hyp.8060

Petford, N., & Atherton, M. (1996). Na-rich Partial Melts from Newly Underplated Basaltic Crust: the Cordillera Blanca Batholith, Peru. *Journal of Petrology, 37*(6), 1491–1521. http://doi.org/10.1093/petrology/37.6.1491

Polk, M. H. (2016). " They Are Drying Out " : Social-Ecological Consequences of Glacier Recession on Mountain Peatlands in Huascarán National Park , Peru. Doctoral Dissertation, University of Texas, Austin, TX

Polk, M. H., Young, K. R., Baraer, M., Mark, B. G., McKenzie, J. M., Bury, J., & Carey, M. (2017). Exploring hydrologic connections between tropical mountain wetlands and glacier recession in Peru's Cordillera Blanca. *Applied Geography, 78*(January), 94–103. http://doi.org/10.1016/j.apgeog.2016.11.004

Portes, R. de C., Spinola, D. N., Reis, J. S., Ker, J. C., Costa, L. M. da, Fernandes Filho, E. I., … Schaefer, C. E. G. R. (2016). Pedogenesis across a climatic gradient in tropical high mountains, Cordillera Blanca, Peruvian Andes. *Catena, 147*, 441–452. http://doi.org/10.1016/j.catena.2016.07.027

Pouyaud, B., Zapata, M., Yerren, J., Gomez, J., Rosas, G., Suarez, W., & Ribstein, P. (2005). On the future of the water resources from glacier melting in the Cordillera Blanca, Peru. *Hydrological Sciences Journal, 50*(6), 999–1022. http://doi.org/10.1623/hysj.2005.50.6.999

Rabatel, A., Francou, B., Soruco, A., Gomez, J., Cáceres, B., Ceballos, J. L., ... & Scheel, M. (2013). Current state of glaciers in the tropical Andes: a multi-century perspective on

glacier evolution and climate change. *The Cryosphere*, 7(1), 81. http://doi.org/10.5194/tc-7-81-2013

Racoviteanu, A. E., Arnaud, Y., Williams, M. W., & Ordoñez, J. (2008). Decadal changes in glacier parameters in the Cordillera Blanca, Peru, derived from remote sensing. *Journal of Glaciology, 54*(186), 499–510. http://doi.org/10.3189/002214308785836922

Roy, J. W., & Hayashi, M. (2009). Multiple, distinct groundwater flow systems of a single moraine-talus feature in an alpine watershed. *Journal of Hydrology*, *373*(1–2), 139–150. http://doi.org/10.1016/j.jhydrol.2009.04.018

Salzmann, N., Huggel, C., Rohrer, M., Silverio, W., Mark, B. G., Burns, P., & Portocarrero, C. (2013). Glacier changes and climate trends derived from multiple sources in the data scarce Cordillera Vilcanota region, southern Peruvian Andes. *Cryosphere*, *7*(1), 103–118. http://doi.org/10.5194/tc-7-103-2013

Schaner, N., Voisin, N., Nijssen, B., & Lettenmaier, D. P. (2012). The contribution of glacier melt to streamflow. *Environmental Research Letters*, *7*(3), 034029. http://doi.org/10.1088/1748-9326/7/3/034029

Schauwecker, S., Rohrer, M., Acuña, D., Cochachin, A., Dávila, L., Frey, H., ... & Loarte, E. (2014). Climate trends and glacier retreat in the Cordillera Blanca, Peru, revisited. *Global and planetary change*, 119, 85-97. http://doi.org/10.1016/j.gloplacha.2014.05.005

Schauwecker, S., Rohrer, M., Huggel, C., Endries, J., Montoya, N., Neukom, R., … Suarez, W. (2017). The freezing level in the tropical Andes, Peru: An indicator for present and future glacier extents. *Journal of Geophysical Research, 122*(10), 5172–5189. http://doi.org/10.1002/2016JD025943

Somers, L. D., McKenzie, J. M., Zipper, S. C., Mark, B. G., Lagos, P., & Baraer, M. (2018). Does hillslope trenching enhance groundwater recharge and baseflow in the Peruvian Andes? *Hydrological Processes*, *32*(3), 318–331. http://doi.org/10.1002/hyp.11423

Somers, L., Gordon, R., McKenzie, J., Lauta, L., Wigmore, O., Glose, A., … Condom, T. (2016). Quantifying groundwater- surface water interactions in a proglacial valley, Cordillera Blanca, Peru. *Hydrological Processes*, *2929*(June), 2915–2929. http://doi.org/10.1002/hyp.10912

Squeo, F. a., Warner, B. G., Aravena, R., & Espinoza, D. (2006). Bofedales: High altitude peatlands of the central Andes. *Revista Chilena de Historia Natural*, *79*, 245–255. http://doi.org/10.4067/S0716-078X2006000200010

Thompson, L. G., Mosley-Thompson, E., Davis, M. E., & Brecher, H. H. (2011). Tropical glaciers, recorders and indicators of climate change, are disappearing globally. *Annals of Glaciology*, *52*(59), 23–34. http://doi.org/10.3189/172756411799096231

Vilímek, V., Klimeš, J., & Červená, L. (2015). Glacier-related landforms and glacial lakes in Huascarán National Park, Peru. *Journal of Maps*, *5647*(January), 1–10. http://doi.org/10.1080/17445647.2014.1000985

Vuille, M. (2013). El cambio climático y los recursos hídricos en los Andes Tropicales. *Banco Interamericano de Desarrollo*, 29.

Vuille, M., Carey, M., Huggel, C., Buytaert, W., Rabatel, A., Jacobsen, D., … Sicart, J. (2018). Earth-Science Reviews Rapid decline of snow and ice in the tropical Andes – Impacts , uncertainties and challenges ahead. *Earth-Science Reviews*, *176*(November 2016), 195–213. http://doi.org/10.1016/j.earscirev.2017.09.019

Vuille, M., Francou, B., Wagnon, P., Juen, I., Kaser, G., Mark, B. G., & Bradley, R. S. (2008). Climate change and tropical Andean glaciers: Past, present and future. *Earth-Science Reviews*, *89*(3–4), 79–96. http://doi.org/10.1016/j.earscirev.2008.04.002

Vuille, M., Franquist, E., Garreaud, R., Sven, W., Casimiro, L., & Cáceres, B. (2015). *Journal of Geophysical Research : Atmospheres*. http://doi.org/10.1002/2015JD023126.Received

Vuille, M., Kaser, G., & Juen, I. (2008). Glacier mass balance variability in the Cordillera Blanca, Peru and its relationship with climate and the large-scale circulation. *Global and Planetary Change*, *62*(1–2), 14–28. http://doi.org/10.1016/j.gloplacha.2007.11.003

Young, K. R. (2014a). Ecology of land cover change in glaciated tropical mountains. *Revista Peruana de Biologia*, *21*(3), 259–270. http://doi.org/10.15381/rpb.v21i3.10900

Young, K. R. (2014b). Ecology of Land Cover Change in Glaciated Tropical Mountains Ecología de los cambios de cobertura del paisaje de glaciares de montañas tropicales, *21*(December), 259–270.

Tables

Table 1. Summary of catchment morphology, including the altitudinal range (m), mean catchment elevation (masl), proportion of bedrock geology, as well as percent area coverage of glaciers and pampas. Relative groundwater contributions represent results from Baraer et al., (2015).

	Llanganuco	**Quilcayhuanca**	**Querococha**	**Pachacoto**
Alt. range (m)	3043	2436	1149	1280
Mean elev (masl)	4817	4686	4549	4756
Gl. Area (%)	42	21	2.8	16
Pampa area (%)	1.2	4.1	9.4	11.6
GW (%)	24	40	80	60

Table 2. Summary of methods and techniques used in studies of CB groundwater.

Tributary catchment	Groundwater study methods
Llanganuco	• Detailed geochemical analysis (Chavez, 2013) • Hydrochemical mixing model (Baraer et al., 2015) • Piezometer installation and time series data (Chavez, 2013) • Tracer dilution gaging (Gordon et al., 2015)
Quilcayhuanca	• Detailed geochemical analysis (Chavez, 2013) • Tracer dilution gaging (Gordon et al., 2015) • Electrical and seismic geophysical methods (Glas, 2018) • Ground penetrating radar (Maharaj, 2011) • Heat tracing and energy balance modeling (Maharaj, 2011; Somers et al., 2016) • Hydrochemical mixing model (Michel Baraer et al., 2015) • Piezometer installation and time series data (Chavez, 2013) • Shallow boreholes (Baraer et al., 2015; Chavez, 2013) • Vertical streambed temperature tracing (Maharaj, 2011)
Querococha	• Ground penetrating radar (Maharaj, 2011) • Hydrochemical mixing model (Baraer et al., 2015) • Shallow boreholes (Maharaj, 2011) • Vertical streambed temperature tracing (Maharaj, 2011)
Pachacoto	• Hydrochemical mixing model (Baraer et al., 2015)

Figures

Figure 1. Callejon de Huaylas drainage basin and watershed characteristics. Pampa wetland delineation was automated, using flat valley bottoms above 3500 masl as boundary conditions59. Projected freezing line heights (FLH) for optimistic (RCP 2.6) and pessimistic (RCP8.5) climate modeling scenarios, taken from Schauwecker et al., (2017). Digital elevation model derived from Advanced Spaceborne Thermal Emission and Reflection Radiometer-derived digital elevation model with a cell size of 30 m. Glaciers delineated using Global Land Ice Measurements from Space database88

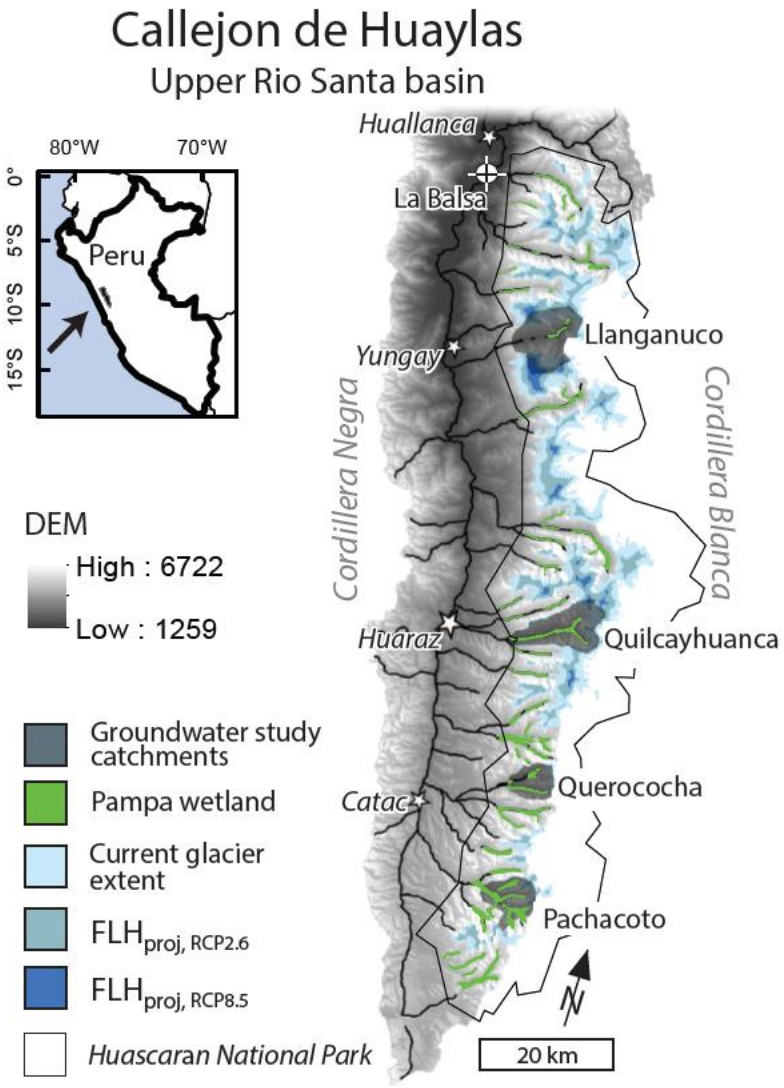

Figure 2. (a) Proglacial lakes in the upper Llanganuco valley, partially filled with sediment. (b-d) Hypothesized pampa formation includes the infilling of lakes with sediment, which occupies the uppermost sections of submerged talus. White arrow indicates direction of glacial retreat. Darker Green area along lake bottom is representative of coarse grained talus that is infilled with fine lacustrine particles.

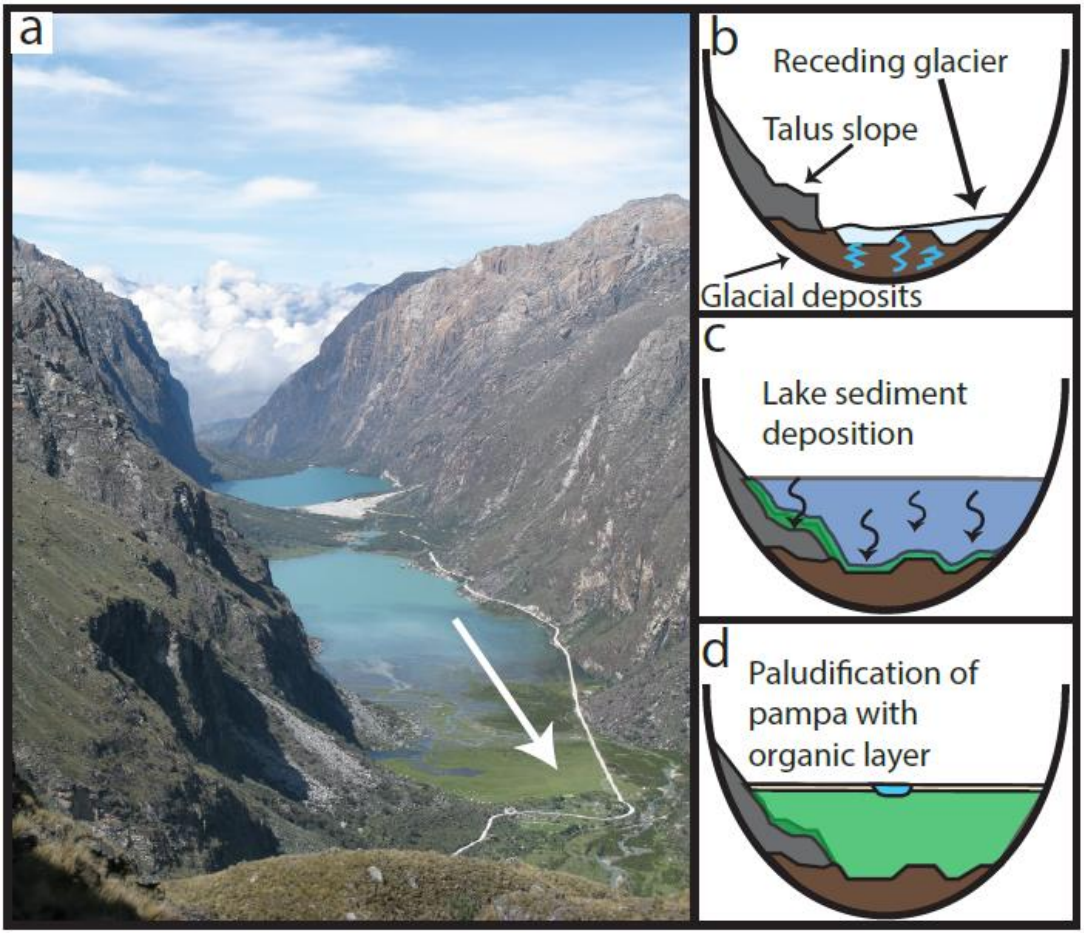

Figure 3. Photographs of pampas included in groundwater studies for the Cordillera Blanca: (a) Pachacoto , (b) Llanganuco , (c) Querococha and (d) Quilcayhuanca. Different bedrock lithology leads to wider pampa area in southern valleys (a) and (c), while pampas are narrower in (b) and (d).

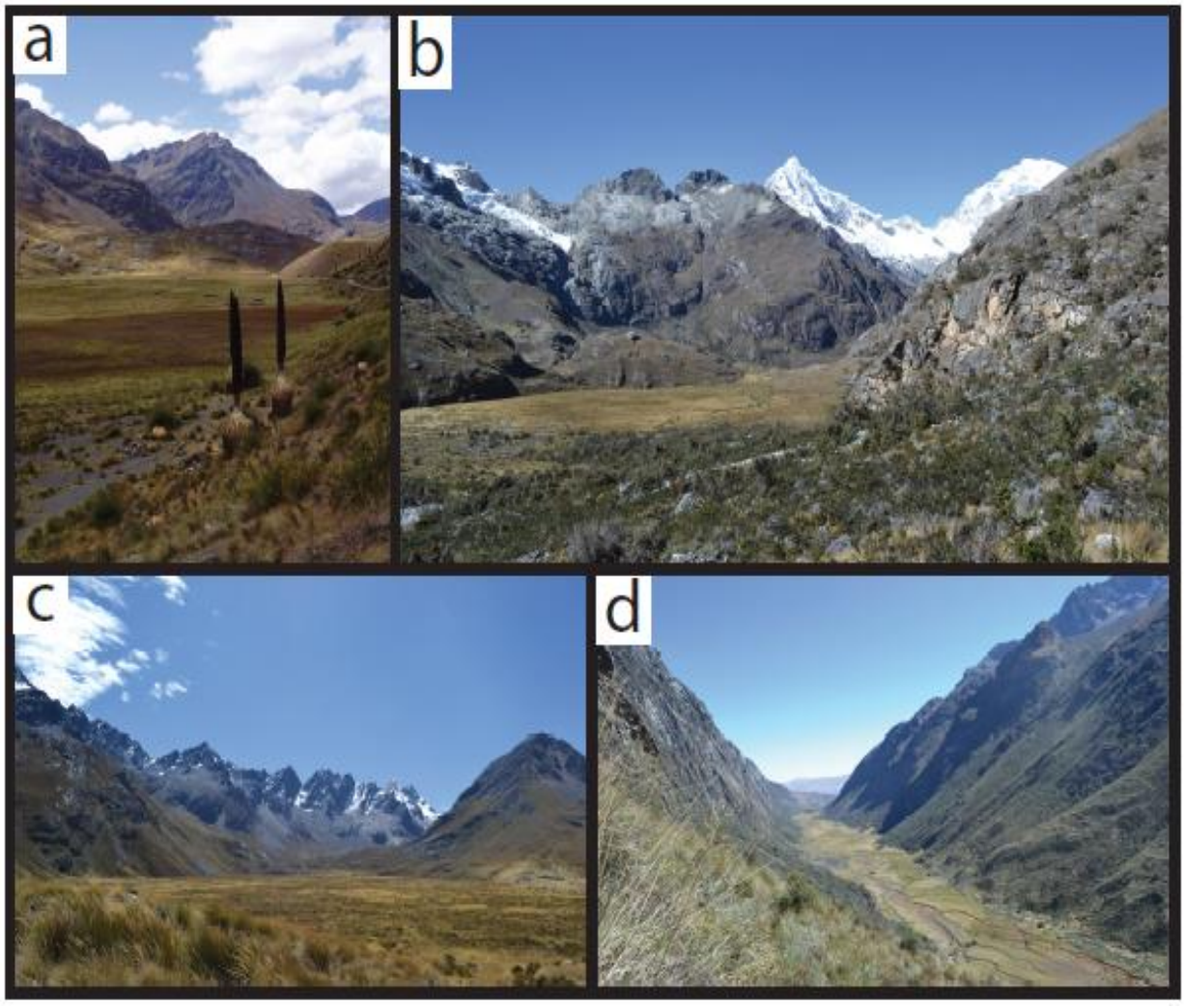

Figure 4. (a) Conceptual diagrams of groundwater flow for northern and central valleys (north of Huaraz) and (b) southern valleys (south of Huaraz) of the Cordillera Blanca. White arrows indicate direction of groundwater recharge, flow, and exchange.

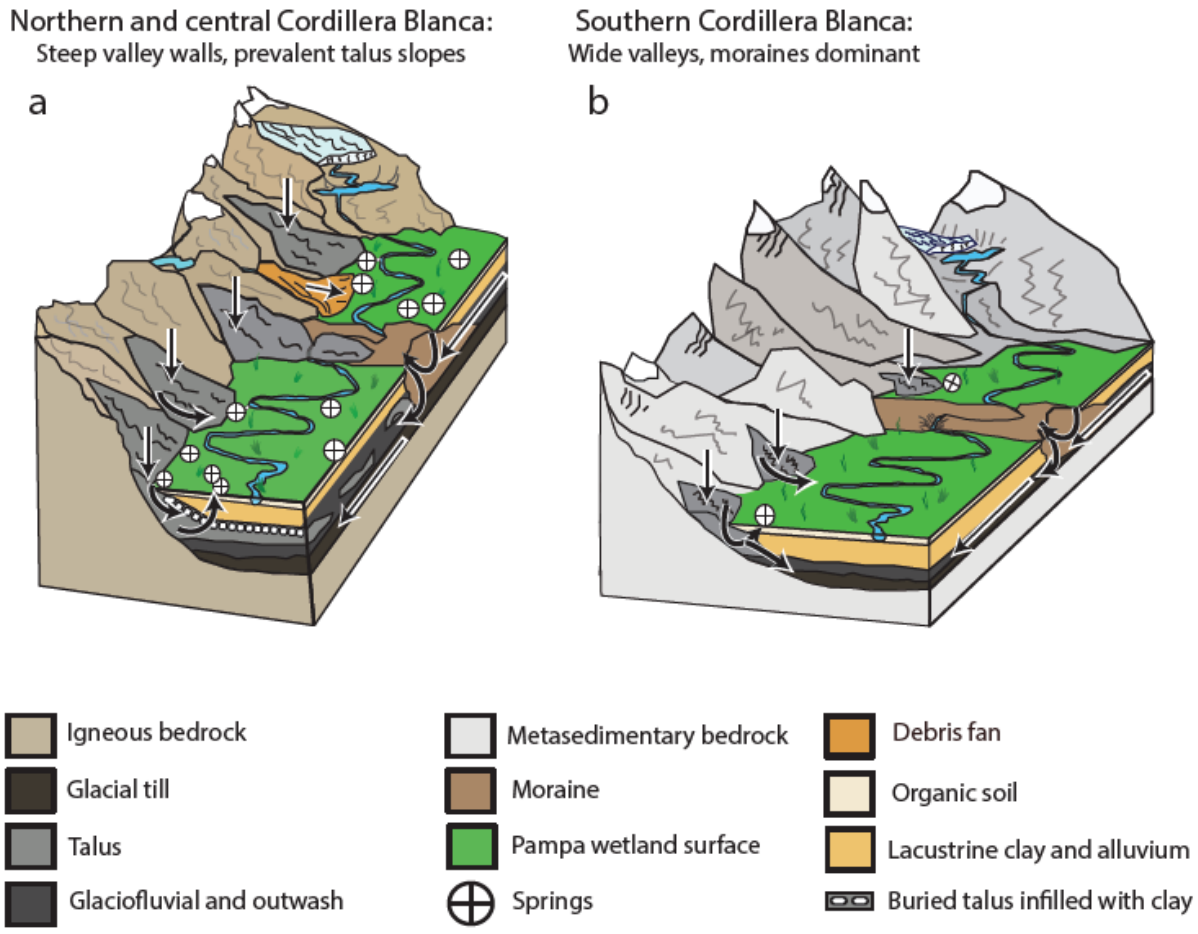

Chapter 3

Historical changes in New York State streamflow: attribution of temporal shifts and spatial patterns from 1961-2016

Abstract

To better understand the effects of climate change on streamflow, the hydrologic response to both temperature and precipitation need to be examined at the local and state-wide scale. New York State is hydrologically diverse, where regional clusters of watersheds respond differently to warming temperatures and increased seasonal precipitation rates. Connections between streamflow and climate were examined for 98 gaging stations across New York State and surrounding areas, for a historical period of 56 years of daily average streamflow. Gages were grouped into clusters if their mean annual discharge rates were strongly correlated to one another. Within each cluster, sharp temporal changes in discharge, or change points, were identified. These change points clustered both spatially and by flow regime, with high and median flows increasing in the Adirondacks and Central New York around 1970. This same time period saw shifts in only low flows in the Finger Lakes region in response to the end of a centennial drought in the Northeastern US. The difference between these regions is indicative of distinct basin-specific characteristics including land cover type and soil thickness. Low flows in the Catskills increased in 2003, which coincides with increases in summer precipitation. Our results support previous studies that have shown that streamflow in New York State is strongly tied to precipitation, and the strength of that connection is modulated by land cover, geographic position, and seasonal soil moisture conditions. Across New York State, earlier center of volume dates in the first five months of the year are inversely tied to increases in January streamflow rates, the result of warmer winter temperatures and increased precipitation as rain. The transition to the post- 1970s pluvial period also brought more frequent peak over threshold flows statewide, and this wetter period has continued to the present day.

1. Introduction

Historical trends and shifts in streamflow inform our understanding of the connections and teleconnections between stream discharge and climate. Precipitation and streamflow are typically strongly related, but can show varying degrees of disconnection due to factors such as snowpack storage, antecedent soil moisture, basin topography, land cover, and flow regulation resulting from dam releases, irrigation, and municipal allocation (Rice et al., 2015) . To examine the (dis)connections between climate variation and streamflow behavior, a state-scale analysis is useful, particularly for those states that may have complex topography and are at risk of drought and flood. State-wide, or meso-scale assessments of hydrologic change are beneficial to decision making and planning that is tailored to a specific region, municipality, or basin morphology (de Moel et al., 2015).

Changes in the magnitude, frequency, and timing of streamflow over time can be attributed to natural climatic variability, as well as anthropogenic influences such as changing land use or atmospheric forcing. Decadal-scale oscillations of atmospheric and sea surface temperatures have been associated with abrupt shifts in streamflow, while signals due to anthropogenic climate change are observed as long-term monotonic trends. This study focuses on shifts and trends in streamflow in New York State over the past half century. The timing and nature of shifts across low, median, and high flow magnitudes is compared to step increases in precipitation rates, which sheds light on the connectivity between streamflow and atmospheric processes. Similarly, changes in the frequency of high flows and the timing of spring runoff are included in our study.

The Northeastern United States has been included in a range of recent studies to better understand historical changes in climate and streamflow variability across the contiguous US

(e.g. Ahn & Palmer, 2015; Hayhoe et al., 2010; Ivancic & Shaw, 2015; McCabe & Wolock, 2014; Parr et al., 2015; Rice et al., 2015). Among these and other studies, the attribution of hydrologic change has received particular attention because the Northeastern US (NE) has undergone both shifts and trends in temperature and precipitation due to both anthropogenic and atmospheric forcing. Since the 1960s, the NE region has warmed by 0.46 - 0.7°C per decade during the winter (Burakowski et al., 2008; Hayhoe et al., 2007), accompanied by earlier spring snowmelt and lower snow-to-precipitation ratios (Dudley et al., 2017; Dyer & Mote, 2006; Hodgkins & Dudley, 2006; Huntington et al., 2004). Regionally, both precipitation and temperature have shown step increases between 1968 and 1972, marking a positive shift in the running mean and the end of a drought during the 1960s that was the most severe on record (Burakowski et al., 2008; Frei et al., 2015; Leathers et al., 2000).

In response to the end of the 1960s drought, marked increases in streamflow magnitude and shifts in timing of streamflow have been observed throughout New England and the Mid-Atlantic, including parts of New York State. The timing of annual median and minimum flows (McCabe & Wolock, 2002), mean daily flows (Ivancic & Shaw, 2017), seasonal daily flows (Sagarika et al., 2014), and flood magnitude and frequency (Armstrong et al., 2015) have been linked to wetter conditions post-1970. The 1960s drought was most severe between 1962 and 1966, and has been attributed to internal atmospheric variability as opposed to external climatic forcing (Seager et al., 2012). This record drought in the NE was also associated with cool surface temperatures, below average sea surface temperatures (SSTs), very low soil moisture, and was intensified by a persistent negative phase of the North Atlantic Oscillation (NAO) (Bradbury et al., 2002; Namias, 1966). Although the 1960s drought is indicative of record drought conditions, these conditions were more similar to pre-1960s precipitation amounts than

the post-1970s wetter conditions that brought higher extreme precipitation and higher total annual rain amounts to the region (Pederson et al., 2013).

Both the magnitude and frequency of very heavy precipitation events have increased by 71% over the last century in the NE (Guilbert et al., 2015), with more stations across the Northeast exhibiting wetter precipitation trends from 1961 to 2000, in contrast to 1926 to 1960 (Griffiths & Bradley, 2007). Corresponding upward trends in annual peak discharge have been observed in parts of New England (Collins, 2009a), however flood frequency, magnitude and duration have shown more fragmented patterns in the NE (Archfield et al., 2016). The NE has also exhibited increases in the 5-, 10-, and 20- year return period flow rates and peak annual flows since 1963 (Barrett & Salis, 2017), but annual maximum daily flows across the region have not shown such increases (Ahn & Palmer, 2015). These fragmented spatial patterns of flooding in the presence of more frequent and larger heavy precipitation events reflect the complex relationships between landscape properties, climate regime, antecedent moisture conditions, and flood generation (Ivancic & Shaw, 2015; Viglione et al., 2016). The spatially variable conditions that influence the temporal behavior of streamflow underline the importance of exploring historical trends and patterns at detailed spatial scales.

Most historical analyses of hydrologic change have considered undisturbed (reference) watersheds from the Geospatial Attributes of Gages for Evaluating Streamflow (GAGES II, Falcone et al., 2010) dataset, which consists of multiple basin characteristics for more than 9000 gages maintained by the US Geological Survey (USGS) across the US. A subset of more than 1500 reference watersheds in this data set are considered to be relatively free of human disturbances, and are defined as pristine catchments with the absence of upstream control structures, extractions, pumping, or diversions with at least 20 years of continuous data

(Whitfield et al., 2012). Historical analyses of streamflow behavior have largely focused on these reference watersheds (e.g. Archfield et al., 2016; Collins, 2009b; Demaria et al., 2016; McCabe & Wolock, 2014; Sagarika et al., 2014), where observed temporal variability in streamflow characteristics can be more confidently linked to long-term trends or abrupt shifts in climate. To expand spatial coverage beyond the limitations of reference watersheds, some investigators have cautiously included non-reference watersheds that exhibit varying degrees of regulation based on the assumption that natural signals can be identified in streams with limited human disturbance (Barrett & Salis, 2017; Rice et al., 2015). Ivancic and Shaw (2017) included both regulated and reference gages in a cluster analysis of change point timing of mean annual flow across the US from 1940 to 2014. They attributed spurious spatial distribution of streamflow patterns to human influence, whereas change points associated with climatic forcing were assumed to occur in grouped clusters.

In this study, we assess changes across multiple flow magnitude, frequency, and timing metrics for gages in New York State and adjacent areas over the past half century using a combination of trend and change point analysis. Our study includes both reference and non-reference watersheds to maximize the potential for natural signal detection, with the assumption that consistent spatially clustered patterns observed at multiple watersheds are likely due to climatic controls. We then compare results to long-term changes and shifts in temperature in temperature and precipitation in the context of geographic position of the gage's corresponding cluster. The timing of change points provides insight into the connections between streamflow and atmospheric processes, while the presence of long-term trends indicates external forcing by anthropogenic climate change. This study provides an account of change across a diverse range of flow variables, with high spatial coverage across elevations, climate divisions, and large

drainage basins (Figure 1). Our statewide approach informs a regional understanding of the connections between streamflow and climate, and provides a historical framework from which future predictions in streamflow can be refined based on long-term climate change.

1.1 Study Area

In the Northeastern US, atmospheric moisture is transferred from the Atlantic Ocean, the Gulf of Mexico, and the Great Lakes, with snowmelt an increasingly important hydrologic driver as elevation and latitude increase. New York State (NYS) is at the intersection of the New England, Mid-Atlantic, Ohio, and Great Lakes hydrologic regions and varies in elevation by more than 1600 m (Figure 1). The underlying bedrock of the state is largely Devonian sedimentary rock, with a crystalline metamorphic dome to the North that comprises the Adirondack Mountains, and areas near New York City that consists of highly metamorphosed rock at the northern edge of the US East Coast Piedmont region. For most of the state, glacial deposits and erosional features dominate the landscape in the form of the glacially scoured lakes, thick alluvial and till deposits and lacustrine sediment-filled basins that are rich in clay and silt. The Appalachian plateau to the south includes the Catskill Mountains that reach elevations of 1200 m. The highlands of the north and south are divided by a lowland region that spans from the Great Lakes, through the Mohawk River valley toward the Hudson valley to the East.

The humid continental climate of New York State spans 10 US climatological divisions (www.ncdc.noaa.gov) controlled by large-scale atmospheric circulation, topography, and large lake systems. The temperature regimes in the region are highly seasonal, while precipitation remains relatively constant throughout the year. Large precipitation events in New York State are produced by westerly Alberta Clippers, coastal ‘Noreasters, and warm season tropical systems that originate in the Gulf of Mexico (Frei et al., 2015). Hydrologic regimes in upstate New York

(north of New York City) are characterized by summer low flows and large snowmelt-driven spring runoff pulses (Shaw et al., 2006). In areas of New York State to the east and south of the Great Lakes, large lake-effect precipitation events are commonly observed in the fall and winter from warm lake waters, with high intensity snow events occurring in December and January (Briley et al., 2017). Several studies of hydrologic change have focused on the Catskill region because of its role as the principal source of New York City's water supply (Burns et al., 2007; Cockburn & Garver, 2015; Gianfagna et al., 2015; Matonse & Frei, 2013; Pradhanang et al., 2013; Seager et al., 2012). The Catskills, like the Adirondacks, are largely mountainous and forested, while much of the Finger Lakes region and western NYS contain high amounts of both forest and cropland (Figure 1a). Southeastern portions of the state, including New York City and Long Island are highly urbanized, and stream gages in this area and other urbanized areas of the state can be expected to reflect a high amount of regulation in their records (Busciolano, 2005).

2. Data and Methods

2.1 Data

The data sets used in this analysis include daily average discharge at 98 gaging stations maintained by the U.S. Geological Survey (USGS) throughout New York State and surrounding areas, which includes 14 reference watersheds of minimal disturbance and 84 gages throughout the state that exhibit some degree of human influence (Table 1). Records were selected with more than eight continuous years of data for every decade from water years 1961 to 2016, and incomplete records were extended using the monthly mean and Streamflow Record Extension Facilitator (SREF, Granato, 2008, Table 2). The SREF methodology uses the line of organic correlation (LOC) to predict flows for missing daily records from highly correlated, neighboring stations by minimizing errors in both the horizontal and vertical directions. The MOVE.3

(Maintenance of variance, Vogel & Stedinger, 1985) was used for this analysis within the SREF platform. Complete records that were used in the MOVE.3 calculations are referred to here as index gages, and were determined by the strength of correlation to the station with missing values (Gazoorian, 2015). After employing the SREF-MOVE.3 gap filling technique, 87% of the gages used in this study contain 56 years of continuous record (starting in 1961), while the remaining13% of gages have start dates between 1963 and 1975. The drainage areas associated with each gage in this study varied over three orders of magnitude, from approximately 10 km^2 to 9000 km^2 (Table 1), and are distributed throughout the state across land cover types, climate regions, and elevations (Figure 1).

We used monthly precipitation and temperature data from the Parameter Elevation Regressions on Independent Slopes Model (PRISM) dataset (http://www.prism.oregonstate.edu) for a record length of 1962 to 2016. This gridded dataset is based on interpolative calculations of meteorological station data, with consideration of topography, slope, orographic, and coastal effects (Daly et al., 1994). Monthly gridded PRISM data were resampled from 4 km to 800 m grids, and spatially averaged over the watershed area for each associated stream gage in our study. Time series of monthly values were aggregated by season for water years 1962-2016 for trend and change point detection.

2.2 Spatial Clustering

Spatial correlation across stream gages reduces the number of signals detected when investigating trends and change points over many sites, and should not be ignored when performing hypothesis tests across a region (Douglas et al., 2000). To address this, the daily streamflow records were aggregated to mean annual flow, and standardized by subtracting the mean and dividing by the series standard deviation as in McCabe and Wolock (2014). Pearson

correlation coefficients were computed against all possible pairs of normalized records, and the difference from unity was used as a measure of dissimilarity between gages. At the start, each gage was assigned to its own cluster, then joined iteratively with its most similar cluster until only a single cluster remained. For this study, six total clusters were chosen in order to represent the diverse topography and climate regions of New York State. These clusters contain groups of stream gages with similar annual mean time series (function 'hclust' from the R package 'stats', R Core team, 2015). Spatial clustering provides a framework for examining regional variability in streamflow, and can inform our understanding of how streamflow responds to basin drainage boundaries, land cover, and flow regulation. Although all gages in the Northeast are correlated to each other to a certain degree ($r > 0.5$, McCable and Wolock, 2014), this type of spatial grouping can help explain shifts in streamflow that are caused by regional climatic processes. By explaining hydrologic phenomena in terms of clusters instead of individual gages, we can address some of the similarities between gages that arise from spatial correlation (Douglas et al., 2000).

2.3 Flow duration curves

A flow duration curve illustrates the relationship between ranked annual daily flow magnitudes and the probability of their exceedance (p). Annual flow duration curves (FDCs) were calculated for each water year across all study gages according to methods outlined by Vogel and Fennessey (1994), and annual time series were computed for the p= 0.1, 0.2, 0.3, 0.4, 0.5, 0.6, 0.7, 0.8, 0.9, and 0.99 probabilities of flow exceedance, where the highest annual flows exhibit the lowest p for each water year. By including this wide range of flow exceedance probabilities (EPs), the response of stream systems to external forcing can be explored with respect to processes that govern high, median, and low flow regimes. Low flows associated with

higher EPs are usually observed during the summer, and reflect levels of groundwater supplying base flow to watersheds. High flows with lower likelihood of exceedance may be generated by a combination of snowmelt, heavy precipitation and high antecedent soil moisture conditions, and usually occur in the spring for upstate New York. By examining the entire flow regime and how it changes over time, we can better predict the sensitivity of certain regimes (high, median, low) to changes in climate as it relates to seasonality and physical setting.

2.4 Peaks over threshold

Flood and high flow frequency were examined over the 56 year period using a peaks-over-threshold (POT) technique, where a POT sample consists of the occurrence of average daily discharge value above a chosen threshold (Lang et al., 1999). This technique of evaluating peak flows increases the sample size to more than one event per year, as is the case with the annual peak flow time series. Threshold selection for this method can be carried out in a variety of ways, such as the lowest annual peak flow for the time series or an average of three to four peaks per year (Langbein, 1949; Reed & Robson, 1999). Irving and Waylen (1986) suggested a return period of 1.2 to 2 years as a threshold, and it has also been suggested to set the threshold according to physical overflowing water level of a specific stream (bankfull, e.g. Karim et al., 2017). We based our threshold detection on statistical properties of the daily average discharge series for each station, similar to the method of threshold selection presented by Madsen et al. (1997, Equation 1).

$$Q_t = \mu_q + k\sigma_q \quad (1)$$

Where the threshold (Q_t) is calculated based on the mean of the series (μ_q) summed with its standard deviation (σ_q) multiplied by a frequency factor of 1.5, which is lower than the value of

k=3 used by Madsen et al. (1997). A choice of k=1.5 leads to a lower threshold and includes more data than a choice of k=3, necessitating rigorous testing for independence of each peak.

The peaks occurring above Q_t for each water year were tested for independence to ensure that more than one peak was not counted for a single flood or high flow event. Independence criteria have varied in the literature, for example, Cunnane (1979) suggested that the local minimum discharge value between any two peaks should be smaller than two-thirds of the lower peak value, and that peaks should be separated by a time determined by onset timing of each peak in the hydrograph. Criteria suggested by the Water Resources Council (USWRC, 1982) identify independent peaks as separated by five days added to the logarithm of the basin area in square miles. If a pair of peaks do not meet these criteria, then the second of the two is rejected from the data set. We combined these two approaches, using the following independence criteria:

$$\Delta \geq 5 \ + \log(A)$$

$$x_{min} < \frac{2}{3}(\min[\mathrm{a}, \mathrm{b}]) \qquad 2$$

Where Δ is the separation distance between peaks, A is the contributing basin area (mi^2), x_{min} is the magnitude of the lowest flow between two successive peaks, (a) and (b). Annual occurrences of independent POT were examined for trends and change points over the period of record.

2.5 Winter- spring center of volume (WSCOV)

The timing of annual spring snowmelt was evaluated using the winter-spring center of volume (WSCOV) approach, which has been widely used in the literature to evaluate the effects of climate change in snowmelt- dominated regions (e.g. Burns et al., 2007; Dudley et al., 2017b; Hodgkins et al., 2003). The WSCOV is the Julian day where half the winter/ spring flow has passed the stream gage, evaluated only during the months January through May.

Although this day is largely controlled by spring snowmelt in the Northeastern US, it is also sensitive to rain-on-snow events, spatial distribution of snowmelt runoff, and the ratio of groundwater to snowmelt (Whitfield, 2013). These sensitivities are acknowledged and considered in the discussion section of this paper. To explore the temporal relationship between WSCOV and streamflow, monthly average flows across all gages were tested for monotonic trends and were graphically compared using LOESS smoothing. The LOESS (short for LOcal regrESSion) data smoothing method fits many regression models to local subsets of time series data in order to describe the variation in the data, point by point.

2.6 Hypothesis testing

We used the non-parametric Mann Kendall test (Kendall, 1975; Mann, 1945) to detect monotonic trends at a significance level of $\alpha=0.1$ for each FDC exceedance probability, as well as the POT and WSCOV time series. The test is a rank-based hypothesis test that is commonly used in hydrology because it is more suitable for the typical non-normal distributions of hydrometeorological variables (e.g. Anderson & Gough, 2017; Hirsch, 1982; Villarini et al., 2011). The slope of identified trends was calculated using a Sen slope estimation method (Helsel and Hirsch, 1992; Sen, 1968), which computes the mean of all possible pair-wise slopes in the data and has been widely used to evaluate trend magnitudes in hydrology (e.g. Gan, 1998; Hodgkins & Dudley, 2006).

Monotonic trends can sometimes be falsely identified in the presence of abrupt shifts in the mean of a series (McCabe & Wolock, 2002). These shifts may be attributed to the nonstationary behavior of hydrologic systems caused by stream channel adjustments (Slater et al., 2015), land cover change (Milly et al., 2008), and the interaction of long-term climate warming with oceanic-atmospheric oscillations (Vogel et al., 2011). Nonstationarity of a

watershed can also be due to human impact, permanently changing the landscape and altering soil permeability, evapotranspiration rates, and vegetative cover (Dey & Mishra, 2017). To detect the presence and timing of significant shifts in the mean, we used the non-parametric Pettitt test (Pettitt, 1979), which has been used in previous studies of hydrologic change points (e.g. Demaria et al., 2016; Sagarika et al., 2014).

3. Results

3.1 Spatial Clustering

Stream gages in this study were grouped into six clusters based on spatial clustering analysis; groupings show gauges with annual flows that are closely correlated with one another (Table 3, Figure 2). The resulting clusters were spatially coherant, although generally not confined to major basin drainage divides or to topographic position (Figure 1b). The ADKCNY cluster overlaps with the CAT cluster by approximately 1600 km^2, while it shares roughly 350 km^2 of watershed area with the FL watersheds. Most of the EA gages were clustered together in the Ohio River drainage basin, but also included two gages off the coast of Lake Erie. The Housatonic gages were generally confined to the Housatonic drainage basin, but those gages clustered in the Adirondack- Central New York (ADK-CNY) region spanned across the Mid-Atlantic and Great Lakes drainage basin, as well as across high (Adirondack highlands) and low (Mohawk valley) topographic positions. This was also the case for the Finger Lakes (FL) cluster. Most watersheds included in the Catskill (CAT) cluster were in forested areas, although some of the more southern Catskill gages were found in more urbanized areas closer to New York City and contain a high amount of dams and impoundments.

3.2 Precipitation and temperature

Trends in precipitation rates were generally driven by increasing change points, detected by the Pettitt test at a significance level of α=0.15. All changes in precipitation throughout the study period were increasing, and the year of increase depends on the regional cluster and the season of the year (Figure 3). A shift toward wetter conditions occurred in the late 1960s and early 1970s for the Housatonic, Adriondack and Catskill clusters, with a later shift toward wet summer and fall occurring in the 1980s state-wide. These shifts were significant at α=0.1, but not α=0.05 levels. Winter precipitation increased in 1972 for the ADK-CNY cluster, followed by wintertime precipitation increases occurring between 1990 and 2010 across the other regions of the state. Summertime precipitation increased across the more eastern spatial clusters (Housatonic, Catskill, ADK-CNY) in the early 2000s, while Fall increases were concentrated in the late 1980s.

Temperatures have increased across New York State by 0.14°C per decade, exhibiting similar patterns throughout the study area (Figure 4). A change point toward warmer temperatures was detected in the mid-1980s for temperatures in the winter and spring, while summer temperatures shifted upward later that decade. Although temperatures are generally getting warmer throughout the state, the LOESS regression reveals a shift from increasing to decreasing slopes during the mid-1990s in the winter. This break in slope can be explained by two anomalously cold winters (2013/2014 and 2014/2015) that have been linked to instabilities in the atmospheric jet stream over Canada (Anderson & Gough, 2017). The loss of Arctic sea ice has been associated with a weakened polar Arctic vortex, which causes colder air to reach portions of Eurasia and North America, causing anomalously cold winters (Zhang et al., 2016).

3.3 Flow duration curves

Across the gages and corresponding high (EP < 0.4), median (0.4 ≤ EP < 0.6), and low flows (EP≥ 0.6), approximately one fifth exhibited significant (α=0.1) monotonic trends without the presence of a shift or change point. All trend slopes were increasing, and ranged from 2% to 7% per decade. These trends were evident in gages representing each spatial cluster in the study. The results from the Pettitt test revealed statistically significant step changes across streamflow regimes, at a significance level of α=0.05 (Figure 5). With the exception of Long Island gages and a single gage in the FL cluster, all step increases were positive shifts toward higher flow rates, typically ranging from 20% to 40% higher for all flow regimes. Isolated gages that exhibited step changes above 100% were assumed to be altered by human interference and not typical of the shifts that would be expected due to climatic controls.

Increases in streamflow rates for given EPs occurred in the early 1970s (ADK-CNY, FL) and mid-2000s (CAT, ADK-CNY) at more than 30% of gages in each respective cluster (Figure 5). Step changes detected outside these times were assumed to be isolated occurrences and either affected by regulation or other non-climatic controls. Between 1972 and 1974, Finger Lakes low flows (exceedance probabilities greater than 60%) increased as step changes, while median and high flows did not exhibit this pattern. Similar timing was evident in the ADK-CNY region, although here the change was more concentrated in median and high flows with exceedance probabilities (EPs) at or below 40%. From the mid-1990s to mid-2000s, the CAT and ADK-CNY regions had significant increases in streamflow, particularly in mid-and low flows. Figure 6 shows these shifts in time series for a Catskill watershed (site number 01423000) and an Adirondack watershed (site number 04252500).

A limitation of the Pettitt change point test is that only the single highest magnitude change is detected, while there may be other, more subtle step changes in the record. To explore the possibility of multiple step changes, all records were re-evaluated after 1972, as well as before 1995 for the Catskill gages. For the post-1972 period, both the Finger Lakes and ADK-CNY clusters exhibited spurious decreases in flow magnitude between 1980 and 1982, while the ADK-CNY flows also increased abruptly along with the Catskills in 2003. The changes in flow magnitudes in the Catskills were further inspected using a LOESS regression procedure for Schoharie Creek at Prattsville, NY (Site ID 01350000, Figure 7). Across low (EP =0.7, 0.9), median (EP= 0.5), and high (EP= 0.1, 0.3) flow regimes, there was a period of diminished flow magnitudes during the 1960s, increasing to a higher regime in the 1970s, remaining at similar levels through the 1980s before beginning to rise again in the mid-1990s. This pattern was less pronounced in the highest (EP=0.01) and lowest (EP=0.9) flow regimes, and was apparent in most other Catskill records.

3.4 Peaks over threshold

Pettitt change point analysis reveals a point in time where a shift occurs toward more frequent peaks in all clusters over the study period (Figure 8). Shifts primarily occurred between 1968 and 1973, with some shifts toward higher frequencies in 1995 across the Mohawk Valley and Western New York. Under the assumption of non-stationarity, the POT threshold was shifted at each gage's most significant change point, to incorporate the mean and variance of the series before and after the change. Figure 9 shows the POT results with a stationary threshold (9a) and a nonstationary threshold (9b). Although accounting for non-stationarity reduced the number of watersheds exhibiting step changes, the same temporal shifts (1968-1972, 1995) were present at a significance level of $p \leq 0.10$ (Figure 9b). Shifting the threshold also gave rise to a

number of significant decreasing change-points, although these were spurious both spatially (clusters) and temporally (change point year).

3.5 Winter-spring center of volume

At almost all sites, the Julian day representing the winter-spring center of volume (WSCOV) has shifted earlier by 2 to 3 days per decade. LOESS regression lines show similar patterns in more than 75% of gages, where a steady decrease toward earlier WSCOV dates pauses during the 1980s, before continuing toward earlier dates after 1990 (Figure 10). This pause coincides with the pattern observed in the low- to median flows at Schoharie Creek (Figure 5), where flows remained relatively constant from 1980 to 1990 before continuing to increase.

The monthly average flow for January through May across all regional clusters in the state, significantly increased ($p \leq 0.1$) in the month of January, while few gages exhibited any change in flow rate in the remaining months of February-May (Figure 11). More than 60% of all gages included in this study showed significant increases in average January flow, compared to less than 5% of all gages showing increases for the rest of the winter- spring season. January flows are increasing on average 1% each year across all clusters. The LOESS curve of annual average January flow shows a strong positive trend, which decreases toward a zero slope between 1985 and 1995 before continuing its positive excursion toward 2016 (Figure 12a).

4. Discussion

Step increases that occurred in 2003 and 2004 for low flows in the CAT and ADK-CNY clusters are concurrent with a significant (α=0.05) step increase in total summer precipitation in the Catskill region. This increase coincides with the end of a severe drought in the summer and

winter of 2002 that occurred in central and southeastern portions of New York State (NOAA/ NWS, 2015). These results are consistent with increases in warm season precipitation magnitude that have been observed in the Catskills (Burns et al., 2007), New England (Hodgkins & Dudley, 2008) and a higher frequency of extreme warm season rain events in the Northeastern United States (Frei et al., 2015). Low flows are generally associated with the summer season when soil moisture conditions are at their lowest and ET is at a maximum. This linkage suggests that the step changes toward higher low flow levels were connected to summer precipitation, which may have raised the water table or lake levels in the associated basins to contribute to increased base flows (Smakhtin, 2001). During the same time period, increasing shifts were observed in winter precipitation, either in the form of rain or snow. If the precipitation is stored as snowpack, this can also raise water tables in the spring and summer, contributing to higher groundwater levels that influence summer base flows.

The increased summer precipitation in the Catskills could also be linked to increases in median and high flow conditions, although in the Catskills the most dominant high flow change point occurred in the mid- 1990s, when there was an increase in winter precipitation. In general, more winter precipitation falling as either rain or snow can lead to stronger high flow responses because this is the time of year when soil moisture is highest, either from infiltration of stored snowmelt or from winter rain events and reduced evapotranspiration (Matonse & Frei, 2013). The strongest high flow response revealed by the current study occurred between 1972 and 1974 in the ADK-CNY region, which contain the highest levels of snowpack in the state (NOAA/ NWS HRSC, 2017).

The increases in flow magnitude and frequency circa 1972 reflect numerous reported shifts in the literature from relatively dry conditions to the “post 1970s pluvial” period for the

Northeast and Mid-Atlantic regions (Ahn & Palmer, 2015; Sagarika et al., 2014). According to tree ring data and historical precipitation records, this pluvial period is unprecedented and reflects a regional regime change toward persistently wetter conditions (Pederson et al., 2013). Gages in the ADK-CNY cluster exhibited a step increase in high and median flows during this time, although the only step increases observed in the precipitation between 1968 and 1972 were for $p \leq 0.15$ for all four seasons. In 1973, the step change toward higher low flows in the Finger Lakes cluster do not seem to coincide with any step increases in precipitation. This can be because the increases are due to a more gradual increase of soil moisture and groundwater levels, or changes in land use that are conducive to higher rates of infiltration. Slight decreases in forested land cover, increases in developed land, and dam construction have been reported for this region (Suro & Gazoorian, 2011), although these changes were likely gradual, taking place over multiple years and not responsible for the 1970s change point observed throughout the region.

The beginning of the 1970s pluvial not only brought increased streamflow to the region, but also more frequent high flow events according to our POT results. The computation of the associated threshold value uses the long-term mean and standard deviation, which is likely non-stationary in nature and likely shifted upward from pre-1970 to post-1970 (McCabe & Wolock, 2002). An upward shift in the threshold should dampen the frequency of events in the higher regime, when compared with a threshold representative of a nonstationary series. In nature, this shift represents a flow regime where a new mean channel capacity may have been established by channel widening or incision (Slater et al., 2014). Even with these considerations, a shifted increase in the frequency of peak events over threshold was found in the transition from pre- to the post- 1970s pluvial across all clusters (Figure 9).

The transition from drier to wetter conditions after the 1960s drought has been associated with a shift from a very negative phase of the North Atlantic Oscillation (NAO) toward more positive and neutral phases. Frontal systems tend to pass through New York State more frequently during positive NAO phases (Notaro et al., 2006) and allow for more coastal storms to deliver moisture to the mid-Atlantic. The NAO reached a maximum in 1989, part of a decade-long positive excursion that coincides with a slow-down in the negative trend of WSCOV across the region. If the phase of the NAO had a causal relationship with the slowdown, it could either have caused more late spring precipitation, fewer winter rain events, or cooler spring temperatures that lead to later snowmelt. Positive phases of NAO have been linked to warmer temperatures in the Northeast (Notaro et al., 2006), although a positive NAO phase was linked to colder air temperatures in eastern Canada, along with a negative phase of the Atlantic Multidecadal Oscillation (AMO)(Hurrell, 1996).

The changes in streamflow observed in this study are likely the result of complex interactions between climatic variables, topography, land cover, and land use. New York State has undergone some land use change, including dam construction, agricultural land being converted to secondary forest growth, and some growth in urban impervious surfaces (Suro & Gazoorian, 2011). Dams and reservoir impoundments have been shown to lower the magnitude of high and low flows, while forested landscapes can have mixed effects on streamflow (Shaw et al., 2014). The Catskill region contains the highest concentration of dam impoundments in the state(CITE), which may partially explain the muted high flow response during the step change in the early 2000s, along with the timing of the precipitation increase, which only occurred in the summer for the CAT cluster.

The step increase in streamflow during the early 1970s in the ADKCNY and FL clusters could reflect differences in sediment thickness and land cover. Between 1971 and 1974, Low flows increased in the FL cluster, while median and high flows increased at the same time in ADKCNY. The Finger Lakes region contains thicker unconsolidated sediments and till than the Adirondack highlands, where the thickest overburden reaches more than 300 m in the glacial valley bottoms of western NY (Mullins and Hinchey, 1989, Soller et al., 1993). In the Adirondack highland region, still deposits are generally 0 to 5 m thick, although more than 30 meters of unconsolidated sediment have been observed in the northeastern tip of New York State near the Vermont border (Denny, 1974). More forested land cover and thinner Adirondack soils may not be able to support higher base flow levels, whereas in the Finger Lakes region, thicker aquifers and higher crop land coverage increases infiltration rates and leads to higher groundwater levels in a wetter climate.

Because the vast majority of shifts were positive for low, median, and high flows as well as peak frequency, it is possible that these increases would be even higher in the absence of human influence. Increases in impervious surface can increase flow magnitudes across the regime by affecting infiltration rates (Konrad & Booth, 2005), while dams and impoundments can damper high flow responses. Overall, the region surrounding New York State has undergone some conversions to urban and forested land cover, no abrupt changes have been reported in the literature for the period 1968-1972.

The monotonic trend in WSCOV dates across the state are likely driven by an increase in January streamflow. As the WSCOV date is getting earlier on average by two days per decade, January streamflow has been increasing by 10% per decade, with no other months exhibiting significant changes over the period of study. Furthermore, a deviation from the trend is observed

in the same time period for both January Flow and WSCOV, occurring between 1985 and 1998 (Figure 12). The symmetrical trend structures further support the strong linkage between the WSCOV and January streamflow rates. The January flow increases are likely attributed to a combination of warmer winters (Figure 4a), coupled with increases in winter precipitation across all clusters (Figure 3b).

5. Conclusion

Results from this study suggest that changes in streamflow have a strong connection to changes in precipitation and to geographic location. The timing of change points can provide insight into hydrologic processes that are connected to low, median and high flow regimes, as well as to flood and high flow frequency. Across New York State, seasonally fluctuating soil moisture conditions have a strong effect on flow generation for both lower and upper flow regimes. Clustered time series of streamflow reveal patterns of spatial correlation that correspond to a combination of basin characteristics, including topography, landscape position, land use, and drainage divides. Climatic controls on streamflow are observed by the coincidence of increasing shifts in seasonal precipitation and annual low, median, and high flow shifts that occur regionally across New York State. The beginning of an extended, anomalously wet period after 1970 resulted in marked increases in Adirondack high flows and Finger Lakes low flows. The transition from the 1960s to the 1970s also marks a change toward more frequent high flows, according to the POT analysis.

With the exception of the WSCOV, changes in streamflow across New York State were largely abrupt positive shifts, or change points that are associated with natural climate variability (Sagarika et al., 2014). Decadal-scale climatic oscillations are fluctuating along with warming temperature trends of 0.17°C per decade, indicating that hydrologic step changes such as those

that are observed in the historical record will be influenced by long-term, superimposed trends. More evaporative transport is expected for the Northeastern US over the next century, particularly in the winter (Hayhoe et al., 2008). Our historical analysis of change point timing suggests that winter precipitation is connected to both high and low flow regimes, and that those increases will likely continue in a warming climate. The monotonic trend detected in the WSCOV date indicates that this date will continue to advance toward earlier in the year, coupled with the continued increase of January streamflow rates, less precipitation as snow, and more overall rainfall during the winter months.

References

Ahn, K., & Palmer, R. N. (2015). Trend and Variability in Observed Hydrological Extremes in the United States. *Journal of Hydrologic Engineering*, *21*(2), 4015061. http://doi.org/10.1061/(ASCE)HE.1943-5584.0001286

Anderson, C. I., & Gough, W. A. (2017). Evolution of winter temperature in Toronto, Ontario, Canada: A case study of winters 2013/14 and 2014/15. *Journal of Climate*, *30*(14), 5361–5376. http://doi.org/10.1175/JCLI-D-16-0562.1

Archfield, S. A., Hirsch, R. M., Viglione, A., & Bloschl, G. (2016). Fragmented patterns of flood change across the United States. *Geophysical Research*, *43*. http://doi.org/10.1002/2016GL070590.Received

Barrett, K. R., & Salis, W. (2017). Prevalence and Magnitude of Trends in Peak Annual Flow and 5-, 10-, and 20-Year Flows in the Northeastern United States. *Journal of Hydrologic Engineering*, *22*(3), 4016059. http://doi.org/10.1061/(ASCE)HE.1943-5584.0001474

Bradbury, J. A., Dingman, S. L., & Keim, B. D. (2002). New England Drought and Relations With Large Scale Atmospheric Circulation Patterns. *Journal of the American Water Resources Association*, *38*(5), 1287–1299. http://doi.org/10.1111/j.1752-1688.2002.tb04348.x

Briley, L. J., Ashley, W. S., Rood, R. B., & Krmenec, A. (2017). The role of meteorological processes in the description of uncertainty for climate change decision-making. *Theoretical and Applied Climatology*, *127*(3–4), 643–654. http://doi.org/10.1007/s00704-015-1652-2

Burakowski, E. A., Wake, C. P., Braswell, B., & Brown, D. P. (2008). Trends in wintertime climate in the northeastern United States: 1965-2005. *Journal of Geophysical Research*

Atmospheres, *113*(20), 1–12. http://doi.org/10.1029/2008JD009870

Burns, D. A., Klaus, J., & McHale, M. R. (2007). Recent climate trends and implications for water resources in the Catskill Mountain region, New York, USA. *Journal of Hydrology*, 336(1–2), 155–170. http://doi.org/10.1016/j.jhydrol.2006.12.019

Busciolano, R. J. (2005). Statistical analysis of long-term hydrologic records for selection of drought-monitoring sites on Long Island, New York (No. 2004-5152). US Geological Survey.

Cockburn, J. M. H., & Garver, J. I. (2015). Abrupt change in runoff on the north slope of the Catskill Mountains, NY, USA: Above average discharge in the last two decades. *Journal of Hydrology: Regional Studies*, *3*, 199–210. http://doi.org/10.1016/j.ejrh.2014.11.006

Collins, M. J. (2009a). Evidence for changing flood risk in New England since the late 20th century. *Journal of the American Water Resources Association*, *45*(2), 279–290. http://doi.org/10.1111/j.1752-1688.2008.00277.x

Collins, M. J. (2009b). Evidence for changing flood risk in New England since the late 20th century. *Journal of the American Water Resources Association*, *45*(2), 279–290. http://doi.org/10.1111/j.1752-1688.2008.00277.x

Cunnane, C. (1979). A note on the Poisson assumption in partial duration series models. *Water Resources Research*, *15*(2), 489–494. http://doi.org/10.1029/WR015i002p00489

Daly, C., Neilson, R., & Phillips, D. (1994). Development and application of topographic descriptors for conditional analysis of rainfall. *Journal of Applied M*. http://doi.org/10.1002/asl.228

de Moel, H., Jongman, B., Kreibich, H., Merz, B., Penning-Rowsell, E., & Ward, P. J. (2015). Flood risk assessments at different spatial scales. *Mitigation and Adaptation Strategies for Global Change*, *20*(6), 865–890. http://doi.org/10.1007/s11027-015-9654-z

Demaria, E. M. C., Palmer, R. N., & Roundy, J. K. (2016). Regional climate change projections of streamflow characteristics in the Northeast and Midwest U.S. *Journal of Hydrology: Regional Studies*, *5*, 309–323. http://doi.org/10.1016/j.ejrh.2015.11.007

Denny, C. S. (1974). Pleistocene geology of the northeast Adirondack region, New York (No. 786). US Govt. Print. Off.,.

Dey, P., & Mishra, A. (2017). Separating the impacts of climate change and human activities on streamflow: A review of methodologies and critical assumptions. *Journal of Hydrology*, *548*, 278–290. http://doi.org/10.1016/j.jhydrol.2017.03.014

Douglas, E. M., Vogel, R. M., & Kroll, C. N. (2000). Trends in floods and low flows in the United States: Impact of spatial correlation. *Journal of Hydrology*, *240*(1–2), 90–105. http://doi.org/10.1016/S0022-1694(00)00336-X

Dudley, R. W., Hodgkins, G. A., & Letcher, B. H. (2008). Impacts of Low-Flow and Stream-Temperature Changes on Endangered Atlantic Salmon-Current Research (No. 2008-3044). Geological Survey (US).

Dudley, R. W., Hodgkins, G. A., McHale, M. R., Kolian, M. J., & Renard, B. (2017a). Trends in snowmelt-related streamflow timing in the conterminous United States. *Journal of Hydrology*, *547*, 208–221. http://doi.org/10.1016/j.jhydrol.2017.01.051

Dudley, R. W., Hodgkins, G. A., McHale, M. R., Kolian, M. J., & Renard, B. (2017). Trends in

snowmelt-related streamflow timing in the conterminous United States. *Journal of Hydrology*, *547*, 208–221. http://doi.org/10.1016/j.jhydrol.2017.01.051

Dyer, J. L., & Mote, T. L. (2006). Spatial variability and trends in observed snow depth over North America. *Geophysical Research Letters*, *33*(16). http://doi.org/10.1029/2006GL027258

Falcone, J. A., Carlisle, D. M., Wolock, D. M., & Meador, M. R. (2010). GAGES: A stream gage database for evaluating natural and altered flow conditions in the conterminous United States. *Ecology*, *91*(2), 621. http://doi.org/10.1890/09-0889.1

Frei, A., Kunkel, K. E., & Matonse, A. (2015). The Seasonal Nature of Extreme Hydrological Events in the Northeastern United States. *Journal of Hydrometeorology*, *16*(5), 2065–2085. http://doi.org/10.1175/JHM-D-14-0237.1

Gan, T. Y. (1998). Hydroclimatic trends and possible climatic warming in the Canadian Prairies. *Water resources research*, 34(11), 3009-3015.

Gazoorian, C. L. (2015). Estimation of unaltered daily mean streamflow at ungaged streams of New York, excluding Long Island, water years 1961-2010 (No. 2014-5220). US Geological Survey.

Gianfagna, C. C., Johnson, C. E., Chandler, D. G., & Hofmann, C. (2015). Watershed area ratio accurately predicts daily streamflow in nested catchments in the Catskills, New York. *Journal of Hydrology: Regional Studies*, *4*, 583–594. http://doi.org/10.1016/j.ejrh.2015.09.002

Granato, G. E. (2008). Computer Programs for Obtaining and Analyzing Daily Mean Streamflow

Data from the U . S . Geological Survey National Water Information System Web Site

Griffiths, M. L., & Bradley, R. S. (2007). Variations of twentieth-century temperature and precipitation extreme indicators in the northeast United States. *Journal of Climate*, 20(21), 5401-5417.

Guilbert, J., Betts, A. K., Rizzo, D. M., Beckage, B., & Bomblies, A. (2015). Characterization of increased persistence and intensity of precipitation in the northeastern United States. *Geophysical Research Letters*, 42(6), 1888-1893.

Hayhoe, K., VanDorn, J., Croley, T., Schlegal, N., & Wuebbles, D. (2010). Regional climate change projections for Chicago and the US Great Lakes. *Journal of Great Lakes Research*, *36*(SUPPL. 2), 7–21. http://doi.org/10.1016/j.jglr.2010.03.012

Hayhoe, Katharine, Cameron Wake, Bruce Anderson, Xin-Zhong Liang, Edwin Maurer, Jinhong Zhu, James Bradbury, Art DeGaetano, Anne Marie Stoner, and Donald Wuebbles. (2008). Regional climate change projections for the Northeast USA. *Mitigation and Adaptation Strategies for Global Change* 13, no. 5-6 425-436. http://doi.org/10.1007/s11027-007-9133-2

Helsel, D. R., & Hirsch, R. M. (1992). Statistical methods in water resources (Vol. 49). Elsevier.

Hirsch, R. M. (1982). A comparison of four streamflow record extension techniques. *Water Resources Research*, *18*(4), 1081–1088. http://doi.org/10.1029/WR018i004p01081

Hodgkins, G. A., & Dudley, R. W. (2006). Changes in the timing of winter-spring streamflows in eastern North America, 1913-2002. *Geophysical Research Letters*, *33*(6), 1–5. http://doi.org/10.1029/2005GL025593

Hodgkins, G. A., Dudley, R. W., & Huntington, T. G. (2003). Changes in the timing of high river flows in New England over the 20th Century. *Journal of Hydrology, 278*(1–4), 244–252. http://doi.org/10.1016/S0022-1694(03)00155-0

Huntington, T. G., Hodgkins, G. A., Keim, B. D., & Dudley, R. W. (2004). Changes in the proportion of precipitation occurring as snow in New England (1949-2000). *Journal of Climate, 17*(13), 2626–2636. http://doi.org/10.1175/1520-0442(2004)017<2626:CITPOP>2.0.CO;2

Hurrell, J. W., Kushnir, Y., Ottersen, G., & Visbeck, M. (2003). An overview of the North Atlantic oscillation. *The North Atlantic Oscillation: climatic significance and environmental impact*, 1-35.

Irvine, K. N., & Waylen, P. R. (1986). Partial Series Analysis of High Flows in Canadian Rivers. *Canadian Water Resources Journal*, *11*(2), 83–91. http://doi.org/10.4296/cwrj1102083

Ivancic, T. J., & Shaw, S. B. (2015). Examining why trends in very heavy precipitation should not be mistaken for trends in very high river discharge. *Climatic Change*, *133*(4), 681–693. http://doi.org/10.1007/s10584-015-1476-1

Ivancic, T. J., & Shaw, S. B. (2017). Identifying spatial clustering in change points of streamflow across the contiguous US between 1945 and 2009. *Geophysical Research Letters*, 44(5), 2445-2453.. http://doi.org/10.1002/2016GL072444

Karim, F., Hasan, M., & Marvanek, S. (2017). Evaluating annual maximum and partial duration series for estimating frequency of small magnitude floods. *Water (Switzerland)*, *9*(7). http://doi.org/10.3390/w9070481

Kendall, M. G. (1975). Rank Correlation Methods, Charles Griffin, London (1975).

Konrad, C., & Booth, D. (2005). Hydrologic changes in urban streams and their ecological significance. *American Fisheries Society Symposium*, 157–177. Retrieved from http://water.usgs.gov/nawqa/urban/pdf/157-178_Konrad.pdf

Lang, M., Ouarda, T. B. M. J., & Bobée, B. (1999). Towards operational guidelines for over-threshold modeling. *Journal of hydrology*, 225(3-4), 103-117.

Langbein, W. B. (1949). Annual floods and the partial-duration flood series. *Eos*, Transactions American Geophysical Union, 30(6), 879-881.

Leathers, D. J., Grundstein, A. J., & Ellis, A. W. (2000). Growing season moisture deficits across the northeastern United States. *Climate Research*, *14*(1), 43–55. http://doi.org/10.3354/cr014043

Madsen, H., Rasmussen, P. F., & Rosbjerg, D. (1997). Comparison between the peaks-over-threshold method and the annual maximum method for flood frequency analysis. *Water Resources Research*, *33*(4), 747–757. http://doi.org/10.1080/02626667.2013.831174

Matonse, A. H., & Frei, A. (2013). A seasonal shift in the frequency of extreme hydrological events in Southern New York State. *Journal of Climate*, *26*(23), 9577–9593. http://doi.org/10.1175/JCLI-D-12-00810.1

McCabe, G.J., Wolock, D. M. (2014). Spatial and temporal patterns in conterminous United States streamflow characteristics. *Geophysical Research Letters*, *41*, 6889–6897. http://doi.org/10.1002/2014GL061980.Received

McCabe, G. J., & Wolock, D. M. (2002). A step increase in streamflow in the conterminous

United States. *Geophysical Research Letters*, *29*(24), 38-1-38–4. http://doi.org/10.1029/2002GL015999

Milly, P. C., Betancourt, J., Falkenmark, M., Hirsch, R. M., Kundzewicz, Z. W., Lettenmaier, D. P., & Stouffer, R. J. (2008). Stationarity is dead: Whither water management?. *Science*, 319(5863), 573-574.

Mullins, H. T., & Hinchey, E. J. (1989). Erosion and infill of New York Finger Lakes: Implications for Laurentide ice sheet deglaciation. *Geology*, 17(7), 622-625.

Namias, J. (1966). Nature and possible causes of the Northeastern United States Drought during 1962-65. *Monthly Weather Review*, *94*(9), 543–554. http://doi.org/10.1175/1520-0493(1966)094<0543:NAPCOT>2.3.CO;2

NOAA/ National Weather Service Climate Prediction Center, Drought monitoring website (2015) http://www.cpc.ncep.noaa.gov

NOAA/ National Weather Service National Operational Hydrologic Remote Sensing Center website (2017), http://www.nohrsc.noaa.gov

Notaro, M., Wang, W.-C., & Gong, W. (2006). Model and Observational Analysis of the Northeast U.S. Regional Climate and Its Relationship to the PNA and NAO Patterns during Early Winter. *Monthly Weather Review*, *134*, 3479–3505. http://doi.org/10.1175/MWR3234.1

Parr, D., Wang, G., & Ahmed, K. F. (2015). Hydrological changes in the U.S. Northeast using the Connecticut River Basin as a case study: Part 2. Projections of the future. *Global and Planetary Change*, *133*, 167–175. http://doi.org/10.1016/j.gloplacha.2015.08.011

Pederson, N., Bell, A. R., Cook, E. R., Lall, U., Devineni, N., Seager, R., … Vranes, K. P. (2013). Is an epic pluvial masking the water insecurity of the greater New York city region. *Journal of Climate*, *26*(4), 1339–1354. http://doi.org/10.1175/JCLI-D-11-00723.1

Pettitt, A. (1979). A Non-Parametric Approach to the Change-Point Problem Published by : Wiley for the Royal Statistical Society Stable URL : http://www.jstor.org/stable/2346729 A Non-parametric Approach to the Change-point Problem, *28*(2), 126–135.

Pradhanang, S. M., Frei, A., Zion, M., Schneiderman, E. M., Steenhuis, T. S., & Pierson, D. (2013). Rain-on-snow runoff events in New York. *Hydrological Processes*, *27*(21), 3035–3049. http://doi.org/10.1002/hyp.9864

Robson, A., & Reed, D. (1999). Flood estimation handbook. Institute of Hydrology, Wallingford.

Rice, J. S., Emanuel, R. E., Vose, J. M., & Nelson, S. A. C. (2015). Their Relationships With Watershed Spatial Characteristics. *Water Resources Research*, 6262–6275. http://doi.org/10.1002/2014WR016367.Received

Sagarika, S., Kalra, A., & Ahmad, S. (2014). Evaluating the effect of persistence on long-term trends and analyzing step changes in streamflows of the continental United States. *Journal of Hydrology*, *517*, 36–53. http://doi.org/10.1016/j.jhydrol.2014.05.002

Seager, R., Pederson, N., Kushnir, Y., Nakamura, J., & Jurburg, S. (2012). The 1960s drought and the subsequent shift to a wetter climate in the Catskill Mountains region of the New York City watershed. *Journal of Climate*, *25*(19), 6721–6742. http://doi.org/10.1175/JCLI-D-11-00518.1

Sen, K. P. (2018). Estimates of the Regression Coefficient Based on Kendall â€™ s Tau Author (s): Pranab Kumar Sen Source : Journal of the American Statistical Association , Vol . 63 , No . 324 (Dec ., 1968), pp . Published by : Taylor & Francis , Ltd . on behalf of the A, *63*(324), 1379–1389. http://doi.org/10.2307/2281868

Shaw, S., Schneider, R., McDonald, A., Riha, S., & Tryhorn, L. Robin Leichenko, 4 Peter Vancura, 4 Allan Frei, 5 and Burrell Montz6 Sector Lead 2 Cornell University, Department of Earth and Atmospheric Sciences 3 Cornell University, Department of Natural Resources 4 Rutgers University, Department of Geography.

Shaw, S. B., Marrs, J., Bhattarai, N., & Quackenbush, L. (2014). Longitudinal study of the impacts of land cover change on hydrologic response in four mesoscale watersheds in New York State, USA. *Journal of Hydrology*, *519*(PA), 12–22. http://doi.org/10.1016/j.jhydrol.2014.06.055

Slater, L. J., Singer, M. B., & Kirchner, J. W. (2015). Hydrologic versus geomorphic drivers of trends in flood hazard. *Geophysical Research Letters*, 42(2), 370-376. http://doi.org/10.1002/2014GL062482.

Smakhtin, V. U. (2001). Low flow hydrology: A review. *Journal of Hydrology*, *240*(3–4), 147–186. http://doi.org/10.1016/S0022-1694(00)00340-1

Soller, D.R., 1993, Map showing the thickness and character of Quaternary sediments in the glaciated United States east of the Rocky Mountains—Northeastern states, the Great Lakes, and parts of southern Ontario and the Atlantic offshore area (east of 80°31′ west longitude): U.S. Geological Survey Miscellaneous Geologic Investigations Map I-1970-A, scale 1:1,000,000, available at http://ngmdb. usgs.gov/Prodesc/proddesc_10047.htm

Suro, T. P., & Gazoorian, C. L. (2011). Changes in low-flow frequency from 1976-2006 at selected streamgages in New York, excluding Long Island (No. 2011-5112). US Geological Survey.

USWRC (United States. Interagency Advisory Committee on Water Data. Hydrology Subcommittee), 1982. Guidelines for deter- mining flood flow frequency. Reston, VA: US Department of the Interior, Geological Survey, Office of Water Data Coordination.

Viglione, A., Merz, B., Viet Dung, N., Parajka, J., Nester, T., & Blöschl, G. (2016). Attribution of regional flood changes based on scaling fingerprints. *Water resources research*, 52(7), 5322-5340.

Villarini, G., Smith, J. A., Ntelekos, A. A., & Schwarz, U. (2011). Annual maximum and peaks-over-threshold analyses of daily rainfall accumulations for Austria. *Journal of Geophysical Research Atmospheres*, *116*(5), 1–15. http://doi.org/10.1029/2010JD015038

Vogel, R. M., & Fennessey, N. M. (1994). Flow-Duration Curves. I: New Interpretation and Confidence Intervals. *Journal of Water Resources Planning and Management*, *120*(4), 485–504. http://doi.org/10.1061/(ASCE)0733-9496(1994)120:4(485)

Vogel, R. M., & Stedinger, J. R. (1985). Minimum variance streamflow record augmentation procedures. *Water Resources Research*, *21*(5), 715–723. http://doi.org/10.1029/WR021i005p00715

Vogel, R. M., Yaindl, C., & Walter, M. (2011). Nonstationarity: Flood magnification and recurrence reduction factors in the united states. *Journal of the American Water Resources Association*, *47*(3), 464–474. http://doi.org/10.1111/j.1752-1688.2011.00541.x

Whitfield, P. H. (2013). Is “Centre of Volume” a robust indicator of changes in snowmelt timing? *Hydrological Processes*, *27*(18), 2691–2698. http://doi.org/10.1002/hyp.9817

Whitfield, P. H., Burn, D. H., Hannaford, J., Higgins, H., Hodgkins, G. A., Marsh, T., & Looser, U. (2012). Reference hydrologic networks I. The status and potential future directions of national reference hydrologic networks for detecting trends. *Hydrological Sciences Journal*, *57*(8), 1562–1579. http://doi.org/10.1080/02626667.2012.728706

Zhang, J., Tian, W., Chipperfield, M. P., Xie, F., & Huang, J. (2016). Persistent shift of the Arctic polar vortex towards the Eurasian continent in recent decades. *Nature Climate Change*, 6(12), 1094.

Tables

Table 1. US Geological Survey stream gages included in historical trend and changepoint analysis. Locations, drainage area, and length of historical records are listed for both reference gages (*) and gages that exhibit some degree of regulation.

*reference watersheds with minimum human disturbance

STATION ID	NAME	DRAINAGE AREA (KM^2)	LAT	LONG	LENGTH OF RECORD (YRS)
1197500	Housatonic River near Great Barrington, MA	730.38	42.23192	-73.3547	56
1199000	Housatonic River at Falls Village, CT	1642.06	41.95732	-73.3693	56
1199050	Salmon Creek at Lime Rock, CT	76.146	41.94232	-73.391	55
1200000	Tenmile River near Gaylordsville, CT	525.77	41.65876	-73.5287	56
1200500	Housatonic River at Gaylordsville, NY	2579.64	41.65315	-73.4898	56
1208990*	saugatuck River near Redding, CT	54.39	41.29454	-73.3951	52
1304000	Nissequogue River near Smithtown, NY	69.93	40.84944	-73.2242	56
1304500	Peconic River at Riverhead, NY	193.473	40.91361	-72.6867	56
1305500	Swan River at East Patchogue, NY	20.9013	40.76694	-72.9936	56
1308000	Sampawams Creek at Babylon, NY	58.793	40.70417	-73.3139	56
1308500	Carlls River at Babylon, NY	91.686	40.70861	-73.3283	56
1309500	Massapequa Creek at Massapequa, NY	99.974	40.68889	-73.4547	56
1311500	Valley Stream at Valley Stream, NY	9.7643	40.66361	-73.7044	56
1315500	Hudson River at North Creek, NY	2051.28	43.70083	-73.9833	56
1318500	Hudson River at Hadley, NY	4309.76	43.31889	-73.8442	56
1321000	Sacandaga River near Hope, NY	1271.69	43.35278	-74.2703	56
1325000	Sacandaga River at Stewarts Bridge near Hadley, NY	2732.45	43.31139	-73.8672	56
1331500	Hoosic River at Adams, MA	120.953	42.61119	-73.124	56
1333000*	Green River at Williamstown, MA	110.334	42.70897	-73.1968	56
1334000	Walloomsac River near North Bennington, VT	287.49	42.91286	-73.2565	56
1334500	Hoosic River near Eagle Bridge, NY	1320.9	42.93861	-73.3769	56
1336000	Mohawk River below Delta Dam near Rome, NY	393.68	43.26444	-75.4364	56
1347000	Mohawk River near Little Falls, NY	3475.78	43.01472	-74.7794	56
1350000*	Schoharie Creek at Prattsville, NY	613.83	42.31944	-74.4367	56
1351500	Schoharie Creek at Burtonsville, NY	2294.74	42.8	-74.2628	56
1357500	Mohawk River at Cohoes, NY	8935.5	42.78528	-73.7075	56
1362200*	Esopus Creek at Allaben, NY	164.983	42.11694	-74.3803	53
1362500	Esopus Creek at Coldbrook, NY	497.28	42.01417	-74.2706	56
1365000*	Rondout Creek near Lowes Corners, NY	99.197	41.86639	-74.4872	56
1371500	Wallkill River at Gardiner, NY	1800.05	41.68611	-74.1653	56
1372500	Wappinger Creek near Wappingers Falls, NY	468.79	41.65306	-73.8725	56

1375000	Croten River at New Croton Dam	979.02	41.22503	-73.8589	56
1376800	Hackensack River at West Nyack, NY	79.513	41.09556	-73.9639	56
1377000	Hackensack River at Rivervale, NJ	150.22	40.99917	-73.9892	56
1413500*	East Branch Delaware River at Margaretville, NY	422.17	42.14472	-74.6536	56
1414500*	Mill Brook near Dunraven, NY	65.268	42.10611	-74.7306	56
1415000*	Tremper Kill near Andes, NY	85.988	42.12	-74.8186	56
1417000	East Branch Delaware River at Downsville, NY	963.48	42.075	-74.9764	56
1420500	Beaver Kill at Cooks Falls	624.19	41.94639	-74.9797	56
1423000*	West Branch Delaware River at Walton, NY	859.88	42.16611	-75.14	56
1425000	West Branch Delaware River at Stilesville, NY	1181.04	42.07472	-75.3961	56
1426500	West Branch Delaware at Hale Eddy, NY	1541.05	42.00306	-75.3836	56
1428500	Delaware River near Barryville NY	5231.8	41.50889	-74.9858	56
1434000	Delaware River at Port Jervis, NY	7951.3	41.37056	-74.6975	56
1435000*	Neversink River near Claryville, NY	172.494	41.89	-74.59	56
1436000	Neversink River at Neversink, NY	239.834	41.82	-74.6356	56
1437500	Neversink River at Godeffroy, NY	795.13	41.44111	-74.6019	56
1438500	Delaware River at Montague, NJ	9013.2	41.30917	-74.7953	56
1440000*	Flat Brook near Flatbrookville, NJ	165.76	41.10611	-74.9525	56
1500000	Ouleout Creek at East Sidney, NY	266.77	42.33333	-75.235	56
1503000	Susquehanna River at Conklin, NY	5780.88	42.03528	-75.8031	56
1509000	Tioughnioga River at Cortland, NY	756.28	42.60278	-76.1594	56
1512500	Chenango River near Chanango Forks, NY	3840.97	42.21806	-75.8483	56
1518000	Tioga River at Tioga, PA	730.38	41.90841	-77.1294	56
1520000	Cowanesque River near Lawrenceville, PA	771.82	41.99674	-77.14	56
1521500	Canisteo River at Arkport, NY	79.254	42.39583	-77.7114	56
1523500	Canacadea Creek near Hornell, NY	149.961	42.33472	-77.6831	56
1524500	Cansisteo River at Hornell, NY	409.22	42.31389	-77.6511	56
1526500	Tioga River near Erwins, NY	3566.43	42.12111	-77.1292	56
1529500	Cohocton River near Campbell, NY	1217.3	42.2525	-77.2167	56
1529950	Chemunch River at Corning, NY	5195.54	42.14639	-77.0575	42
1531000	Chemung River at Chemung, NY	6490.54	42.00222	-76.6347	56
1542810*	Waldy Run near Emporium, PA	13.5716	41.57895	-78.2925	52
3007800	Allegheny River at Port Allegany, PA	642.32	41.81868	-78.2928	42
3010500	Allegheny River at Eldred, PA	1424.5	41.9634	-78.3861	56
3011020	Allegheny River at Salamanca, NY	4164.72	42.15639	-78.7153	56
3011800*	Kinzua Creek near Guffey, PA	100.492	41.76645	-78.7186	51
3014500	Chandokoin River at Falconer, NY	502.46	42.1125	-79.2039	56
3015500*	Brokenstraw Creek at Youngsville, PA	831.39	41.85256	-79.3173	56
3021350*	French Creek near Wattsburg, PA	238.28	42.01533	-79.7826	42
4215500	Cazenovia Creek at Ebenezer, NY	349.65	42.82972	-78.775	56
4218518	Ellicott Creek below Williamsville, NY	211.344	42.97778	-78.7636	44
4223000	Genesee River at Portageville, NY	2548.56	42.57028	-78.0422	56
4224775*	Canaseraga Creek above Dansville, NY	230.251	42.53556	-77.7042	42

4227500	Genesee River near Mount Morris, NY	3688.16	42.76667	-77.8389	56
4228500	Genesee River at Avon, NY	4333.07	42.91778	-77.7572	56
4230380	Oatka Creek at Warsaw, NY	101.269	42.74417	-78.1375	53
4230500	Oatka Creek at Garbutt, NY	518	43.01	-77.7914	56
4231000	Black Creek at Churchville NY	336.7	43.10056	-77.8822	56
4231600	Genesee River at Ford St Bridge	6407.66	43.14172	-77.6163	56
4232050	Allen Creek near Rochester, NY	77.959	43.13028	-77.5186	56
4232482	Keuka Lake Outlet at Dresden, NY	536.13	42.68028	-76.9539	52
4234000	Fall Creek near Ithaca, NY	326.34	42.45333	-76.4728	56
4235000	Canandaigua Outlet at Chapin, NY	505.05	42.91806	-77.2328	56
4239000	Onondaga Creek at Dorwin Ave, Syracuse, NY	229.215	42.98333	-76.1508	56
4240010	Onondaga Creek at Spencer St, Syracuse	284.9	43.0575	-76.1625	46
4240120	Ley Creek at Park St, Syracuse, NY	77.441	43.07722	-76.1703	56
4240300	Ninemile Creeke at Lakeland, NY	297.85	43.08083	-76.2264	56
4243500	Oneida Creek at Oneida, NY	292.67	43.0975	-75.6392	56
4252500	Black river Near Boonville, NY	787.36	43.51167	-75.3067	56
4256000*	Independence River at Donnattsburg NY	229.733	43.74681	-75.3334	56
4258000	Beaver River at Croghan NY	753.69	43.89722	-75.4042	56
4260500	Black River at Watertown, NY	4827.76	43.98556	-75.9247	56
4262500	West Branch Oswegatchie River near Harrisville NY	668.22	44.18556	-75.3308	56
4263000	Oswegatchie River near Huevelton NY	2553.74	44.59944	-75.3789	56
4266500	Racquette River at Piercefield, NY	1867.39	44.23472	-74.5719	56
4280000	Poultnet River below Fair Haven, VT	484.33	43.62423	-73.3115	56
4292500	Lamoille River at East Georgia, VT	1776.74	44.67921	-73.0726	56

Table 2. Missing records and data infilling techniques used. In cases of two or three days of missing data, gaps were filled using the monthly mean daily flow value (MMQ). In cases of larger gaps , maintenance of variance was performed using data from neighboring index stations (Granato, 2009).

STATION ID	MISSING RECORDS (DAYS)	INDEX STN ID/INFILLING
1200000	1303	1372500
1306495	3	MMQ
1306500	355	1304000
1308000	367	1308500
1315500	2	MMQ
1318500	2	MMQ
1321000	2	MMQ
1336000	2	MMQ
1376800	2	MMQ
1377000	2	MMQ
1420500	2	MMQ
1428500	2	MMQ
1435000	2	MMQ
1436000	2	MMQ
4240120	794	1509000
4240300	641	1509000
4280000	2	MMQ

Table 3. Six cluster groupings and their corresponding spatial characteristics.

Cluster	# of gages	total basin area (km2)	Dominant land cover type	Altitudinal range	HUC02 hydrologic region	NOAA climate divisions
Housatonic (HS)	10	4289	Forested and Pasture, someUrban	35-1063	New England	Northwest Connecticut, Hudson
Long Island (LI)	9	1016	Urban	11-310	Mid- Atlantic	Coastal
Catskill (CAT)	21	14886	Forested, some crop land and urban	14-1218	Mid-Atlantic	Hudson, Coastal, Eastern Plateau, Poconos
Adirondack-central New York (ADK-CNY)	22	34980	Forested, some crop land and urban	47-1654	Great Lakes, Mid Atlantic	Eastern plateau, Mohawk Valley, Northern Plateau, Central Lakes, Western Vermont
Finger Lakes (FL)	21	20403	Crop land, some forest and urban	103-802	Great Lakes, Mid Atlantic	Central Lakes, Western Plateau, Great Lakes, Upper Susquehana
Erie-Allegheny (EA)	10	7198	Forested, crop land, some urban	145-796	Great Lakes, Ohio	Pennsylvania Northwest Plateau, Western Plateau, Great Lakes

Figures

Figure 1a. Locations of stream gages with respect to land cover (National land cover database) and NOAA climate divisions (black lines). **1b**. DEM of study area with locations of stream gages and major hydrologic region boundaries (black line, HUC02).

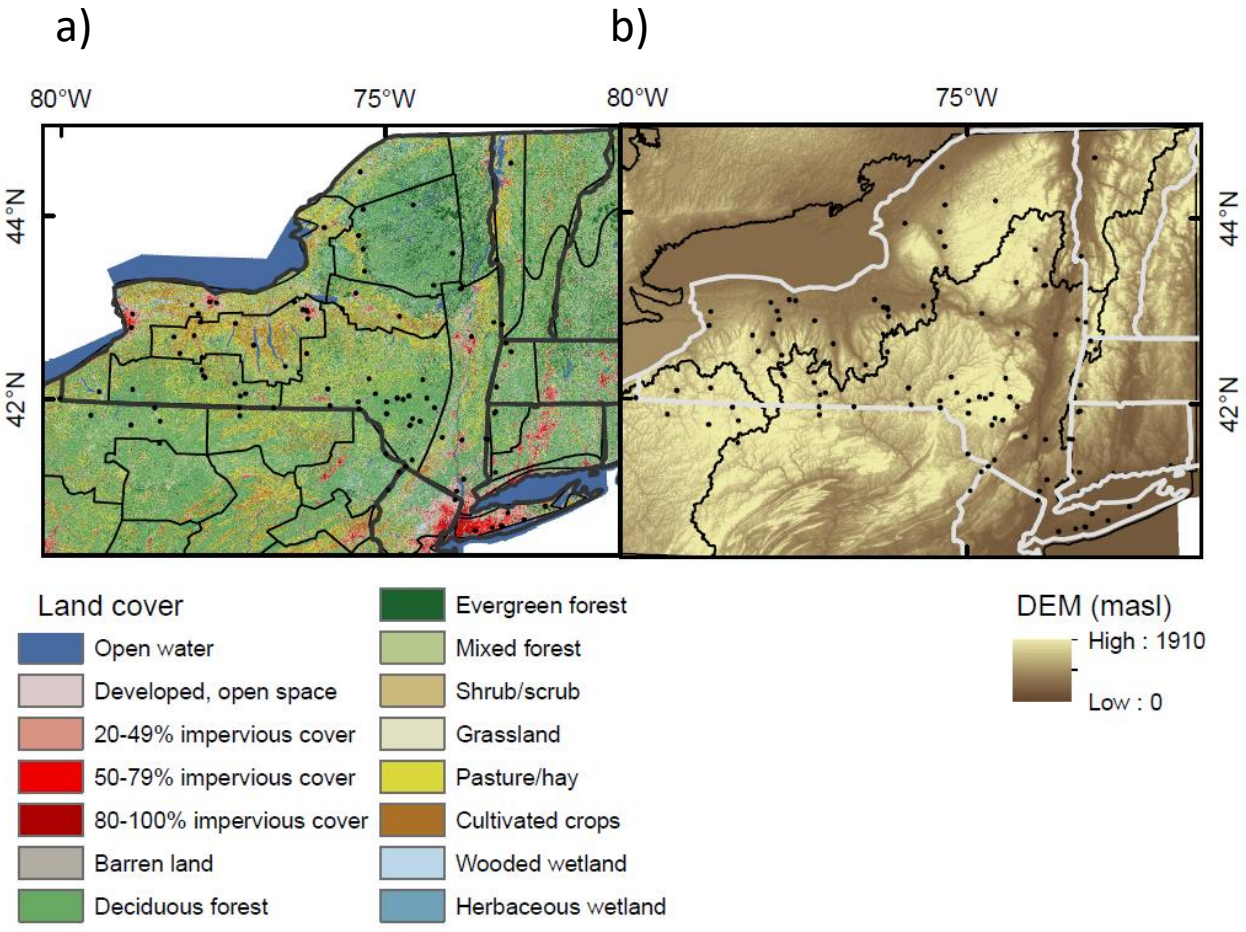

Figure 2. Contributing watersheds included in this study, colored by cluster. Clusters are based on the correlation coefficient between mean annual flows. Hatched areas represent overlapping area between two clusters.

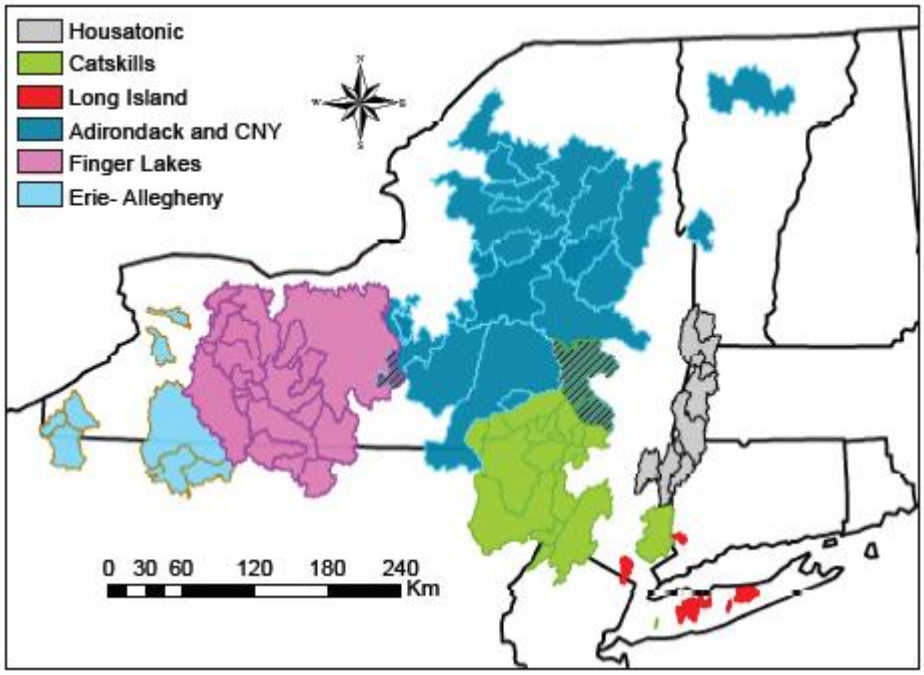

Figure 3. Seasonal occurrence of precipitation change points, colored by cluster. All change points detected in the PRISM-based precipitation rates were positive across all watersheds.

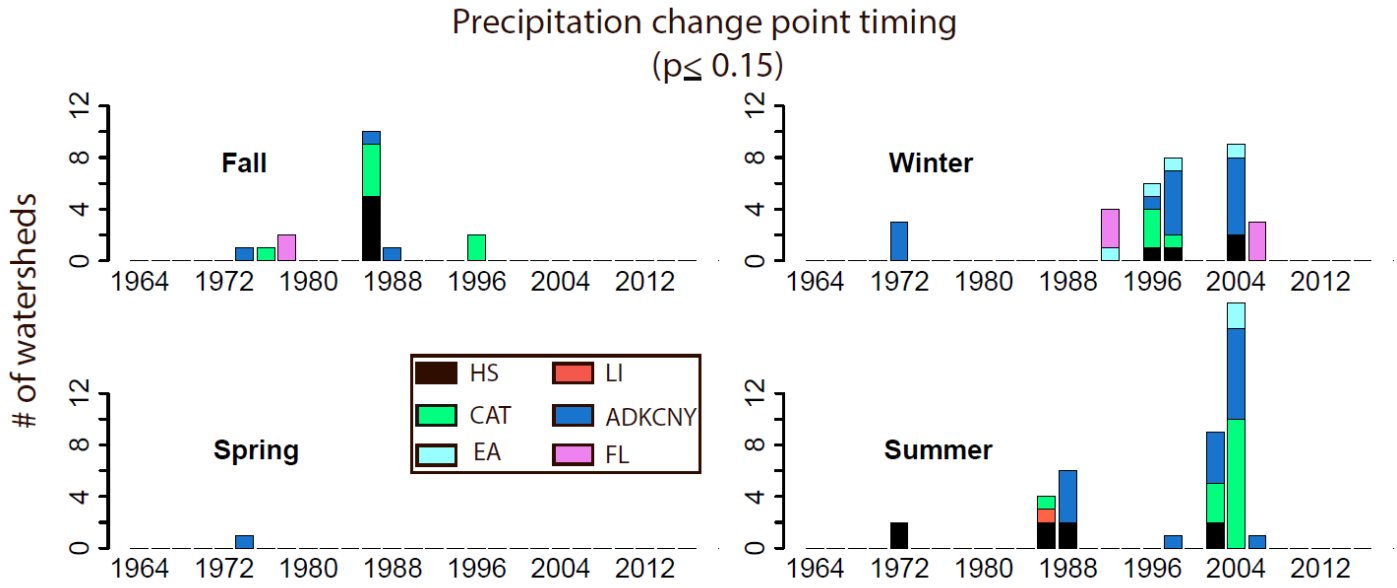

Figure 4. Time series of seasonal normalized temperature across all study watersheds, normalized by subtracting the mean and dividing by the standard deviation to highlight temporal shifts. Grey area shading represents the range of normalized temperatures. Smooth spline interpolation is plotted in black, while the LOESS function is plotted in red with a smoothing factor of 0.6.

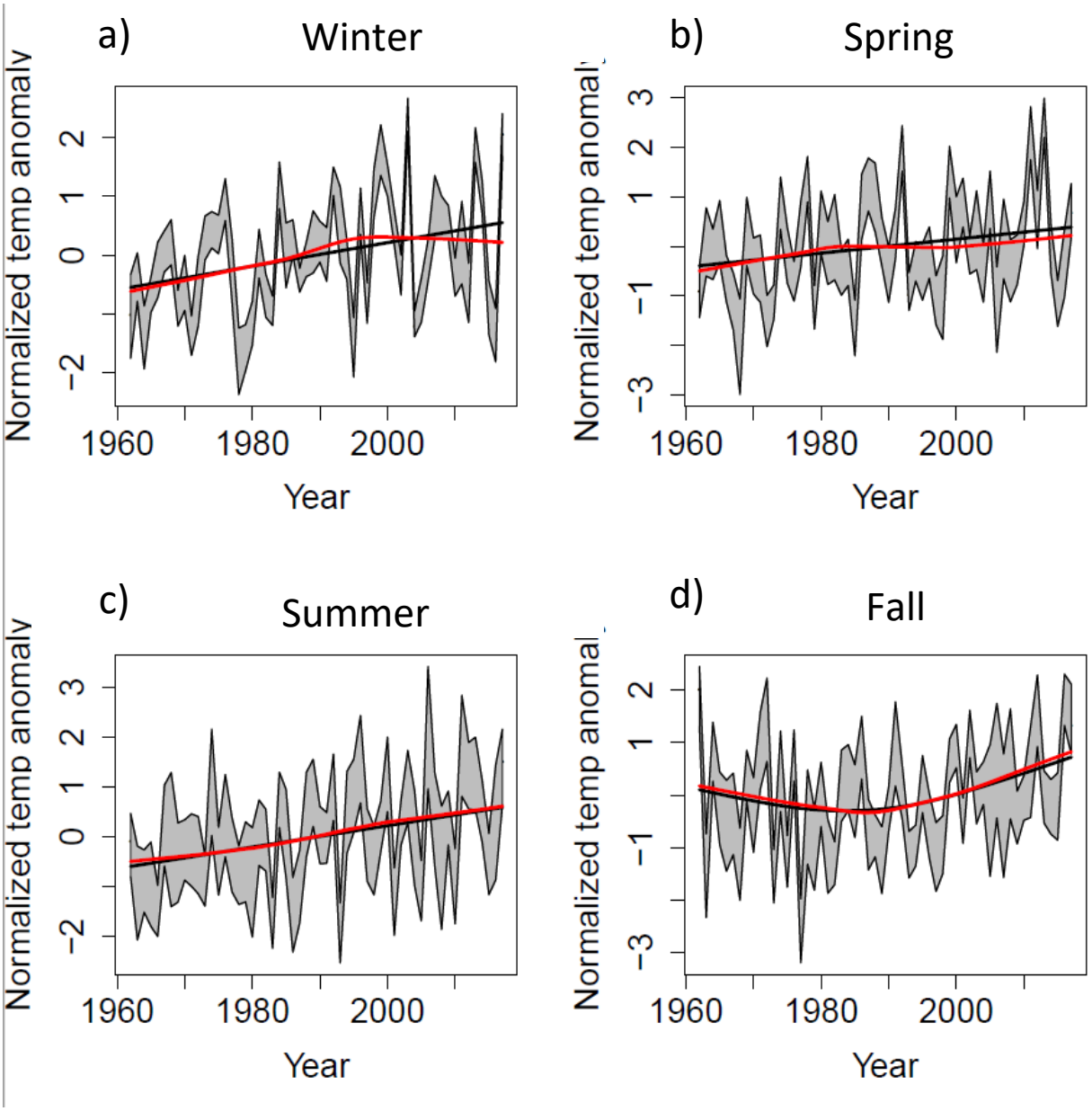

Figure 5. Occurrence of significant (α=0.05) change points for three clusters, CAT, ADK-CNY, and FL. Shaded legend is representative of the number of gages, where the total gages for the CAT, CNY-ADK, and FL clusters are 22, 27, and 21, respectively. Regions with the darkest shading represent years in which more than 30% of gages are exhibiting similar behavior. These behaviors are considered to be driven by climatic forces.

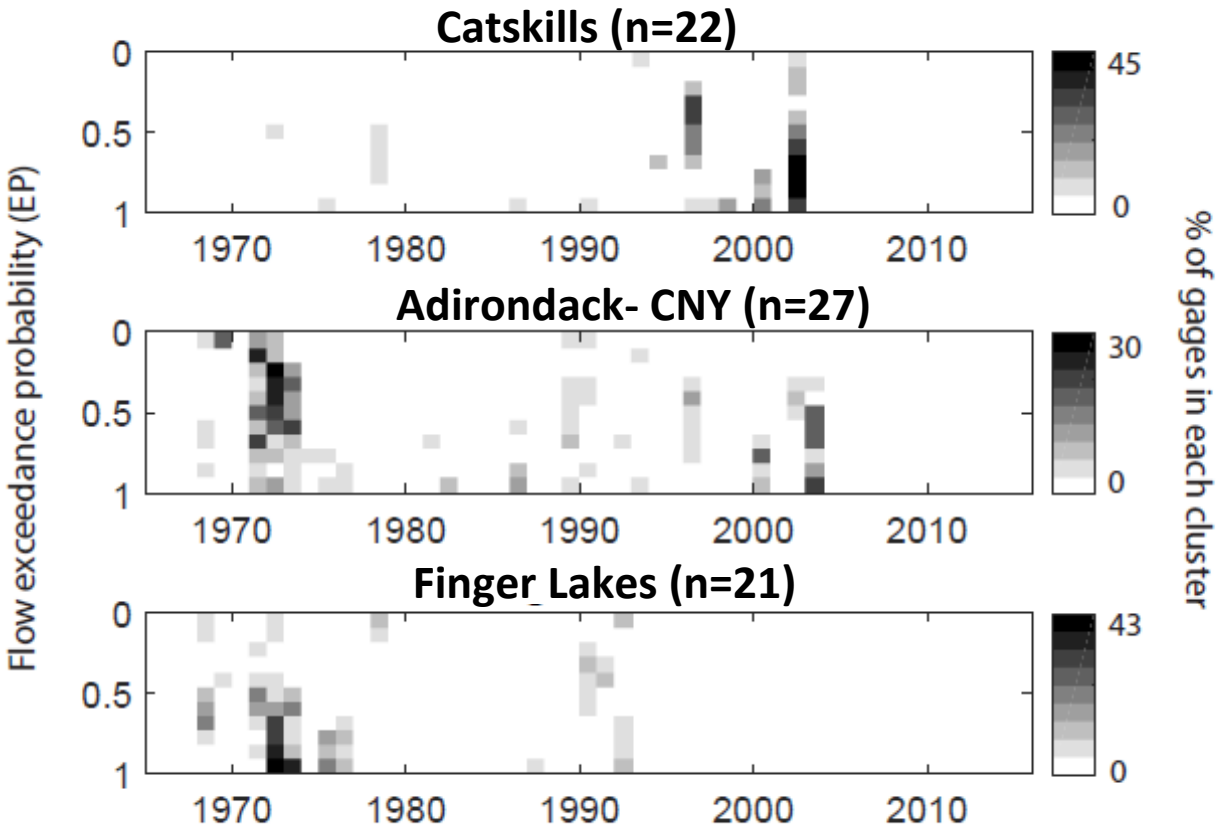

Figure 6. Normalized flow time series for each of nine annual exceedance probabilities (Ep= 0.1, 0.2, 0.3, 0.4, 0.5, 0.6, 0.7, 0.8, 0.9) at two USGS gaging stations. The long term mean anomaly of daily discharge is plotted in red, with that mean shifting upon a significant (α=0.05) Pettit test result. Discharge is normalized by subtracting the mean and dividing by the standard deviation of the entire daily flow series.

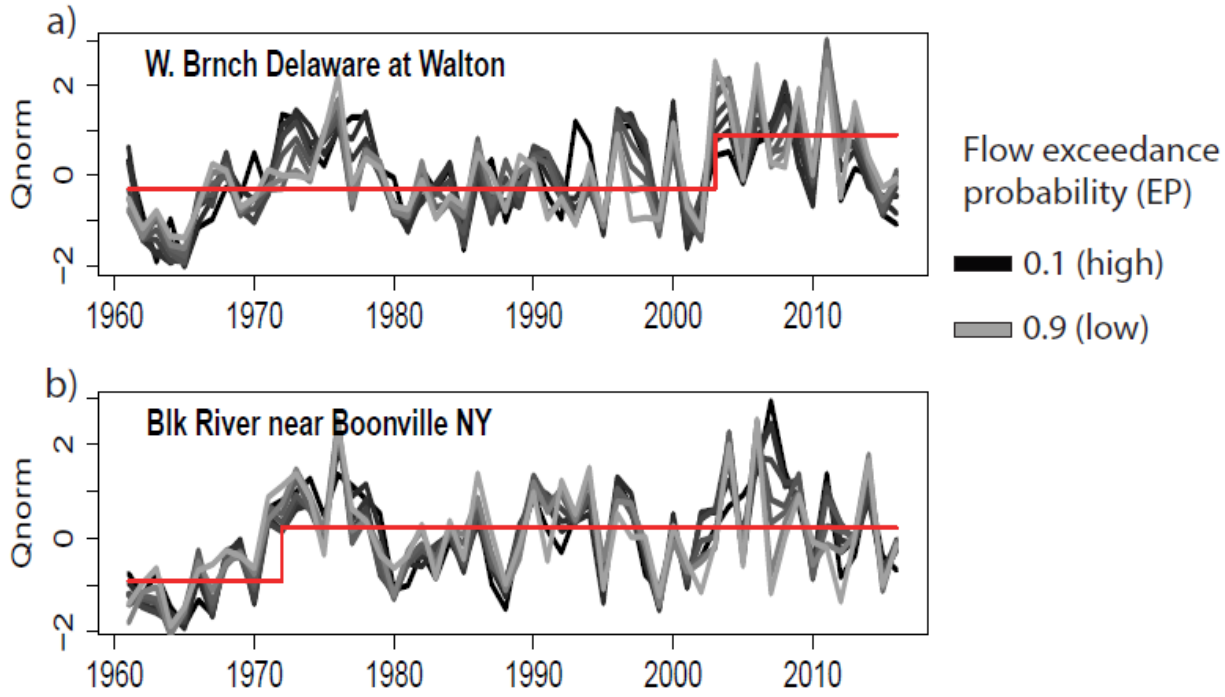

Figure 7. Annual normalized flow values at USGS gaging station 0350000 at Prattsville, NY for EP= 0.01, 0.1, 0.3, 0.5, 0.7, 0.9 (black dots). The LOESS smoothed curve is plotted as solid black line. Median and low flows show increases in magnitude since the 1960s, while the highest flow magnitudes show little to no pattern.

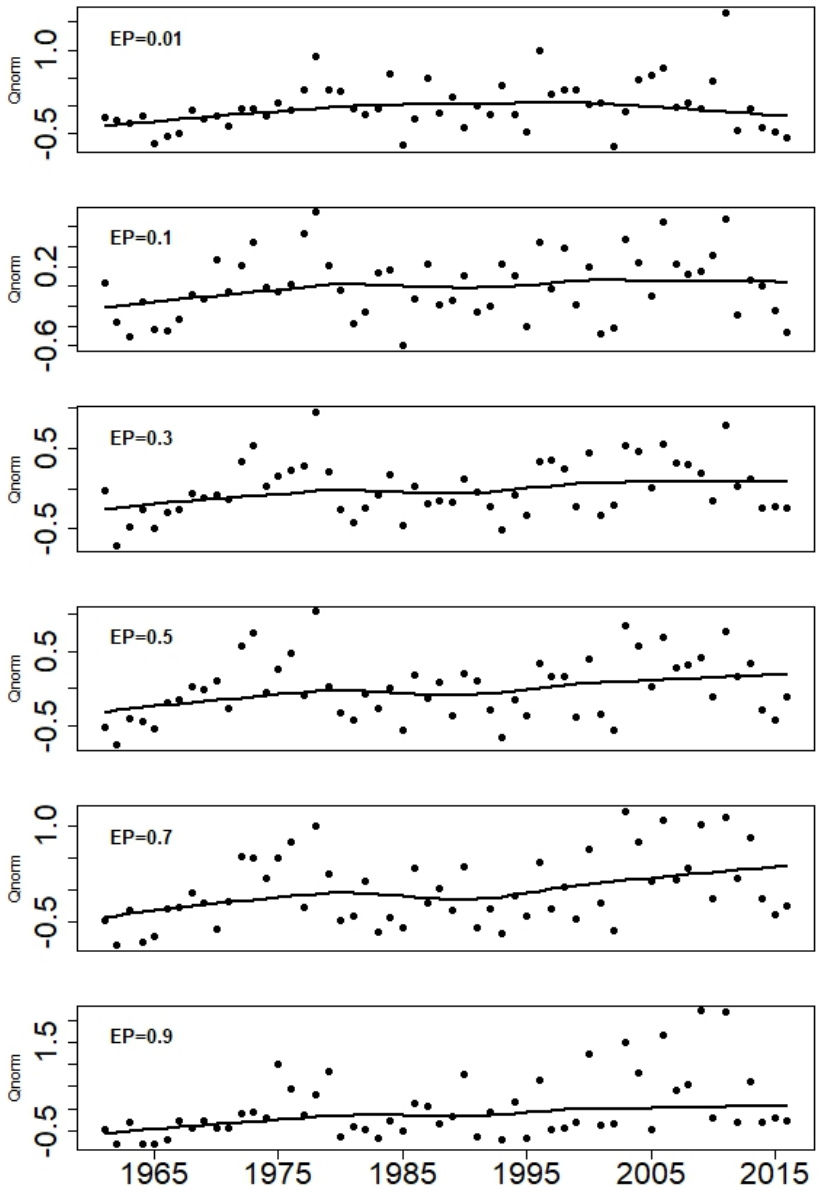

Figure 8. Timing of the change point increase in peaks over threshold (POT). Change points were detected at a significance level of $\alpha=0.1$

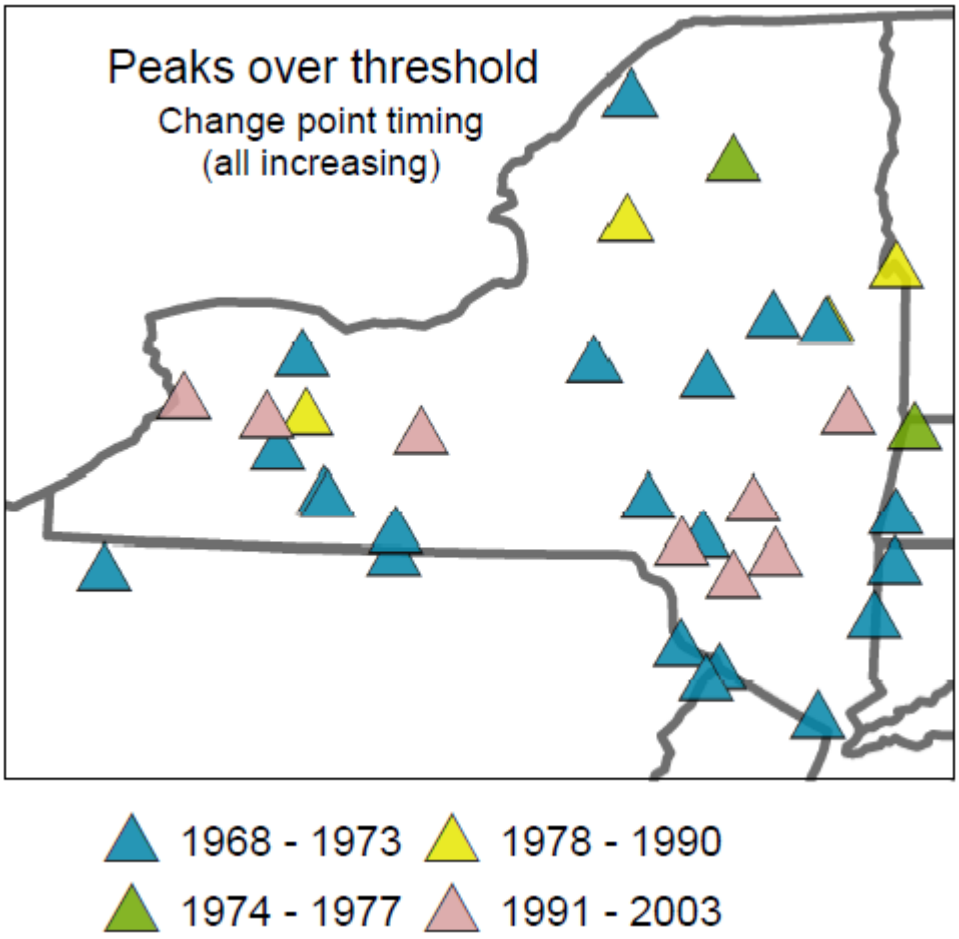

Figure 9. Peaks over threshold (POT) results for USGS gage 04292500 (Lamoille River at East Georgia, VT) using a stationary mean (9a) and nonstationary mean (9b) in the calculation of the method's threshold value. Both cases show a significant (α=0.05) increase in the frequency of peak events in the early 1970s. The black line shows the median number of peaks before and after the changepoint.

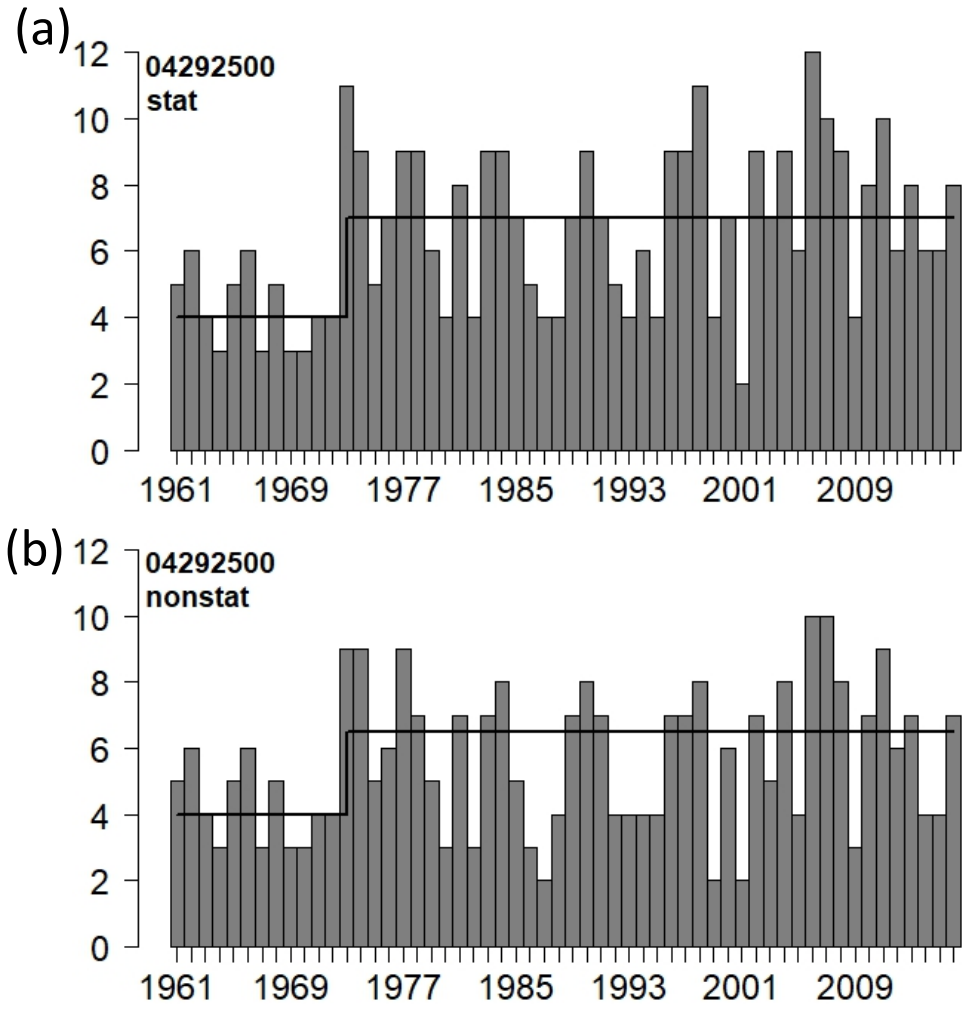

Figure 10. Winter-spring center of volume (WSCOV) plotted as the Julian day between Jan 1 and May 31 for the Independence River at Donnatsburgh, NY (site ID 04296000). LOESS smoothed curve plotted as solid black line, exhibiting a relatively steady decrease toward January over the study period.

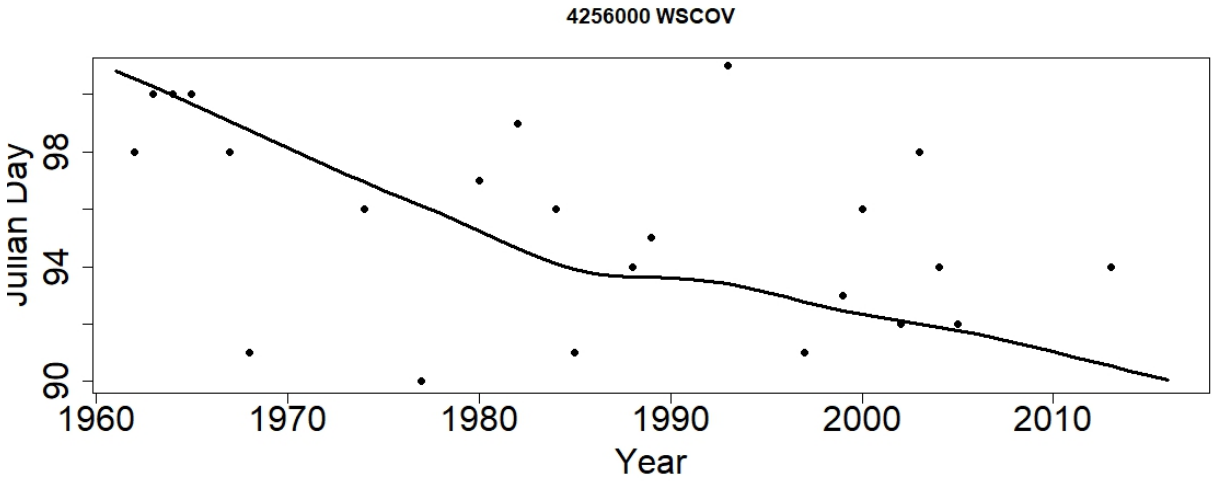

Figure 11. Significant ($p \leq 0.1$) trends detected by Mann-Kendall tests for each month from January to May since 1961 across all gages. Slopes were calculated using Sen's method for those trends that were significant, plotted on the x axis as a percentage change.

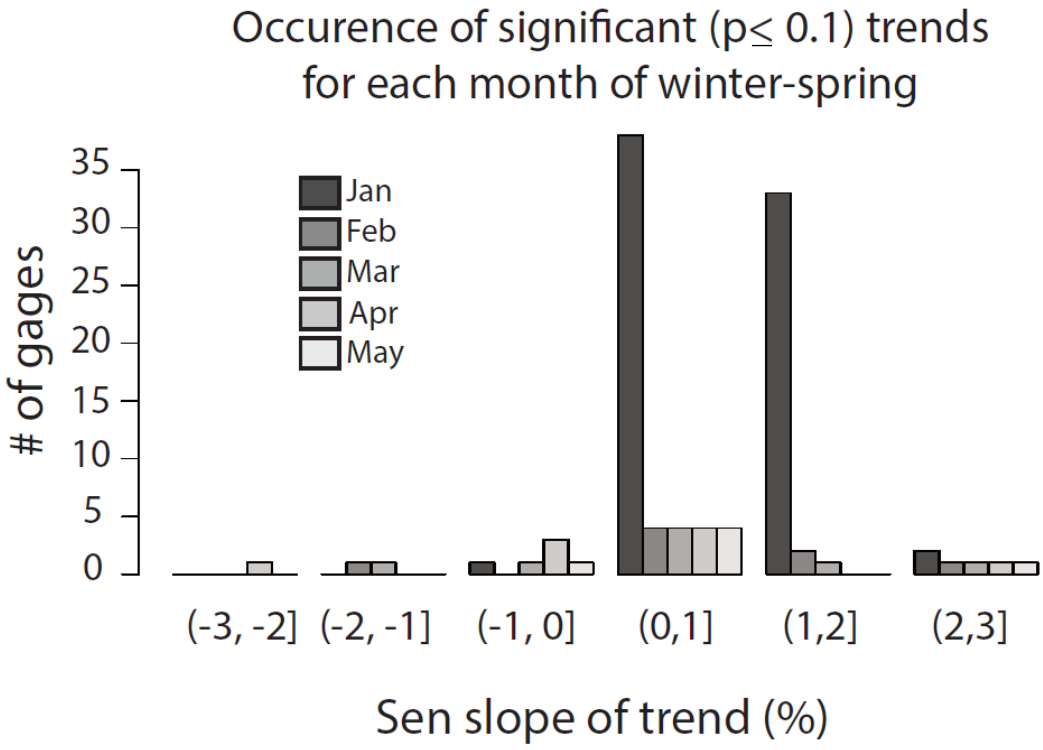

Figure 12. Smoothed annual January streamflow (a) and WSCOV dates (b) as LOESS smoothing functions, averaged and colored by cluster. Shaded region indicates the time period in which both measures' smoothing functions deviate from the overall trend. January streamflow was normalized by subtracting the mean and dividing by the standard deviation of the time series.

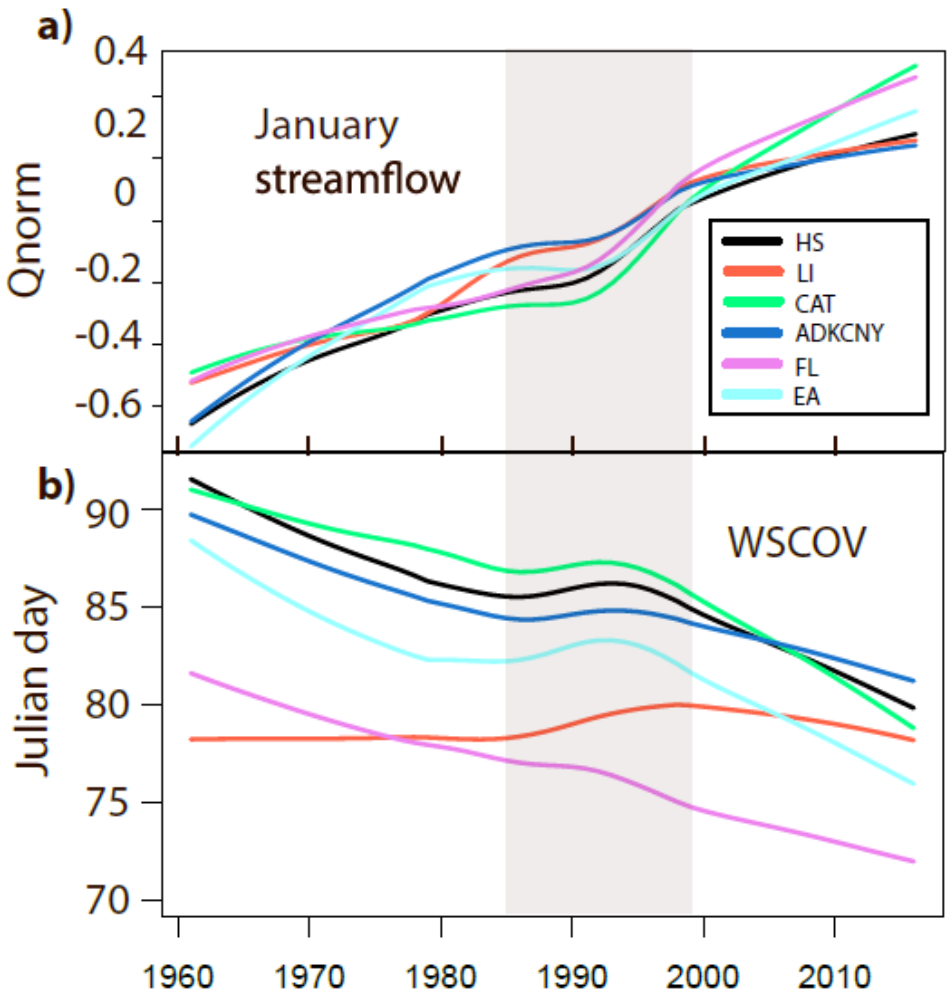

Vita

EDUCATION

PhD Earth Sciences, Syracuse University, Syracuse, NY anticipated 2018

MS Education, University of Southern Maine, Portland, ME 2008

BS Geological Sciences, University of Maine, Orono, ME 2002

RESEARCH FOCUS

My research serves to answer questions surrounding climate change and the hydrologic cycle, integrating the fields of hydrology, hydrogeology, and geophysics. Specifically, I am interested in groundwater as a buffer for changing meteorological patterns, as evidenced by both geophysical and more traditional hydrologic data. I use spatial and time series analysis to shed light on preferential flow of water through the subsurface that is contributing to water availability for downstream communities. I aim to integrate this research with my teaching practice, building on my experience as a teacher and mentor of middle, high school, and undergraduate students, striving to make my research program accessible to students with diverse abilities and backgrounds. International and interdisciplinary collaboration play an important role in my work in order to contribute globally to questions of shifting water resources.

RESEARCH EXPERIENCE

Impacts of climate change on streamflow magnitude, frequency, and timing Jan 2017- present

Research Intern, US Geological Survey, Troy, NY. Supervisor: Dr. Douglas Burns

- Performed statistical trend analysis of 60+ years of historical streamflow records for more than 100 USGS stream gages in New York State and surrounding areas
- Analyzed hydrologic data sets for trends and change points in magnitude, flow frequency, and timing of high flows

- Processed 5000+ raster- format GIS layers to determine climate- change related streamflow regime shifts using PRISM model outcomes
- Communicated results to state and federal government researchers, technicians, and stakeholders

Groundwater- surface water interactions in glaciated tropical catchments Jul 2014- present

Doctoral Researcher, Syracuse University, Syracuse, NY. Supervisor: Dr. Laura Lautz

Cordillera Blanca range and Santa river basin, Northwestern Peru.

- Designed geophysical field surveys using four integrated methods: Seismic refraction, electrical resistivity tomography, Resistivity depth soundings, and ambient passive seismic methods
- Responsible for geophysical instrument acquisition and international transport logistics
- Coordinated high- altitude (4000+ m) geophysical field campaigns over three proglacial valleys
- Collected geochemical and hydrologic data as part of an interdisciplinary research effort, including water samples analyzed for major dissolved ions and stable water isotopes
- Processed and interpreted geophysical data sets to understand hydrologic processes
- Collaborated with and communicated results to local Peruvian government authorities

TEACHING EXPERIENCE

Teaching assistant Jan- May 2018

Course: Introduction to Earth Science (EAR 105)

Syracuse University, Syracuse, NY. Supervisor: Dr. Robert Moucha

- Instructed two labs and one recitation of 20 students each
- Led three field trips that focused on glacial geology
- Assessed student performance weekly with oral and written feedback

Teaching assistant and TA coordinator Aug- Dec 2017

Course: Climate Change, Past and Present (*EAR 111*)

Syracuse University, Syracuse, NY. Supervisor: Dr. Zunli Lu

- Supervised teaching assistants for eight sections of lecture-based recitation for 170+ students
- Course topics: stable isotope geochemistry, climate feedback cycles, ocean acidification
- Instructed three sections of 20 students each
- Assessed teaching assistant performance via peer evaluation
- Assessed student performance weekly with oral and written feedback

Teaching assistant Aug- Dec 2017

Course: The Dynamic Earth (*EAR 110*)

Syracuse University, Syracuse, NY. Supervisor: Dr. Robert Moucha

- Instructed three sections of 20-24 students in laboratory- based geosciences course
- Course topics: optical mineralogy, petrology, glacial geology, plate tectonics
- Led field trips to two local areas of geologic interest for 60+ students

Guest Lecturer and grader Aug- Dec 2016

Course: Introductory Geophysics (*EAR 400/600*)

Syracuse University, Syracuse, NY. Supervisor: Dr. Robert Moucha

- Responsible for grading lab reports and summative exams for a class of 12 graduate and undergraduate students

Science department head Aug 2012- Jun 2014

Lincoln International Middle School, Buenos Aires, Argentina

- Leader of curricular design for 6th, 7th, 8th grade physical and life science courses
- Oversaw grade-level assessments and instructional design
- Coordinated and led grade level field trips to three locations in Argentina

Classroom teacher Aug 2008- Jun 2014

Courses: 6th, 7th, 8th grade math and science, 9th grade physical chemistry

Lincoln International School, Buenos Aires, Argentina

- Instructed over 25 classes of 20-24 students in algebra, physics, chemistry, biology, and earth science
- Implemented service learning techniques, as well as flipped classroom, inquiry- guided learning, and laboratory- based instruction.
- Provided bilingual instruction for non- English speaking students
- Mentored a graduate student (Master's level) who was working toward teaching certification
- Coached after school chess team and led environmental community service activities

Classroom teacher Aug 2006- Jun 2008

Course: 8th grade physical science

Massabessic Middle School, Waterboro, Maine

- Instructed 14 classes of 25-35 students in physical and earth science
- Implemented interdisciplinary, project- based learning using a team teaching approach

COMPETETIVE RESEARCH GRANTS

- EMPOWER NRT Seed Grant in Professional Networking (EMPOWER NRT is an NSF national research traineeship at Syracuse University) ($2300), 2017
- NSF Graduate Student Preparedness Award (Given to PhD students on existing NSF awards to broaden professional experience in the geosciences) ($5000), 2017
- Geological Society of America Graduate Student Research Grant ($2400), 2016

AWARDS

- Syracuse University KD Nelson award for outstanding graduate research in field-oriented geophysics and tectonics ($700), 2017
- National Science Foundation EMPOWER NRT Research Fellowship given to outstanding PhD students whose research falls within the water- energy nexus ($32,000), 2016
- Syracuse University Water Fellowship in recognition of outstanding incoming PhD students in Earth Sciences and Civil, Environmental Engineering ($23,830), 2014

PUBLICATIONS

Lautz, L, McCay, D, Driscoll, C, **Glas, R**, Gutchess, K, Millard, G, Johnson, A. In press. Designing student-centered STEM graduate programs for a multitude of career pathways. Eos.

Tacsi, A., Condom, T., Suarez, W., Garcia, J., Cochachin, A., **Glas, R**, Mejia, A. (2018) Hydro-glaciological modeling of the Yanamarey micro-basin under climate change scenarios, Cordillera Blanca, Peru. In review. *Hydrological Processes*

Glas, R., Lautz, L., McKenzie, J., Chavez, D., Moucha, R., Mark., B. (2018). Proglacial aquifer structure and formation in the Cordillera Blanca, Peru. In Prep for Jun 2018 submission to *Hydrogeology Journal*, (Final draft in co-author review)

Glas, R., Lautz, L., McKenzie, J., Chavez, D., Maharaj, L., Baraer, M., Mark, B. (2017). Groundwater and Surface Water Hydrology of the Cordillera Blanca, Peru. In Review, *WIREs Water*

Somers, L., Gordon, R., McKenzie, J., Lautz, L., Wigmore, O., Glose, A., **Glas, R.,** Aubry-Wake, C., Mark, B., Baraer, M., Condom, T. (2016). Quantifying groundwater- surface water interactions in a proglacial valley, Cordillera Blanca, Peru. *Hydrological Processes*, *2929* (June), 2915–2929

SERVICE TO THE PROFESSION

Geophysics field volunteer, USGS Nov 2017

US Geological Survey, Troy, NY. Geophysical field data collection in central New York State using time-domain electromagnetics

Geophysics field volunteer, USGS Oct 2017

US Geological Survey, Ithaca, NY. Geophysical field data collection in Tully, NY using electrical resistivity tomography

Student Volunteer, SAGEEP symposium Mar 2017

Symposium for the Application of Geophysics to Engineering and Environmental Problems (SAGEEP) annual meeting, Denver, CO

Geophysical Data Analysis and Translation Services Oct 2016- present

Peruvian National Water Authority, Huaraz, Peru. Geophysical data inversions, model interpretations, and technical manuscript translations by correspondence

Session Convener, Northeast GSA meeting Mar 2016

Geological Society of America Northeast Meeting, Albany, NY. Session title: Geophysics in the Hydrogeologist's Toolbox

SERVICE TO THE UNIVERSITY AND COMMUNITY

Peer Mentor Aug 2016- present

Syracuse University, Syracuse, NY. Mentoring two graduate students in chemistry and civil/ environmental engineering. Focus on course program completion and networking skills

Geology Graduate Student Organization Aug 2014- present

Syracuse University, Syracuse, NY. Served as treasurer (2014-2015) and active member. Assisted in the organization and implementation of the Central New York Geology Graduate Student Symposium 2015, 2016, 2017, 2018

Host for visiting scientist Oct 2016

Syracuse University, Syracuse, NY. Arranged and coordinated department- wide events for a two day visit by a senior researcher in the Department of Earth Sciences KD Nelson lecture series

K-12 outreach participant Oct 2014 & 2015

Syracuse University, Syracuse, NY. Worked with visiting 9th grade honors earth science students from Liverpool High School, Designed and implemented two hands- on activities to teach concepts of groundwater and surface water flow

Volunteer and outreach coordinator Feb- May 2015

Nottingham High School and Syracuse University, Syracuse, NY. Guest teacher (2 weeks) in four sections of high school earth sciences, coordinated volunteer opportunities for Syracuse University graduate students at Nottingham High School

CONFERENCE PRESENTATIONS

Glas, R., Burns, D., Lautz, L. Changing Streamflow Regimes in New York State: Trends, Patterns, and Attribution. Proceedings of the Geological Society of America Annual Meeting, 2017 Oct 21- 25: Seattle, WA

Glas, R., Lautz, L., Moucha, R., McKenzie, J., Mark, B. Alpine Groundwater Storage in the Tropics: Using Hydrogeophysics to Constrain Boundary Conditions for Future Groundwater Models in the Cordillera Blanca, Peru. Symposium for the Application of Geophysics to Engineering and Environmental Problems Annual Meeting, 2017 March 19-23: Denver, CO

Glas, R., Lautz, L., McKenzie, J., Mark, B., Aubry-Wake, C., Somers, L., Wigmore, O., Baker, E. Integrating Multiple Geophysical Methods to Quantify Alpine Groundwater- Surface Water Interactions: Cordillera Blanca, Peru. Proceedings of the American Geophysical Union Annual Meeting, 2016 Dec 12-16: San Francisco, CA

Glas, R., Lautz., L., McKenzie, J., Aubry-Wake, C., Baker, E., Somers, L., Mark, B., Wigmore, O. Using Multiple, Integrated Hydrogeophysical Methods to Understand Groundwater-Surface Water Interactions in Glaciated, Tropical Catchments of the Cordillera Blanca, Peru. Proceedings of the Geological Society of America Annual Meeting, 2016 Sep 25- 28: Denver, CO

Glas, R., Lautz., L., McKenzie, J., Aubry-Wake, C., Baker, E., Somers, L., Mark, B., Wigmore, O. Characterization of Aquifer Structure using Seismic Refraction Tomography in the Cordillera Blanca, Peru. Presented at the Foro Internacional de Glaciares y Ecosistemas de Montaña, 2016 Aug 10- 13: Huaraz, Peru

Glas, R., Lautz, L., McKenzie, J., Aubry-Wake, C., Baker, E., Somers, L., Mark, B., Wigmore, O. Observations of Subsurface Heterogeneity in a Tropical Alpine Catchment using Seismic Refraction Tomography. Proceedings of the Geological Society of America Northeast Regional Meeting, 2016 Mar 24-26: Albany, NY

Glas R., Lautz L., McKenzie J., Mark, B., Baker, E., Aubry-Wake, C., Somers, L., Wigmore, O. Characterizing Subsurface Structure and Composition Using Seismic Refraction Surveys of Proglacial

Valleys in the Cordillera Blanca, Peru. Proceedings of the American Geophysical Union Fall Meeting, 2015 Dec 14-18; San Francisco, CA

Baker, E., Lautz, L., Aubry-Wake, C., McKenzie, J., Glas, R., Mark, B., 2015. Infrared Imaging and Modeling of Proglacial Stream Temperature in the Cordillera Blanca, Peru. Proceedings of the American Geophysical Union Annual Meeting, 2015 Dec 14-18: San Francisco, CA

Somers, L., Gordon, R., McKenzie J., Lautz, L., Wigmore, O., Glas, R., BG Mark. Quantifying Groundwater-Surface Water Interactions using a Stream Energy Balance Model and Dye Tracing in a Proglacial Valley of the Cordillera Blanca, Peru. Proceedings of the American Geophysical Union Annual Meeting; 2015 Dec 14-18: San Francisco, CA

MEMBERSHIPS

American Geophysical Union, 2014- present

Association of Women Geoscientists, 2016-2017

American Water Resources Association, 2017

Environmental and Engineering Geophysical Society, 2017

Geological Society of America, 2014- present

WiSE-FPP (Women in Science and Engineering Future Professionals Program), 2014-present